Joana Isabel Silva Rodrigues

BSc Genetics and Biotechnology

Dissecting the role of alpha-synuclein phosphorylation in Parkinson's disease

Dissertation for obtaining a Master's Degree in
Molecular Genetics and Biomedicine

Supervisor: Sandra Tenreiro, PhD, CEDOC – Chronic Diseases Research Center

FACULDADE DE CIÊNCIAS E TECNOLOGIA
UNIVERSIDADE NOVA DE LISBOA

September 2017

Dissecting the role of alpha-synuclein phosphorylation in Parkinson's Disease

Acknowledgments

The work presented here was only possible with the great support I received during this year from the people here mentioned. Thereby, I would like to express my immense gratitude to the followings:

Firstly, I would like to thank Doctor Sandra Tenreiro, for all the support, encouragement, and kindness. Thank you for mentoring me and for all the amazing opportunities you gave me, allowing me to grow as a scientist and as person. To Professor Tiago Outeiro, for giving me the opportunity to work in the Cellular and Molecular Neuroscience Unit and for providing all the necessary conditions to develop my work. To Doctor Hugo Vicente Miranda, for his amazing critical spirit, incentive and support.

I would like to thank CEDOC - NOVA Medical School, as institution and as a community, for receiving me with open arms. Thank you to everyone who assisted me during my experiments. It was a pleasure to work in such a motivational environment.

A very special thank you to “Morsas”, my girls. To Ana, our grandma, for all the amazing support, all the critics and good advices, all the help and care. Thank you for putting up with us and for taking care of us. Thank you for sharing your experiences, making me grow and helping me understand this brave new world. The best advice I got from you was “Nos péis não”, and I will remember it for the rest of my days. To Babita, our jester and my partner in crime. Hamilton brought us together and MCA kept our flame alive. Thank you for always, and I mean ALWAYS, laughing with me and making me laugh. Your puns will always make me happy. ChemiDoc will not be the same without you. You were the best plate-shaking person during my yeast transformations and always will be, no one can ever replace you. Thank you for the best roadtrips ever, I will never hear “Uptown Girl” and “It's Not Unusual” without you popping up in my head. May our childhood bands cheer you up forever. I hope we will be together until we die and, when we die, we will be ghost friends and haunt Ana. To Gabigoo, our sun, thank you for always being there right by my side, literal and figuratively. We shared so much during this year, for the good and the bad, we were always there for each other and always will be. Our friendship came from nothing and became one of the most precious things I have. Thank you for all the laughs, all the good times and all the care. Despite the “All by Myself” jokes, I want you to know that I will be there for you at any time. More recently, thank you for all the goodies you bring home; I figured that your plan is to make me gain weight so the plane cannot take off. To the three of you, thank you for making this year as amazing as it was. Thank you for your friendship and for being my second family during this year, sometimes even my first family. I have not enough words to thank you properly. May this friendship last a lifetime.

To all my friends, either from Torres Novas, UTAD or FCT, for always being there for me, and for sharing my happiness. To Ana Silva, my Azorean friend, my roomate, for our friendship, which grew exponenially over this year. For all the encouragement and for pushing me to do my best. I have a special respect for you, I will be always pride of what you have accomplished. A gigantic thank you to your cooking skills! See you in Azores! To “Gordos & Gorduchos” my family at UTAD, our friendship will always be my most random friendship, our inside jokes, all the memes shared, all the pictures sent and all the random conversations. May this never end, may this family be together for eternity. See you soon. A special thank you to Rita, Cláudia, João and Patrick. Each and every one of you contributed to my happiness in your own peculiar ways, by being there with me or simply by always putting a smile in my face, even when the distance between us was enormous and our schedules were completely unsynchronized. It was a pleasure to have you with me during one more year and, hopefully, in the years to come. I will have you in my heart wherever I go.

Last, but not least, I would like to thank my family, specially my parents, Susana and António, for all the efforts they made and continue to make so I can pursuit this dream. Thank you for all the faith you always had in me, for all the support and patience. The sacrifices made were gigantic, and I hope that I have made you proud and that I will have the opportunity to give you as much as you gave me. Without you, my dream would never become a reality. No matter how far I will go, I will always be there with you. To 'Vó Alice, there were so many times that I thought about you. I will always remember the excitement with which you used to ask about my studies, and your smile every time I explained something to you. I know that you would be proud today. We miss you every single day.

"There's a million things I haven't done. But just you wait"

Lin-Manuel Miranda

Resumo

A doença de Parkinson é a segunda doença neurodegenerativa mais comum, caracterizada pela agregação de alfa-sinucleína nos neurónios dopaminérgicos da *substantia nigra pars compacta* e, consequentemente, pela morte neuronal. Os neurónios dopaminérgicos sobreviventes apresentam depósitos de alfa-sinucleína, denominados Corpos de Lewy.

A origem da doença de Parkinson pode ser esporádica ou ter uma causa genética. Doença de Parkinson associada ao *SNCA*, gene codificante da alfa-sinucleína, apresenta um padrão hereditário autossómico dominante. Atualmente, seis mutações foram identificadas no gene *SNCA.* A alfa-sinucleína é suscetível de sofrer diversas modificações pós-trasducionais, sendo que a fosforilação é uma modificação de elevada importância, pois é a principal modificação encontrada nos agregados, podendo ter um papel na regulação da estrutura, oligomerização e toxicidade da alfa-sinucleína. Porém, ainda está a ser debatido se a fosforilação promove ou previne estas mesmas propriedades, sendo que modelos celulares distintos apresentam resultados contraditórios.

Saccharomyces cerevisiae é um modelo celular estabelecido para o estudo da doença de Parkinson, sendo que permite reproduzir diversas características, tais como agregação e toxicidade celular. Neste estudo, plasmídeos multicópia contendo diferentes variações de alfa-sinucleína fundidas com GFP sob a regulação do promotor *GAL1* foram transformados em levedura. Os efeitos da fosforilação de diversos resíduos na formação de inclusões de alfa-sinucleína e na sua toxicidade foram avaliados. As seis mutações no gene *SNCA* (A30P, E46K, H50Q, G51D, A53E e A53T) foram caracterizadas quanto à formação de inclusões, toxicidade, níveis proteicos, degradação, acidificação vacuolar e produção de ROS.

A avaliação dos efeitos da fosforilação revelou que tanto o bloqueio como a mímica da fosforilação da S129 superam os efeitos da fosforilação da S87, com a alfa-sinucleína S129A promovendo um aumento da toxicidade, enquanto a alfa-sinucleína S129D apresenta um efeito protetor. Em relação à fosforilação dos resíduos de tirosina, o bloqueio da fosforilação do resíduo Y125 provocou uma diminuição na degradação proteica, resultando num aumento de toxicidade, comprovado pelo ensaio de viabilidade celular de citometria de fluxo. As mutações familiares A30P, G51D e A53E demonstraram uma toxicidade inferior à alfa-sinucleína WT, enquanto que as mutações H50Q e A53T apresentaram efeitos semelhantes ao WT. O mutante E46K foi o único que exibiu uma toxicidade mais elevada. Seria de esperar uma maior toxicidade por parte das alfa-sinucleínas mutantes, tendo em conta que estas provocam um parkinsonismo mais severo e um aparecimento precoce da doença. A divergência obtida poderá dever-se ao modelo celular usado, uma vez que as leveduras têm um ambiente celular distinto dos neurónios dopaminérgicos afetados na doença de Parkinson.

Palavras-chave: Doença de Parkinson, alfa-sinucleína, fosforilação, mutações familiares, *S. cerevisiae*

Abstract

Parkinson's disease is the second most common neurodegenerative disorder, characterized by an aggregation of alpha-synuclein in the dopaminergic neurons of the *substantia nigra pars compacta* and, consequently, neuronal death. Surviving dopaminergic neurons present alpha-synuclein deposits, known as Lewy Bodies.

Parkinson's disease can have sporadic or genetic cause. Parkinson's disease associated with *SNCA*, the alpha-synuclein encoding gene, shows an autosomal dominant inheritance pattern. Until now, six *SNCA* mutations were identified. Alpha-synuclein is prone to suffer several post-translational modifications, critical for its function and structural properties. Phosphorylation is a modification of major importance, since it it's the modification most commonly found in aggregates; it may play an important role in regulating alpha-synuclein structure, oligomerization and toxicity. However, whether phosphorylation promotes or prevents these properties is still under debate, with distinct cellular models presenting contradictory results.

Saccharomyces cerevisiae cells are an established model to study Parkinson's disease, since it can reproduce several features, such as protein aggregation and cellular toxicity. For this study, multicopy plasmids containing different alpha-synuclein variants fused with GFP under the regulation of a *GAL1* promoter were transformed in yeast cells. Effects of phosphorylation at different residues in alpha-synuclein inclusion formation and cell toxicity were evaluated. Furthermore, the six known *SNCA* mutations (A30P, E46K, H50Q, G51D, A53E and A53T) were characterized regarding inclusion formation, cell toxicity, protein levels, protein clearance, vacuole acidification and ROS production.

Evaluation of phosphorylation effects revealed that either blockage or mimic of S129 phosphorylation always overcome the S87 phosphorylation effect, with S129A increasing toxicity, while S129D promotes protection. Regarding tyrosine residues phosphorylation, Y125 phosphorylation blockage impaired protein clearance, increasing its toxicity. Concerning familial mutations, A30P, G51D and A53E aSyn, point to a lower toxicity than WT aSyn, while the H50Q and A53T mutations presented results very similar to WT, and E46K aSyn was the only one who presented higher toxicity. This divergence is probably due to the cellular model used, since yeast cells present a distinct cellular environment than the affected dopaminergic neurons in PD.

Keywords: Parkinson's Disease, alpha-synuclein, phosphorylation, familial mutations, *S. cerevisiae*

Index

Figure Index

Table Index

List of abbreviations and acronyms

AD	Alzheimer's Disease
Amp	Ampicillin
aSyn	Alpha-synuclein
Atg	Autophagy-Related Protein
ATP	Adenosine Triphosphate
bSyn	Beta-synuclein
BAX	Bcl-2-Like Protein X
BSA	Bovine Serum Albumine
CDNF	Cerebral Dopaminergic Neurotrophic Factor
CSM	Complete Supplement Media
DA	Dopamine
DDC	DOPA Decarboxylase
DHE	Dihydroethidium
E1	Ubiquitin-Activated Enzyme
E2	Ubiquitin Conjugating Enzyme
E3	Ubiquitin-Protein Ligase
E. coli	*Escherichia coli*
EDTA	Ethylenediamine Tetracetic Acid
ER	Endoplasmic Reticulum
Gal	Galactose
GFP	Green Fluorescent Protein
Glu	Glucose
gSyn	Gama-synuclein
HECT	Homologous to the E6-AP Carboxyl Terminus type
Kan	Kanamycin
LB	Lewy Body
LB media	Luria Broth media
LiAc	Lithium Acetate

LN	Lewy Neurites
L-DOPA	L-3,4-dihydroxyphenylalanine
MAM	Mitochondria-Associated ER Membranes
MANF	Mesencephalic Astrocyte-Derived Neurotrophic Factor
MPTP	1-methyl-4-phenyl-1,2,3,6-tetrahydropyridine
mTOR	Mammalian Target Of Rapamycin
NAC	Non-Amyloid-beta Component
NSF	N-Ethylmaleimide Sensitive Factor
NTF	Neurotrophic Factor
OD	Optical Density
OE	Over-expression
pAG	pAdvanced Gateway
PBS	Phosphate Buffered Saline
PCR	Polymerase Chain Reaction
PD	Parkinson's Disease
PEG	Polyethylene Glycol
pH	Potential of Hydrogen
PI	Propidium Iodide
PIP3	Phosphatidylinositol 3,4,5-triphosphate
PI3K	PI3 Kinase
PTEN	Phosphatidylinositol 3-phosphatase
Raf	Raffinose
RING	Really Interesting New Gene
ROS	Reactive Oxygen Species
RT	Room Temperature
S	Serine
S. cerevisiae	*Saccharomyces cerevisiae*
SDS	Sodium Dodecyl Sulfate
SDS-PAGE	Sodium Dodecyl Sulfate Polyacrylamide Gel Electrophoresis
SNARE	Soluble NSF Attachment Receptor

TBS	Tris Buffered Saline
TBS-T	Tris Buffered Saline – Tween 20
TE	Tris – EDTA
TH	Tyrosine Hydroxylase
UBC	Ubiquitin Conjugating Enzyme
UPR	Unfolded Protein Response
UPS	Ubiquitin-Proteasome System
v-ATPase	Vacuolar-ATPase
WT	Wild-Type
Y	Tyrosine
YNB	Yeast Nitrogen Base
YPD	Yeast Extract Peptone Dextrose
6-OHDA	6-hydroxydopamine

1 Introduction

1.1 Neurodegenerative diseases as proteinopathies

The prevalence of chronic age-related diseases is growing due to the continuing demographic shift of worldwide population towards an older society (Bourdenx et al., 2016). The neurodegeneration process is long and involves the loss of brain and spinal cord cells, moreover, once the patient experiences symptoms, the neurodegeneration is already advanced (Uversky, 2009).

Several neurodegenerative diseases such as Alzheimer's disease (AD), Parkinson's disease (PD), Amyotrophic Lateral Sclerosis, and Huntington's disease share cellular and molecular mechanisms and histopathological features. Although the featured protein and the affected brain areas are different for each disease (Figure 1.1), generally they have a common protein aggregation pathology. Misfolded proteins that accumulate and become aggregate prone and insoluble, are commonly found in brain regions most affected by the disease and have, therefore, become known as pathological hallmarks of neurodegenerative disorders (Swart et al., 2014).

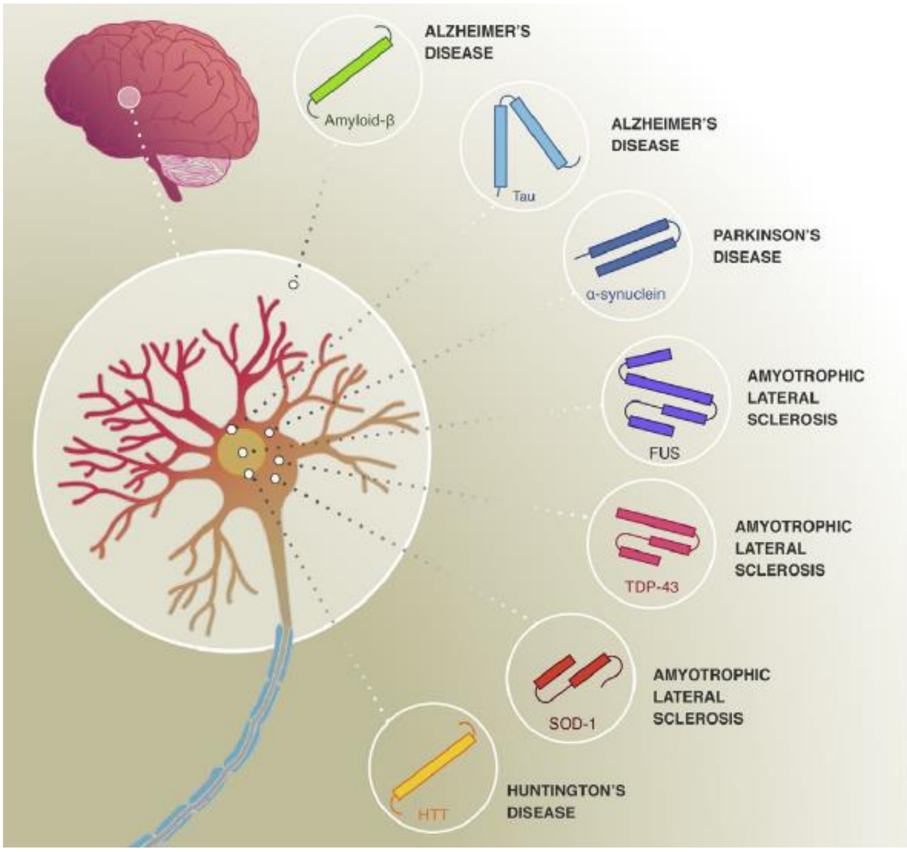

Figure 1.1 Neurodegenerative diseases have in common the presence of misfolded and aggregated proteins and, consequently, the presence of protein deposits.

Each neurodegenerative disease has a specific protein that deposits in a specific region of the neuron, however, there are proteins, like alpha-synuclein, that are prone to aggregate in a variety of neurodegenerative diseases (Eftekharzadeh et al., 2016).

These aggregated proteins have a very ordered structure and often exhibit characteristics of amyloid-like protein assemblies (Swart et al., 2014; Eftekharzadeh et al., 2016). In this state, proteins develop elongated fibers with backbones consisting of many-stranded β-sheets (Eisenberg & Jucker, 2012). Both the structure and the biophysical properties of amyloid fibrils are similar across different amyloid diseases, even though each disease involves the amyloidogenic aggregation of one or many different proteins. Several studies reported that the formation of amyloid fibrils is associated with the loss of protein function or a toxic gain of function (Eftekharzadeh et al., 2016).

Although each disease has specific protein aggregates as hallmarks, there is an overlapping pattern e.g., PD shares the presence of alpha-synuclein (aSyn) inclusion bodies with several other synucleinopathies (Uversky, 2009). Therefore, despite the diversity of proteins involved in each disease, there are common disease mechanisms, indicating typical pathological patterns associated with neuronal decline (Swart et al., 2014).

The main risk factor for all neurodegenerative diseases is still aging, suggesting that a decline in protein quality control associated with aging may contribute to misfolding and, consequently, aggregation of proteins in specific populations of brain cells (Chen et al., 2011).

1.2 Synucleinopathies and Parkinson's Disease

Synucleinopathies exhibit, as hallmark, the presence of aggregated aSyn deposits in intracellular inclusions, but display differences in symptomatology, brain areas and cell types affected, and anatomical sites of onset (Dehay & Fernagut, 2016). Synucleinopathies include several diseases such as PD, amyotrophic lateral sclerosis, neurodegeneration with brain iron accumulation type 1, pure autonomic failure, multiple system atrophy and dementia with Lewy bodies (Uversky, 2009; Tagliafierro, 2016).

PD is the second most prevalent neurodegenerative disorder, following AD, with a prevalence of 1% to 2% in people over 65 years of age (Lau & Breteler, 2006; Massano & Ferreira, 2016). PD is considered a slowly progressive neurodegenerative disease which results from the interaction between genetic and environmental factors wherein multiple neuroanatomical areas are implicated leading to a range of features that begin years before diagnosis. Most PD cases are sporadic; however, approximately 5% to 10% of PD patients have monogenic forms of the disease, exhibiting a Mendelian type of inheritance (Kalia et al., 2015).

The pathological hallmark of PD is the progressive loss of dopaminergic neurons in the *substantia nigra pars compacta* (SNpC) and the presence of Lewy Bodies (LB), as well as, Lewy Neurites (LN) in the surviving neurons (Lau & Breteler, 2006; Massano & Ferreira, 2016). The resultant dopamine (DA) deficiency leads to a movement disorder characterized by classical parkinsonian motor features, described in figure 1.2 (Kalia et al., 2015).

The axons from the SNpC and other key dopaminergic areas in the brain project extensively to form four main pathways namely, the mesocortical, mesolimbic, nigrostriatal and tuberoinfundibular pathways, which are responsible for mediating several non-motor features of PD (Chaudhuri & Schapira, 2009; Kalia et al. 2015). The motor features are identified relatively late in the pathological process, when approximately 70% of the dopaminergic neurons are already dead (Uversky, 2009).

Figure 1.2 Parkinson's disease motor and non-motor features.
The dopamine deficiency resultant from the loss of dopaminergic neurons in the SNpC leads to a series of motor features. Moreover, four main pathways can also be affected leading to the development of non-motor features.

PD management involves primarily the symptomatic treatment with drugs that increase DA concentration or stimulate DA receptors (Kalia et al., 2015). Despite these symptomatic treatment efficiency, nowadays, there are no drugs that slow or change the disease course (Noyce et al., 2016).

The main PD risk factors are age superior than 50 years and male gender, being men 1.5 times more likely to develop the disease (Wooten et al., 2004). Unlike the females, where prevalence tends to stabilize over time, in males the incidence keeps rising after the age of 80 years (Hirsch & Steeves, 2016). In women, loss of estrogen production can also compromise protective effects and, some evidences suggest that early menopause, ovary removal or hysterectomy increases risk in women, similarly to that seen in men. Environmental factors and ethnicity are also considered risk factors for the disease development. The prevalence of PD seems to be higher in Europe, North America and South America (Dexter & Jenner, 2013; Kalia et al. 2015). Overall, age remains the major risk factor for PD for the majority of the patients (Kalia et al., 2015).

1.3 Alpha-synuclein and the synuclein family

The synuclein family is comprised of aSyn, β-synuclein (bSyn) and γ-synuclein (gSyn), which are small proteins highly conserved and highly expressed in neurons. (George, 2001; Sung & Eliezer, 2007). aSyn and bSyn are widely expressed in the central nervous system including neocortex, striatum, hippocampus, thalamus, and cerebellum and are absent from peripheral tissues. In the other hand, gSyn is mostly found in the peripheral nervous system but can also be expressed in other tissues, such as in the brain and ovarian and breast cancer. (Lavedan, 1998; Sung & Eliezer, 2007).

SNCA, the encoding gene of aSyn, which is located on chromosome 4q22.1, has six exons encoding a 140 amino-acid protein (Ozansoy & Ba, 2013). Genome wide association studies and other gene-based approaches have implicated *SNCA* as a very significant genetic risk factor for some synucleinopathies. Nevertheless, while coding missense mutations and multiplication of the *SNCA* locus leads to familiar PD, the exact variants that contribute to sporadic PD remains unclear (Tagliafierro, 2016).

aSyn is an intrinsically disordered protein that has a molecular weight of 14 kDa when unfolded (Bourdenx et al., 2016). Its structure can be divided into three different regions as demonstrated in Figure 1.3: (i) residues between 1 and 60, the N-terminal domain, code for amphipathic α-helices; (ii) residues 61-95, the central region, contains the hydrophobic and highly amyloidogenic non-amyloid-beta component (NAC) region and, at last, (iii) the residues 96-140 make up the C-terminal region rich in acidic residues and prolines. The N-terminal and central regions comprise a membrane-binding domain, while the C-terminal region is thought to be responsible for the protein-protein and protein-small molecule interactions (Breydo et al., 2012). Additionally, the central domain is required for oligomerization and fibrillation of the protein, since if this region is deleted, aSyn loses its ability to form amyloid fibrils (Giasson et al., 2001).

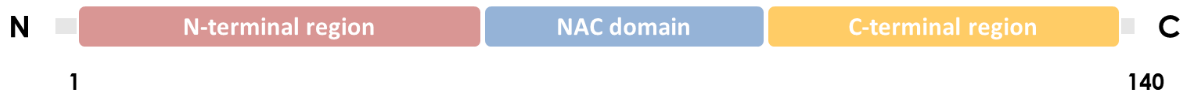

Figure 1.3 aSyn is a small protein divided into three regions.
Firstly, a N-terminal region and a NAC domain, both comprising a membrane-binding domain and, lastly, a C-terminal region putatively responsible for the protein interaction with proteins and small molecules.

In terms of structure, aSyn is naturally unfolded when in its monomeric form, however, under certain conditions, it is prone to aggregate (Tyson et al., 2016). The process of aggregation begins with the formation of relatively soluble oligomers that can self-assemble into insoluble amyloid fibrils, resulting in the formation of deposits (Figure 1.4; Mukaetova-Ladinska & McKeith, 2006). These deposits were first identified by Fritz Heinrich Lewy, which he named "*Negrishen Körperchen"* and are currently known as LB. PD and DLB are defined by the existence of intracytoplasmic LB in surviving neurons soma and LN in processes of degenerating nerve cells. (Dehay & Fernagut, 2016; Peelaerts & Baekelandt, 2016).

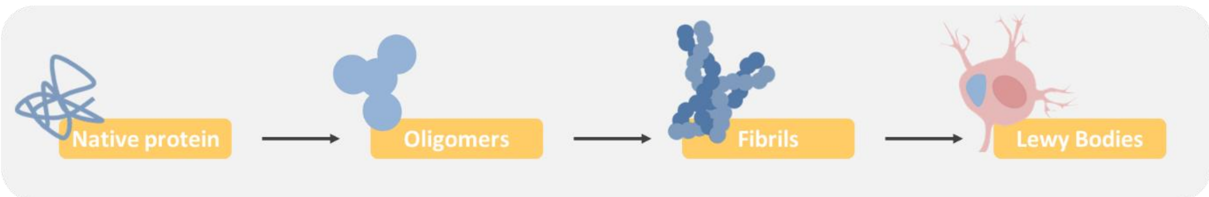

Figure 1.4 aSyn aggregation process culminates with the formation of Lewy Bodies.
aSyn is prone to form intracellular aggregates under certain, yet not completely understood conditions. The aggregation process starts with the formation of oligomeric structures, following fibril formation, and ending with the formation of inclusion bodies, known as Lewy Bodies.

Since aSyn comprises an intrinsically disordered region, corresponding to the C-terminal region, it is considered an intrinsically disordered protein (Bourdenx et al. 2016; Eftekharzadeh et al. 2016). These proteins seem to be highly sensitive to misfolding and aggregation, probably because of their unfolded nature (Eftekharzadeh et al., 2016). They do not fold into a specific secondary structure, as well as tertiary structure when under normal conditions, staying in a partially folded or even unfolded state (Oldfield & Dunker, 2014).

According with several studies, the major theory for aSyn toxicity is its tendency to aggregate. However, it is still unclear whether the toxicity is due to the LB or to the transient oligomeric species that are formed along the aggregation process (Volles & Lansbury Jr., 2003).

1.3.1 Alpha-synuclein – a multifunctional protein

The exact function of aSyn is still unknown, since it is involved in several cellular processes and molecular interactions, especially at presynaptic sites. Although, it is thought to play a role in maintaining a supply of synaptic vesicles, axonal transport and DA synthesis and metabolism (Sidhu et al., 2004; Dunning et al., 2012).

aSyn is mostly present at presynaptic terminals and a role in synaptic plasticity has already been envisioned. Indeed, aSyn may regulate synaptic vesicle mobilization at nerve terminals. Cabin et al. found that cultured hippocampal neurons, where aSyn expression was knocked down, had fewer synaptic vesicles when compared with the control neurons, particularly in the reserve pool (Cabin et al., 2002). Similarly, the levels of synapsin, a protein essential for synaptic vesicle recycling, decreased in cells where aSyn was depleted, suggesting a role of aSyn in genesis or maintenance of the reserve pool of synaptic vesicles (Sidhu et al., 2004).

Regarding the aSyn effects on synapses, other studies demonstrated that aSyn has a role in the assembly of the soluble N-ethylmaleimide sensitive factor (NSF) attachment receptors (SNARE)-complex. This process is essential for several membrane fusion events, indicating a function of aSyn in synaptic vesicle docking and fusion. The SNARE-complex is responsible for zipping the vesicles onto the plasma membrane, which will then undergo fusion followed by synaptic stimulation (Lautenschläger et al., 2017). However, there is still controversy on how aSyn acts on this complex. A study developed by Burré et al. demonstrated that aSyn induces an increase in SNARE-complex assembly (Burré et al., 2010), while others authors defend that aSyn has a negative regulatory function (Darios et al., 2010; Thayanidhi et al., 2010).

Recently, aSyn was proposed to be a curvature-sensing and stabilizing protein, i.e., aSyn is able to sense membrane curvature and stabilize it by inserting its amphipathic helix into the lipid surface (Varkey et al. 2010; Middleton & Rhoades, 2010; Lautenschläger et al. 2017). Nuclear magnetic resonance studies revealed that aSyn could bind to lipid membrane through its N-terminal and NAC domain, possibly tethering two vesicles together or vesicles to the plasma membrane through a double-anchor mechanism, facilitating exocytosis and endocytosis (Fusco et al., 2016). Regarding neurotransmitters release, aSyn function is also debatable, with studies showing an inhibitory effect on neurotransmitter release (Larsen et al., 2006; Gureviciene et al., 2007; Nemani et al., 2010; Scott et al., 2010; Wu et al., 2010; Janezic et al., 2013) and others showing a neurotransmitter release increase (Liu et al., 2004; Watson et al., 2009). Finally, aSyn has also been suggested to have an effect in axonal transport of synaptic vesicles by interacting with numerous proteins that can bind or are a part of the cytoskeleton (Sidhu et al., 2004).

1.3.2 *SNCA* Familial Mutations

PD associated with *SNCA* shows an autosomal dominant inheritance pattern with an early onset and typically develops rapidly. Triplication of the genomic region containing *SNCA* has been described as a cause of PD in several families; nevertheless, *SNCA* duplications have been reported as a more common cause of familial and sporadic PD. These duplications and triplications of the *SNCA* locus cause early-onset PD with the severity, as well as the age of onset, correlating with the number of *SNCA* copies, suggesting a gene-dose effect (Hernandez et al., 2016).Until now, six mutations have already been identified, being the A53T mutation the first acknowledged, followed by A30P and E46K. On the other hand, the G51D, A53E and H50Q mutations were recently identified (Table 1.1; Pasanen et al. 2014). The known mutations are present in the N-terminal region of the protein (Figure 1.5), highlighting the importance of this domain in the pathological dysfunction of aSyn (Xu & Pu, 2016).

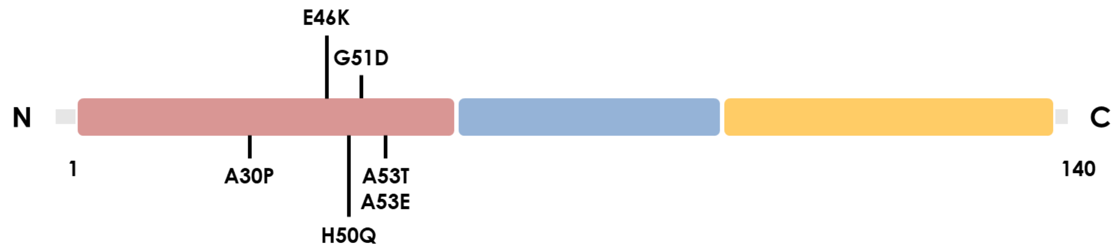

Figure 1.5 Schematic representation of the identified aSyn familial mutations.
Six *SNCA* mutations have already been identified, being all of them in the N-terminal region.

1.3.3 Alpha-synuclein Post-Translational Modifications: Phosphorylation

Post-translational modifications are critical for the function and the structural properties of proteins. aSyn within LBs is subjected to several modifications including phosphorylation, glycation, ubiquitination, cross-linking, truncations and nitration, facilitating misfolding and triggering oligomerization and, consequently, fibrillation (Oueslati et al., 2010; Muntané et al., 2012). Evidences from different models, and biochemical and biophysical studies suggest that phosphorylation of aSyn may play an important role in the regulation of its own structure, membrane binding, oligomerization, fibril formation, LB formation and neurotoxicity *in vivo* (Oueslati et al., 2010).

Table 1.1 Description of aSyn familial mutations and respective clinical features observed.

aSyn Mutation	*SNCA* Alteration	Onset	Clinical Features	Reference
A30P	G>C, residue 88	60-80 years	Cognitive impairment was found in 2 of the 4 patients carrying the mutation, with no other non-motor features Similar to typical PD	(Krüger et al. 1998; Petrucci et al. 2016; Kasten & Klein, 2013)
E46K	G>A, residue 188	60-70 years	Severe parkinsonism with dementia, hallucinations, fluctuations of consciousness and cognitive decline	(Zarranz et al., 2003)
H50Q	T>G, residue 150	55-60 years	Bilateral tremor at the age of 60, with micrographia, slow movements and problems turning Later, presence of rigidity and bradykinesia, apathy, anxiety and mild cognitive impairment	(Appel-cresswell et al., 2013; Proukakis et al., 2013)
G51D	G>A, residue 152	20-60 years	Motor fluctuations, mild to moderate response to L-3,4-dihydroxyphenylalanine (L-DOPA) and a L-DOPA-induced dyskinesia, psychiatric signs, pyramidal tract involvement with a rapid progression of the disease	(Lesage et al., 2013; Petrucci et al., 2016)
A53E	C>A, residue 158	30-60 years	Numbness and occasional hypotensive attacks The phenotype progressed slowly to a parkinsonian syndrome associated with severe spasticity, myoclonic jerks and psychiatric disturbances	(Pasanen et al., 2014; Petrucci et al., 2016)
A53T	G>A, residue 209	40-60 years	Rapid progression and variable occurrence of psychiatric, cognitive, and autonomic disorders	(Polymeropoulos et al., 1997; Petrucci et al., 2016)

Under normal conditions, only 4% of aSyn is constitutively phosphorylated at serine 129 (S129), however, approximately 90% of the protein is phosphorylated at S129 in pathological inclusions in post-mortem brain samples, being this phosphorylation the most abundant aSyn modification in LBs (Anderson et al. 2006; Waxman & Giasson, 2011; Popova et al. 2015; Oueslati, 2016). These numbers corroborate the hypothesis that aSyn phosphorylation may play a role in protein aggregation, stability and toxicity (Samuel et al., 2016).

High levels of aSyn phosphorylated at serine 87 (S87) in synucleinopathies were also reported (Paleologou et al., 2010). Following studies also revealed that aSyn can be phosphorylated at tyrosine 125, 133 and 136 (Y125, Y133 and Y136) and that phosphorylation at these sites suppresses aggregation and toxicity induced by phosphorylated S129 (Oueslati et al., 2010). Human brains also revealed that aSyn could be phosphorylated at tyrosine 39 (Y39) and that phosphorylation at this site, as well as in Y125, had no correlation between increased levels of phosphorylation and the pathological condition (Figure 1.6;Tenreiro et al. 2014).

Distinct *in vitro* phosphorylation experiments demonstrated different results on aSyn aggregation, with some studies revealing increased fibril formation, while others showed a decrease (Fujiwara et al., 2002; Paleologou et al., 2008; Schreurs et al., 2014). Additionally, the use of phosphomutants that either promote or prevents phosphorylation in several *in vivo* models also presented contradictory results (Samuel et al., 2016). Studies in transgenic mouse and *Drosophila melanogaster* revealed a pathogenic role for aSyn phosphorylation, while studies in *Caenorhabditis elegans* and rats showed a protective effect against neuronal dysfunction (Chen & Feany, 2005; Gorbatyuk et al. 2008; Kuwahara et al. 2012). The function of phosphorylation is not the only subject needing elucidation, the stage when this modification occurs is also a matter of debate. Some evidences suggest that aSyn phosphorylation occurs after fibrillization, possibly to clear aSyn aggregates (Samuel et al., 2016).

In yeast, overexpression of S129A aSyn, a mutant that blocks phosphorylation at S129, caused an increase in the growth defect provoked by wild-type (WT) aSyn; however, the S129E mutant, which mimics phosphorylation at the same residue, had no effect in cell growth, suggesting that the lack of phosphorylation of S129 enhances aSyn toxicity. Furthermore, the S129A mutation also increases the percentage of cells with aSyn inclusions, suggesting that phosphorylation blockade leads to an increase in trafficking defects caused by WT aSyn (Sancenon et al., 2012; Tenreiro et al., 2014a).

1.3.4 Mechanisms of alpha-synuclein toxicity

The precise cellular events that lead to the loss of dopaminergic neurons through aSyn action are still poorly understood, however, the generation of reactive oxygen species (ROS) comprises a leading hypothesis, since it can cause oxidative neuronal damage. A strong evidence of oxidative stress in the nigra of PD patients was provided by post-mortem studies, revealing an increase in iron content, mitochondrial dysfunction, oxidative damage to DNA, proteins, and lipids, among others (Junn & Mouradian, 2002).

Figure 1.6 Schematic representation of the aSyn residues prone to suffer phosphorylation. Almost every putative phosphorylation site is localized in the C-terminal region of the protein, except for Y39 and S87

Mitochondria are crucial for the synthesis of adenosine triphosphate (ATP), reduction of oxidative stress, Ca^{2+} storage, lipid metabolism and neuronal survival. Studies conducted by Parihar et al. revealed that aggregated aSyn binds to mitochondria in a concentration-dependent manner (Parihar et al., 2009). Moreover, other studies presented that aSyn, either WT or mutant, was able to interact with membranes being crucial for aSyn cytotoxicity (Smith et al. 2005; Volles & Lansbury Jr, 2007). Impairment of mitochondrial function has been associated with both WT and mutant aSyn overexpression, but the exact interaction between aSyn and mitochondria is still under debate (Wales et al., 2013). Numerous researches reported that mitochondrial function can be altered as a result of aSyn binding to its inner membrane, where it can associate with mitochondrial complex I, decreasing the mitochondrial activity (Liu et al., 2009; Winklhofer and Haass, 2010). Mitochondrial complex I is responsible for catalyzing the first step in the electron transport chain which, in turn, is the main source of ROS (Turrens, 2003). The binding between aSyn and complex I is followed by cytochrome c release to cytosol, and increased in Ca^{2+} and ROS levels, culminating in cell death (Figure 1.7). The precise mechanisms of how complex I inhibition can induce cell death are still poorly understood. Nonetheless, three pathways have been proposed: (i) inhibition of complex I can induce mitochondrial bioenergetics defects, decreasing ATP biosynthesis; (ii) complex I activity inhibition may increase reductive stress, reducing molecular oxygen or activating redox sensitive signaling pathways, possibly increasing cytochrome c intermembrane pool, activating mitochondrial-dependent apoptotic machinery; (iii) impaired substrate oxidation at complex I can imbalance the NAD+/NADH ration, resulting in inhibition of NAD+-dependent enzymes and consequent mitochondrial homeostasis dysregulation (Perier et al., 2005; Imaizumi et al., 2015).

Besides, overexpression of the A53T aSyn mutant in neurons leads to an early time of onset of these events (Devi et al., 2008; Parihar et al., 2008). Alterations in ATP production and differences in mitochondrial membrane potential have also been reported (Parihar et al., 2009; Banerjee et al., 2010).

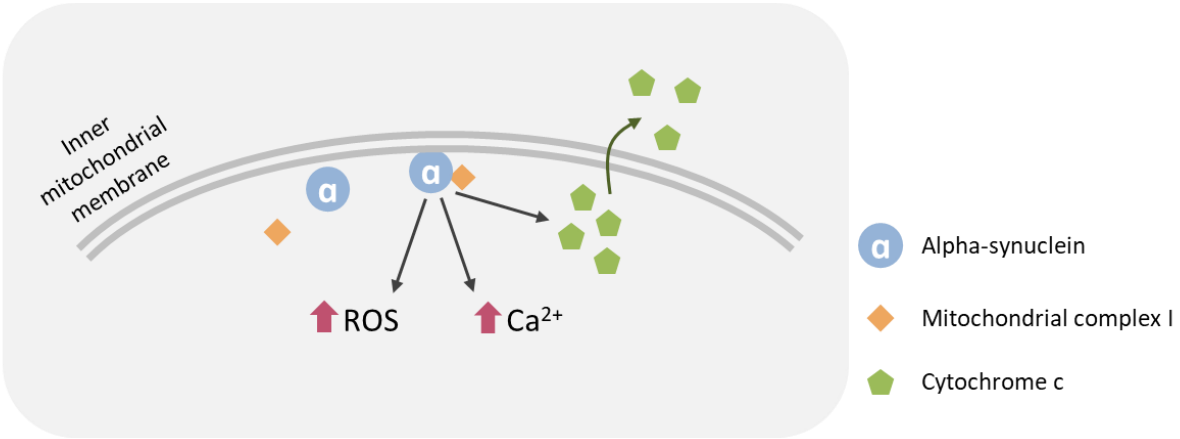

Figure 1.7 aSyn affects mitochondrial function by interacting with mitochondrial complex I.
aSyn is believed to bind to the inner mitochondrial membrane, where it associates with mitochondrial complex I. This assembly results in an increase of ROS production and Ca^{2+} levels and in the release of cytochrome c, culminating with cell death.

Abnormalities in the balance between mitochondrial fusion and fission, vital for the maintenance of mitochondrial activity, can also contribute to neuron dysfunction and cell death. Hence, mitophagy, the delivering of damaged mitochondria to the lysosome, is required for the turnover and removal of dysfunctional mitochondria, avoiding the generation and accumulation of ROS (Villacé et al., 2017). Both WT and A53T aSyn promote an up-regulation of mitophagy leading to an immense mitochondrial degradation, bioenergetic deficits and neuronal death (Chinta et al., 2011; Choubey et al., 2011).

The formation of aSyn aggregates, specially its mutant variations, is linked to an increase in ROS production and, consequently, oxidative stress, which can be defined as a disequilibrium between the levels of ROS produced and the system capability to detoxify the reactive intermediates, creating a hazardous state and contributing to cellular damage (Dias et al., 2013). *In vitro* and *in vivo* studies support the belief that an increased oxidative stress in the brain promotes aSyn aggregation, possibly causing modifications in the nuclear membrane, and subsequent aSyn translocation to the nucleus (Paxinou et al., 2001; Xu et al., 2006). Overall, ROS promotes aSyn aggregation, while overexpression of aSyn leads to an increase in ROS levels, creating a cycle that leads to neurodegeneration (Junn & Mouradian, 2002; Winklhofer & Haass, 2010). Recently, studies revealed that aSyn is in fact not localized to mitochondria, but to a specific domain of the endoplasmic reticulum (ER), called the mitochondria-associated ER membranes (MAM; Guardia-Laguarta et al. 2015; Paillusson et al. 2017). Mitochondria communicates with the ER through MAM to regulate several cellular processes, such as Ca^{2+} homeostasis, mitochondrial transport and biogenesis, mitochondrial ATP production, lipid metabolism, ER stress, ubiquitin-proteasome system (UPS) and autophagy (Paillusson et al., 2017). Alterations in the ER-mitochondria contact can cause deregulation of Ca^{2+} homeostasis, resulting in an inappropriate protein folding, metabolic alterations and apoptosis (Guardia-Laguarta et al., 2015).

ER stress plays a crucial role in the development of several neurodegenerative diseases. ER stress is usually caused by accumulation of misfolded proteins within the ER. To overcome ER stress, cells activate an unfolded protein response (UPR), which protects cells from misfolded proteins accumulation, by ceasing protein synthesis and activating mechanisms capable of decreasing protein accumulation. In this case, proteins are translocated to the cytoplasm, where they undergo degradation by the proteasome, through a process named ER associated degradation. However, if ER stress persists, a cell death cascade is activated (Cooper et al. 2006; Doyle et al. 2011; Colla et al. 2012).

Misfolded aSyn could generate ER stress by, either interacting with ER chaperones or by disturbing ER function, e.g., by affecting Ca^{2+} metabolism (Coune et al. 2012). Colla et al*.* proposed a sequence of events connecting aSyn, ER stress and neurotoxicity i.e., low levels of aSyn in the ER forms aSyn oligomers that assemble leading to the formation of insoluble aSyn aggregates. This compromises the ER membranes integrity and exposes portions of the ER lumen to the cytosol, resulting in chronic ER stress and, subsequently, cell death (Colla et al. 2012).

Moreover, in yeast, aSyn was reported to inhibit trafficking between ER and the Golgi complex, strengthening cell toxicity and cell loss. Decrease of the ER-to-Golgi transport results in an accumulation of protein in the ER, increasing ER stress (Cooper et al., 2006).

Originally, aSyn was described as a nuclear and pre-synaptic protein (Maroteaux et al. 1988). aSyn mutations associated with PD, namely A30P, G51D and A53T, presented increased nuclear localization in comparison to WT aSyn (Kontopoulos et al., 2006; Fares et al., 2014). Deregulation of transcription is recognized as an important mechanism in neurodegeneration; indeed, the overexpression of either WT or mutated aSyn leads to significant changes in the expression of genes involved in neurotransmission, stress response, apoptosis, and transcription factors (Baptista et al., 2003). Regulation of gene expression also depends on transcription factors distribution within the cell and some studies revealed that transcription factors, as well as their regulatory kinases, were present in aSyn aggregates, hence leading to transcription deregulation (Desplats et al., 2011; Wales et al., 2013).

aSyn can also bind directly to histone-free and transcriptionally active DNA, changing its stability and conformation (Hegde & Rao, 2003). Moreover, by increasing ROS levels within the nucleus, glycated aSyn induces histone glycation and, subsequently, DNA damages (Padmaraju et al., 2011).

Regarding neurotransmission, it is known that the synthesis of DA comprises a rate-limiting step, which is the conversion of tyrosine into L-DOPA by phosphorylated tyrosine hydroxylase (TH) before being converted into DA by DOPA decarboxylase (DDC). TH is only activated when phosphorylated, and this process of phosphorylation and dephosphorylation is highly important in the regulation of DA biosynthesis (Kumer & Vrana, 1996). aSyn colocalizes with and binds to the dephosphorylated form of TH, keeping it in its inactive form and, subsequently, causing a decrease in enzymatic activity and DA synthesis (Figure 1.8, Perez et al. 2002).

1.3.5 Alpha-synuclein clearance

Unmodified aSyn is degraded via UPS and chaperone-mediated autophagy, whereas insoluble and aggregated aSyn is degraded through macroautophagy (Cook & Petrucelli, 2010; Ebrahimi-fakhari et al. 2011). The presence of aSyn, ubiquitin and proteasomal subunits within LBs reinforces a relation between aSyn and proteasomal degradation dysfunction in PD pathogenesis (Betarbet et al., 2005).

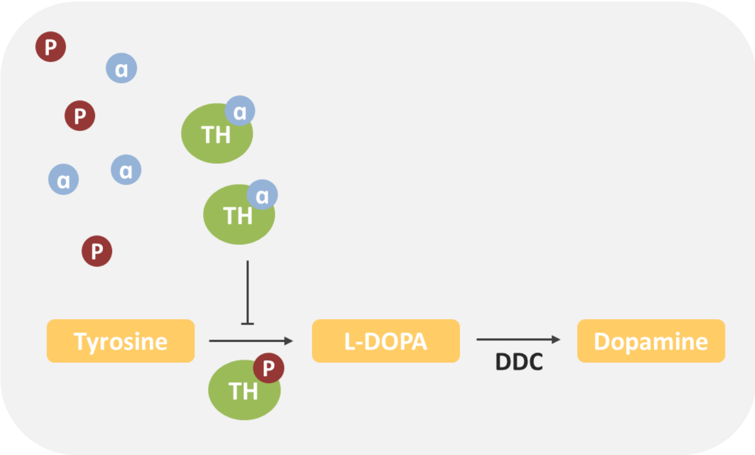

Figure 1.8 Dopamine synthesis is inhibited by aSyn.
TH phosphorylation is required for conversion of tyrosine into L-DOPA, a crucial step for DA synthesis. aSyn binds to TH, hindering TH activation and, consequently, ceasing the conversion of tyrosine into L-DOPA (Perez et al., 2002)

1.3.5.1 Alpha-synuclein degradation through ubiquitin-proteasome system and the Rsp5 agent

The UPS is a multicomponent complex system capable of recognizing and degrading unnecessary, misfolded, mutated and oxidatively damaged proteins (Betarbet et al., 2005; Wijayanti et al., 2015).

Proteins to be degraded are first marked by covalent attachment of a polyubiquitin chain to a lysine residue on the substrate. This process occurs through a series of enzyme-mediated reactions. The ubiquitin-activated enzyme (E1) is responsible for ubiquitin activation, through an ATP-dependent manner. The activated ubiquitin is transferred to a ubiquitin conjugating enzyme (UBC, also known as E2) and, in the end, E2 associates with a ubiquitin-protein ligase (E3), that may or may not have the substrate already bound. Ubiquitin is then transferred to a lysine residue of the substrate, which is then degraded by a proteolytic complex – 26S proteasome (Figure 1.9; Weissman 2001; Betarbet et al. 2005) The selectivity of ubiquitination and the recognition of substrates are mediated by E3s, either alone or in combination with E2s. Additionally, the type of ubiquitin conjugation determines the destiny of the ubiquitylated proteins, i.e., a single ubiquitin tag does not target a protein for degradation, whereas a polyubiquitin chain does. A minimum of four ubiquitin molecules is required to target proteins for degradation (Weissman, 2001).

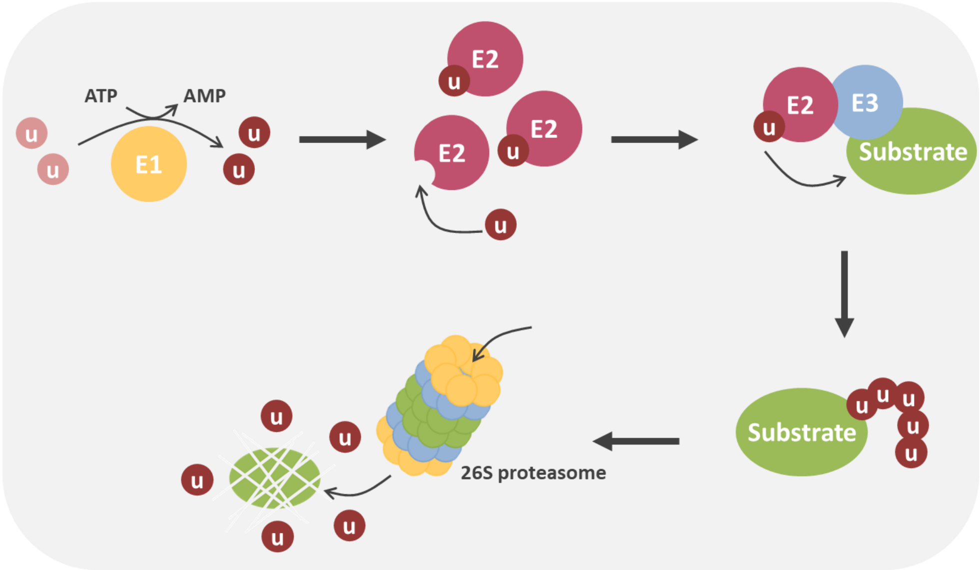

Figure 1.9 Ubiquitin-proteasome system pathway.

The UPS pathway consists of a series of enzymatic reactions: E1 activates ubiquitin, which is then conjugated with E2. E2 interacts with E3, which is bound to the substrate, transferring the ubiquitin to the substrate, which marks the protein for degradation by the 26S proteasome. (u – ubiquitin)

Two distinct families of E3 ligases have been identified until now, namely the Really Interesting New Gene (RING) and the Homologous to the E6-AP Carboxyl Terminus type (HECT), which differ only in the way they transfer ubiquitin from E2 to the substrate (Weissman, 2001). For the present study, the focus will be the HECT family. HECT is a domain of circa 350 amino-acids and is found at the C-terminus of proteins. The majority of the HECT ligases contain protein-protein or protein-lipid interaction domains located in the N-terminus of the protein and, based on this domain architecture, the human HECTs can be divided in three groups: neuronal precursor cell-expressed developmentally down-regulated gene 4 (Nedd4) family, HERC family and other HECTs. The Nedd4 family members have an N-terminal C2 domain responsible for phospholipid binding, two to four WW domains that recognize and bind to substrate proteins and a C-terminal HECT domain. (Rotin & Kumar, 2009; Wijayanti et al. 2015). The Nedd4 family of enzymes binds specifically to substrates containing proline-rich motifs, one of which was found in aSyn (Tofaris et al., 2011).

Rsp5 is the only *Saccharomyces cerevisiae* ortholog of NEDD4, and it is known to be involved in numerous cellular functions, such as mitochondrial inheritance, chromatin remodeling, regulation of transcription and endocytosis, sorting of numerous transmembrane proteins and of cargo into multivesicular bodies from endocytic vesicles or from the Golgi apparatus to endosomes. Usually Rsp5 modifies its protein target at the plasma membrane or Golgi apparatus with ubiquitin chains linked to lysine 63, targeting the protein to being degraded by the endosomal-vacuolar pathway (Rotin & Kumar, 2009). Tofaris et al. stated that Rsp5 promotes aSyn degradation through the endosomal-vacuolar pathway, proving that Rsp5 ligase activity is essential for aSyn degradation and protects from inclusion formation (Tofaris et al., 2011).

1.3.5.2 Autophagy and the importance of an acidic lysosomal environment

Autophagy is a self-degradative pathway, crucial for yeast survival during nutrient deprivation, since it is responsible for macromolecules recycling, providing nutrients and energy. Autophagy substrates comprise aggregate-prone cytoplasmic protein associated with neurodegenerative diseases, such as aSyn (Rubinsztein et al., 2011). Three main forms of autophagy were described: macroautophagy, microautophagy and chaperone mediated autophagy (Cuervo, 2004), differing from each other's in the mechanisms responsible for lysosomal delivery, whereas the final step of lysosomal degradation is common to all forms (Wolfe et al., 2013).

Macroautophagy is the principal mechanism by which aSyn, and other long-lived proteins, are degraded, as well as the only mechanism responsible for mitochondria recycling (Vogiatzi et al., 2008). This process comprises the formation of autophagosomes that fuse with lysosomes to form autophagolysosomes, which content is further degraded by acidic lysosomal hydrolases (Dehay et al., 2010). The presence of aSyn aggregates in the PD patient's brains suggests a deficiency in the protein handling system, which can be confirmed through the evidence of autophagic vesicles accumulation with a lysosomal depletion, as well as with the presence of key components of the autophagosomes-lysosome pathway, such as the LC3 protein, as part of LBs (Dehay et al. 2010; Bourdenx & Dehay, 2016). Moreover, changes in the morphology of the lysosomal system have been observed in PD models (Stefanis et al., 2001). Bourdenx and Dehay proposed that LBs could be originated from defective lysosomes or undegraded autophagic vesicles through the deposition of other undegraded autophagic vesicles during the disease progression (Bourdenx & Dehay, 2016).

Defective lysosomal function is a major factor in neurodevelopmental diseases and has been recognized as a key factor in the pathogenesis of some late-age onset disorders, including PD (Colacurcio & Nixon, 2016). Lysosomes degradation occurs through the action of several hydrolases with an optimum function in acidic conditions (pH 4-5) within lysosomes in order to activate the mentioned enzymes (Wolfe et al., 2013). The lysosomal acidification is maintained by the vacuolar ATPase (v-ATPase), which is an ATP dependent proton pump required to regulate pH homeostasis in organelles (Diciccio & Steinberg, 2011). They are composed by 14 different subunits that are organized into two domains: V_1, a hydrolytic domain, and V_0, a proton-translocation domain (Forgac, 2007). The v-ATPase actively transports H^+ ions into the lysosome using energy from ATP hydrolysis, making the lumen more acidic (Figure 1.10; Colacurcio & Nixon, 2016). Vacuolar acidification mediated by v-ATPase has been identified as a positive regulator of mitochondria stability and lifespan in yeast (Hughes & Gottschling, 2012). However, an increase in lysosomal pH was shown to decrease lysosomal degradation of toxic proteins and lipids, trailed by downregulation of lysosomal enzyme maturation and activity (Lee et al., 2013).

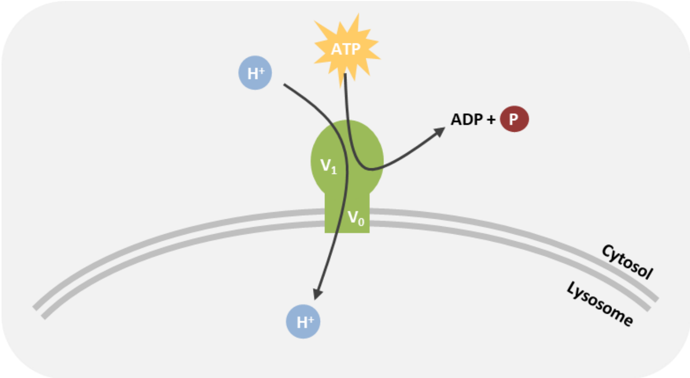

Figure 1.10 Vacuolar ATPase activity involved in lysosomal pH maintenance.
The v-ATPase uses metabolic energy originated from ATP hydrolysis to drive hydrogen proton into the lysosome, maintaining the lysosomal pH.

1.4 CDNF - a non-conventional neurotrophic factor

Neurotrophic factors (NTFs) are secreted proteins that regulate the life and death of neurons during development, responsible for neurons induction, specification, survival, and maturation, as well as neurite growth and branching. Some NTFs can act in the adult brain, supporting, protecting, and repairing mature neurons. Since PD is caused by the degeneration of dopaminergic neurons, many NTFs have been explored for their neurotrophic and protective effects (Sullivan and Toulouse, 2011; Voutilainen et al., 2015; Lindahl et al., 2017) .

Mesencephalic astrocyte-derived neurotrophic factor (MANF) and cerebral dopamine neurotrophic factor (CDNF) comprise a conserved protein family with neurotrophic activities. MANF was first identified by Petrova et al. from a culture medium of a rat astrocyte cell line as a novel neurotrophic factor specific for dopaminergic neurons (Petrova et al., 2003). CDNF, a vertebrate specific paralogue of MANF, was identified by bioinformatics and biochemical approaches (Lindholm et al., 2007). Both neurotrophic factors are structurally different from the classical NTFs and its cytoprotective mechanism of action is still unclear, in contrast with other known NTFs (Lindahl et al., 2017). Several mechanisms of action have been proposed for CDNF, such as actions on mitochondrial complex I, ER stress, oxidative stress, and anti-apoptotic effect. The analysis of CDNF and MANF structure revealed that both proteins can have a double mechanism of action (Airavaara et al. 2012a).

The neurotrophic effects of both CDNF and MANF have been described in different animal models of PD. CDNF had no effects in rat and mouse DA neurons in healthy rodents (Voutilainen et al., 2015). However, when tested in rat 6-hydroxydopamine (6-OHDA) model of PD, CDNF was able to protect and repair DA neurons (Lindholm et al., 2007). In mice treated with 1-methyl-4-phenyl-1,2,3,6-tetrahydropyridine (MPTP), CDNF was shown to protect against MPTP toxicity and to restore motor function (Airavaara et al. 2012b).

Both CDNF and MANF are mainly found in the ER suggesting that their most important function is to regulate ER stress and UPR, however their mechanism of action is still unknown (Voutilainen et al., 2015). Its effect in the ER is corroborated by the fact that extracellular CDNF only rescues neurons degenerated via ER stress (Voutilainen et al., 2015). Also, a study performed by Zhou et al. revealed that pre-treatment with CDNF was able to reduce the expression levels of proteins related to ER stress (Zhou et al., 2016).

Recently, CDNF was shown to activate the survival promoting phosphatidylinositol 3 kinase (PI3K)-Akt signaling pathway which is activated by neurotrophins and growth factors receptors. (Figure 1.11; Voutilainen et al., 2017). In mammalian cells, phosphatidylinositol 3,4,5-triphosphate (PIP3) generation at the plasma membrane is crucial for regulating proliferation and survival by PI3K-Akt signaling pathway. PI3K generates PIP3, while phosphatidylinositol 3-phosphatase (PTEN) degrades this lipid. PIP3 activates Akt which, in turn, activates the kinase mammalian target of rapamycin (mTOR; Rodríguez-Escudeiro et al., 2005). This pathway promotes cell growth, survival and differentiation, and is also capable of downregulating apoptotic signals. (Heras-Sandoval et al., 2014).

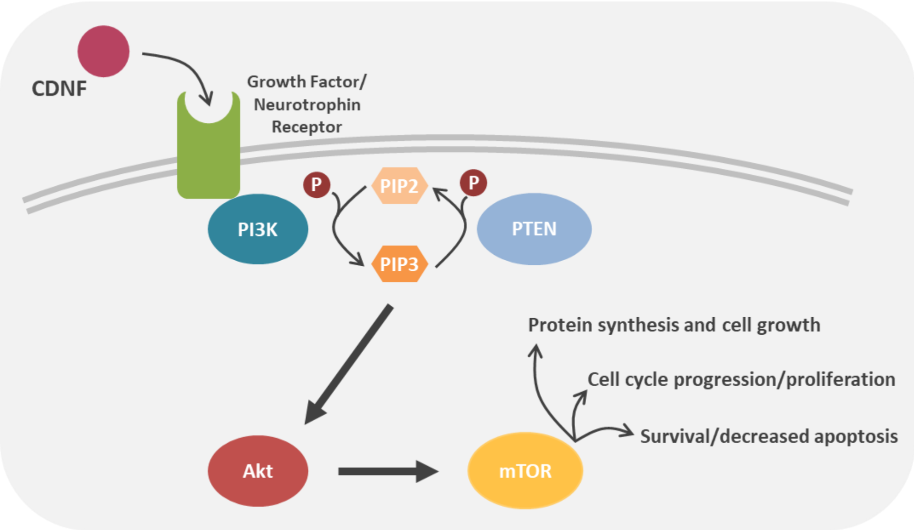

Figure 1.11 Basic schematic representation of the PI3K-Akt signalling pathway.
CDNF was found to activate the survival PI3K-Akt signalling pathway, leading to activation of mTOR which, consequently, alters several cellular pathways.

Latge et al. found that CDNF prevents the toxic effects induced by aSyn oligomers in dopaminergic neurons, however they did not find any evidences that CDNF interacts directly with aSyn, either in monomeric or oligomeric form. In this sense, three different possible CDFN mechanisms of actions were proposed: (i) CDNF binds to a transmembrane receptor, as other NTFs, activating survival pathways that suppress aSyn toxic effects; (ii) CDNF stimulates cellular clearance pathways and (iii) CDNF interacts with bcl-2-like protein X (BAX), inhibiting apoptosis (Latge et al., 2015).

1.5 Yeast as a cellular model to study Parkinson's Disease

Saccharomyces cerevisiae is a single-celled eukaryote, which contains membrane-bound organelles, e.g., the nucleus, the endomembrane system and mitochondria (Duina et al., 2014). The unique features of *S. cerevisiae* granted its establishment as a robust model system in biology. These features include its short generation time, easy handling, non-pathogenic nature, inexpensive culture conditions and its amenability for genetic manipulation (Menezes et al., 2015). Its generation time is about 90 minutes, under optimal laboratory conditions, through a budding process, in which small daughter cells bud of the mother cell (Duina et al., 2014). Thus, sporulation of a particular diploid cell generates different combinations of genotypes with desired genetic traits (Menezes et al., 2015). Molecular genetics is supported by the high efficient homologous recombination pathway which allows to insert, delete or mutate a genomic sequence up to the chromosome level easily (Sugiyama et al., 2009).

Yeast cells have similarities to human cells, sharing fundamental aspects of eukaryotic cell biology, namely the mechanisms of protein folding, quality control and degradation, the components involved in the secretory pathway and vesicular trafficking, mitochondrial dysfunction and oxidative stress and the mechanisms underlying cell death and survival. *S. cerevisiae* was the first eukaryote to have its genome sequenced (Goffeau et al., 1996) and about 60% of the its genes display sequence homology to a human orthologue and, of the human disease-related genes, over 25% have a homologue in yeast (Franssens et al., 2013). Models can be based on the heterologous expression of the human gene if the gene underlying the disease is absent in the yeast genome, or through the study of the function and pathological role of the yeast corresponding gene, provided that it is present in the yeast genome (Tenreiro & Outeiro, 2010).

Yeast models have been proven useful to understand the molecular mechanisms underlying PD, as well as other synucleinopathies, since various features of PD can be reproduced in this model (Tenreiro & Outeiro, 2010). The first yeast model of PD was based on the heterologous expression of human aSyn, which lacks a yeast ortholog. In the yeast model developed by Outeiro and Lindquist, yeast cells express WT aSyn or aSyn mutants fused with green fluorescent protein (GFP) under regulation of the *GAL1* promoter. This promoter is required for galactose catabolism and is only activated in the presence of this sugar (Outeiro & Lindquist, 2003).

The increase in aSyn mediated toxicity is dose-dependent. Indeed, Petroi et al. demonstrated that with only three integrated copies of WT aSyn, growth inhibition and inclusion formation was already visible (Petroi et al., 2012). Microscopy analysis revealed that aSyn is localized in the plasma membrane when one single copy is being expressed, while simply by doubling the number of aSyn copies, aSyn localization shifts, forming cytoplasmic inclusions. Moreover, the number of aSyn copies is also correlated with cytotoxicity, since with one single copy, there is no significant effect on cytotoxicity, meanwhile, with only two copies, cytotoxicity increases drastically (Figure 1.12; Outeiro & Lindquist, 2003; Gitler 2008) The formation of aSyn cytoplasmic inclusions in yeast cells is consistent with previous studies in primary cortical neurons (Mclean et al., 2001). Expression of aSyn in yeast cells is also known to induce oxidative stress and mitochondrial dysfunction and to affect vesicle trafficking (Popova et al., 2015).

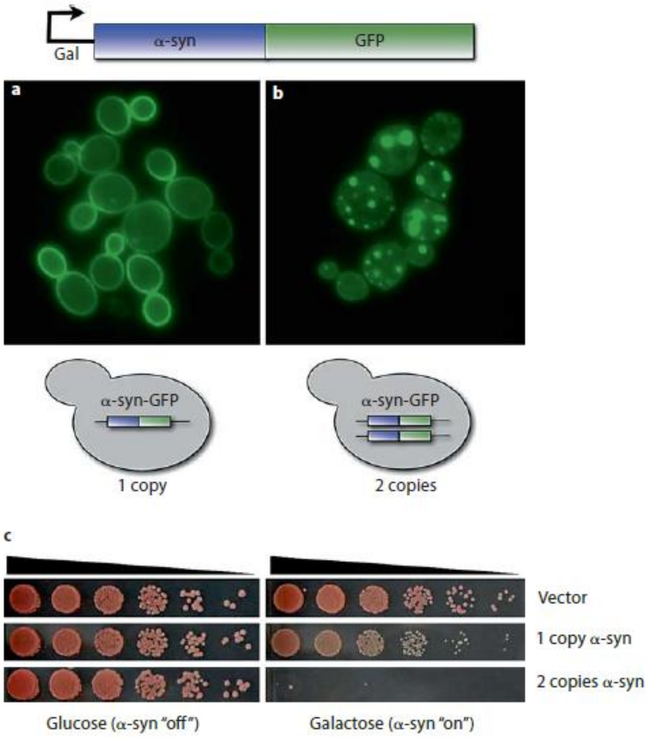

Figure 1.12 Effects of aSyn expression in yeast cells.
In the presence of a single aSyn copy, aSyn strongly localizes to the plasmatic membrane **(A)**, whereas with only two copies of aSyn, its cellular localization changes drastically, forming cytoplasmic inclusions **(B)**. **C)** Cell viability is not significantly affected in cells expressing only one copy of aSyn, meanwhile, when expressing two or more copies, cell growth is completely inhibited (Gitler, 2008).

1.6 Aims

PD is characterized by aSyn aggregation, culminating with the formation of Lewy Bodies. aSyn familial mutations, as well as duplications and triplications, are associated with familial forms of PD. It is known that 90% of aSyn present in pathological inclusions is phosphorylated at S129, and several other phosphorylation sites have already been identified. However, it is still unclear how phosphorylation in different residues modulates distinct aSyn mechanisms of toxicity. In this context, this study aims to clarify the interplay between phosphorylation in distinct aSyn residues using yeast as a cellular model of PD. Moreover, this study also intends to characterize the mechanisms of toxicity for each aSyn familial mutation.

Yeast strains expressing aSyn familial and phosphomutants will be characterized with respect to aSyn cytotoxicity through evaluation of cell viability assessed by spotting assays and flow cytometry. aSyn protein levels, aggregation and protein clearance will be evaluated for all mutants. Known pathways of toxicity associated with aSyn will also be analysed, such as ROS production and autophagy impairment.

2 Materials and Methods

2.1 Yeast Strains and Plasmids

The genotypes of the yeast strains used in this project are described in Table 2.1. All the plasmids containing aSyn variations transformed in yeast cells, described in table 2.2 are under regulation of a *GAL1* promoter.

Table 2.1 Description of yeast strains used in this project

Yeast Strains	Genotype	Reference
W303.1A	MATa can1Δ100 his3Δ11,15 leu2Δ3,112 trp1Δ1 ura3Δ1 ade2Δ1	(Thomas and Rothstein, 1989)
BY4741	MATa his3Δ1 leu2Δ0 met15Δ0 ura3Δ0	(Brachmann et al., 1998)

2.2 *Escherichia coli* manipulation

2.2.1 *E. coli* growth conditions

E. coli cells were cultivated at 37ºC, the optimum growth temperature, in Luria Broth (LB; Sigma-Aldrich, St. Louis, MO, USA) media, supplemented with 2% agar or not, previously autoclaved. LB selective medium were supplemented with 150mg/L of ampicillin (Amp) or 100mg/L of kanamycin (Kan) after sterilization. *E. coli* cells were grown in the appropriated solid media at 37ºC, following storage at 4ºC and regular picking to keep the cultures fresh. For longer periods of storage, glycerol stocks were prepared. *E. coli* cells were inoculated in selective LB liquid media and grown over-night at 37˚C with agitation (220rpm) and the glycerol stocks were made with a 1:1 proportion of bacterial culture mixed with 50% (v/v) glycerol, and stored at -80˚C in cryovials.

2.2.2 *E. coli* transformation

DNA samples (50 to 100ng DNA) were added to 50µL of competent cells, which were then incubated on ice for 30 min. A heat-shock was done by a 40 sec incubation at 42˚C followed by a 2 min incubation on ice. A volume of 0.9mL of LB liquid media was added to the cells that were then incubated during 1 hour at 37˚C with agitation (220rpm). Cells were spun down during 1 min at 5000rpm, 850µL of media was removed, and the cells were plated on selective LB media, using glass beads. The plates were incubated over-night at 37˚C.

2.2.3 Plasmid DNA extraction

For plasmid isolation from *E. coli*, individual clones were inoculated in 3mL of selective LB liquid media and incubated over-night at 37˚C with agitation (220rpm). Using the NZYMiniprep kit (NZYTech, Lisboa, Portugal), the DNA was extracted according to the protocol given by the manufacturer, with the only alteration being the use of 35µL of purified water at 50ºC instead of elution buffer. DNA concentration and purity was assessed by NanoDrop2000/2000c Spectrophometer (Thermo Fisher Scientific Inc., Waltham, MA, USA). The DNA recovered was stored at -20˚C until further use.

Table 2.2 Description of the yeast plasmids used in this project

Plasmid Description	Type of plasmid	Selection mark	Reference
p426_Gal	Multicopy	URA3	(Mumberg et al., 1995)
p426_Gal_aSyn_WT_GFP	Multicopy	URA3	(Outeiro & Lindquist, 2003)
p426_Gal_aSyn_A30P_GFP	Multicopy	URA3	Host laboratory
p426_Gal_aSyn_E46K_GFP	Multicopy	URA3	Host laboratory
p426_Gal_aSyn_H50Q_GFP	Multicopy	URA3	This study
p426_Gal_aSyn_G51D _GFP	Multicopy	URA3	Host laboratory
p426_Gal_aSyn_A53E_GFP	Multicopy	URA3	Host laboratory
p426_Gal_aSyn_A53T_GFP	Multicopy	URA3	Host laboratory
p426_Gal_aSyn_Y39F_GFP	Multicopy	URA3	Host laboratory
p426_Gal_aSyn_S87E_GFP	Multicopy	URA3	Host laboratory
p426_Gal_aSyn_S87A_GFP	Multicopy	URA3	Host laboratory
p426_Gal_aSyn_Y125F_GFP	Multicopy	URA3	Host laboratory
p426_Gal_aSyn_S129D_GFP	Multicopy	URA3	Host laboratory
p426_Gal_aSyn_S129A_GFP	Multicopy	URA3	This study
p426_Gal_aSyn_Y39F_Y125F_GFP	Multicopy	URA3	Host laboratory
p426_Gal_aSyn_S87E_S129A_GFP	Multicopy	URA3	This study
p426_Gal_aSyn_S87A_S129D_GFP	Multicopy	URA3	This study
p426_Gal_aSyn_S87A_S129A_GFP	Multicopy	URA3	Host laboratory
p425_Gal	Multicopy	LEU2	(Mumberg et al., 1995)
pAG425_Gal_CDNF	Multicopy	LEU2	This study
pAG425_Gal_Cerulean_CDNF	Multicopy	LEU2	This study
pAG425_Gal_CDNF_DsRed	Multicopy	LEU2	This study
pRS415	Integrative	LEU2	Stratagene, La Jolla, CA
pRS415_RSP5_WT	Integrative	LEU2	(Haitani et al., 2008)

2.3 *Saccharomyces cerevisiae* manipulation

2.3.1 *S. cerevisiae* growth conditions

Culture media used to grow *S. cerevisiae* cells are described in table 2.3. For solid media, 3% bacteriological agar (HiMedia, Mumbai, India) was added to the media. All media was prepared with purified water and sterilized through autoclaving. For overall yeast cell growth, the Yeast Extract Peptone Dextrose (YNB) rich media was used, whereas for selective yeast growth, selective media was used according to the auxotrophic marks encoded by each plasmid, both at the optimum growth temperature of 30ºC. To grow yeast cells without plasmid expression, selective media was supplemented with glucose 2% (Glu; EMD Chemicals, San Diego, CA, USA) since gene expression is under the regulation of a *GAL1* promoter, which is repressed in the presence of glucose (Glu) as carbon source. To initiate protein expression, cells were grown in selective media supplemented with raffinose 1% (Raf; Sigma-Aldrich, St. Louis, MO, USA) to a final optical density (OD) of 0.6, after which protein expression was induced using selective media supplemented with galactose 1% (Gal; Sigma-Aldrich, St. Louis, MO, USA), activating the *GAL1* promoter. For clearance assays, after protein expression induction for 6 hours, expression was ceased by changing the media for selective media supplemented with Glu. Yeast cells plated in solid media were stored at 4ºC with regular pricking to ensure culture freshness.

Table 2.3 Culture media used for yeast growth

<table>
<tr><th></th><th>Culture Media</th><th>Components</th></tr>
<tr><td>Rich Media</td><td>Yeast Extract Peptone Dextrose (YPD)</td><td>Glucose 2% (EMD Chemicals, San Diego, CA, USA)
Peptone 1% (HiMedia, Mumbai, India)
Yeast Extract 2% (HiMedia, Mumbai, India)</td></tr>
<tr><td rowspan="3">Minimum Media; CSM (Complete Supplement Mixture)</td><td>CSM-URA</td><td>Yeast Nitrogen Base (YNB) without amino-acids 0.67% (Becton Dickinson, Franklin Lakes, Nova Jersey, USA)
CSM-URA 0.077% (MP Biomedicals, Illkirch, France)</td></tr>
<tr><td>CSM-LEU-URA</td><td>Yeast Nitrogen Base (YNB) without amino- acids 0.67% (Becton Dickinson, Franklin Lakes, Nova Jersey, USA)
CSM-LEU-URA 0.067% (MP Biomedicals, Illkirch, France)</td></tr>
<tr><td>CSM-HIS-URA</td><td>Yeast Nitrogen Base (YNB) without Amino Acids 0.67% (Becton Dickinson, Franklin Lakes, Nova Jersey, USA)
CSM-HIS-URA 0.075% (MP Biomedicals, Illkirch, France)</td></tr>
</table>

2.3.2 Yeast Transformation

S. cerevisiae cells, previously grown in YPD liquid media to a final OD of 0.6, were centrifuged, washed with sterile water, and resuspended twice in a solution composed of 1/10 Lithium Acetate (LiAc) 1M, 1/10 Tris-EDTA (TE) 10x and 8/10 sterile water. Salmon sperm DNA previously boiled, the plasmid and a solution composed of 1/10 LiAc 1M, 1/10 TE 1x and 8/10 polietilenoglicol (PEG) 4000 at 50% (w/v), were added to the cells. After 30 min of incubation at 30ºC with agitation and a 20min incubation at 42ºC, the cells were resuspended in sterile water. In the end, the cells were plated in selective medium complemented with glu 2% medium with the help of glass beads, and incubated at 30ºC for two days. Then, three replicas of each transformant were collected and plated in new selective media plates containing glu and incubated during two days at 30˚C.

2.4 Molecular biology: Plasmids construction

2.4.1 Yeast plasmid constructions using site-directed mutagenesis

For site-directed mutagenesis, it was used a DNA template sample, and forward and reverse primers specific for the mutations of interest, designed using the *PrimerX* bioinformatic tool (Table 2.4). The polymerase used was *Pfu Turbo Polymerase* (Agilent Technologies, Santa Clara, CA, USA) and respective buffer, since this polymerase amplifies complex targets in higher yields than *Taq Polymerase* and has proofreading properties.

Table 2.4 Description of plasmids and primers used for site-directed mutagenesis

Plasmid of interest	Template plasmid	Primer Forward	Primer Reverse
p426_Gal_aSyn_H50Q_GFP	p426_Gal_aSyn_WT_GFP	5'GGAGGGAGTGGTGCA GGGTGTGGCAACAG 3'	5'CTGTTGCCACACCCT GCACCACTCCCTCC 3'
p426_Gal_aSyn_S129A_GFP	p426_Gal_aSyn_WT_GFP	5'CTTATGAAATGCCTG CTGAGGAAGGGTATC 3'	5'GATACCCTTCCTCAG CAGGCATTTCATAAG 3'
p426_Gal_aSyn_S87A_S129D_GFP	p426_Gal_aSyn_S87A_GFP	5'GGCTTATGAAATGCCT GATGAGGAAGGGTATC AAG 3'	5'CTTGATACCCTTCCTC ATCAGGCATTTCATAAG CC 3'
p426_Gal_aSyn_S87E_S129A_GFP	p426_Gal_aSyn_S87E_GFP	5'CTTATGAAATGCCTGC TGAGGAAGGGTATC 3'	5'GATACCCTTCCTCAG CAGGCATTTCATAAG 3'

The Polymerase Chain Reaction (PCR) conditions used for all amplifications was: initial denaturation at 95ºC for 1 minute; 18 cycles of denaturation at 95ºC for 50 sec, annealing at 60ºC for 50 sec, following elongation at 68ºC during 8 min; a final elongation at 68ºC for 10 min. After amplification, samples were treated with *DpnI* (Agilent Technologies, Santa Clara, CA, USA) during 7 hours at 37ºC, since this enzyme only cuts methylated plasmids, which happens only in naturally amplified plasmids, allowing *E. coli* transformation with only newly-synthesized plasmids (Figure 2.1).

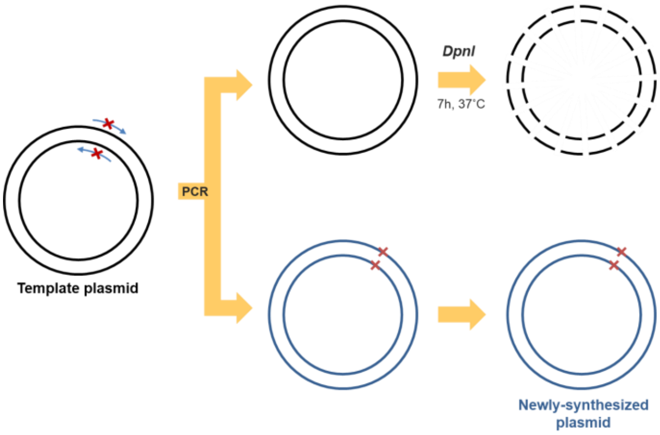

Figure 2.1 Schematic representation of the site-directed mutagenesis protocol.

2.4.2 CDNF plasmids construction by Gateway Recombination Cloning Technology

The CDNF plasmid available was a plasmid for expression on mammalian cells, for this reason, it was necessary to generate a yeast-expressing plasmid containing the CDNF sequence. For that, three different constructions were performed, one with WT CDNF alone, one with a N-terminal fusion with Cerulean and, lastly, one with a DsRed fusion at the C-terminus. Three different pairs of primers were used to amplify three distinct CDNF sequences (Table 2.5 and 2.6) in order to generate pDONR vectors containing each CDNF sequence.

Table 2.5 Description of the PCR reactions performed to amplify the CDNF sequence

Fusion	Primer Forward	Primer Reverse
No fusion	S_CDNF	AS_CDNF
N-terminal fusion	S_CDNF_N_fusion	AS_CDNF
C-terminal fusion	S_CDNF	AS_CDNF_C_fusion

Table 2.6 PCR Reaction Mix used for CDNF amplification

The *KAPA HiFi* was added only after the first PCR cycle.

Component	Volume (µL)
5X KAPA HiFi Buffer (KAPA Biosystems, Wilmington, MA, USA)	2.5
dNTPs (10mM)	0.7
Primer S (10µM)	1
Primer AS (10µM)	1
DNA template (15ng)	1
KAPA HiFi (KAPA Biosystems, Wilmington, MA, USA)	0.5
H_2O	18.3
TOTAL	**25**

The PCR conditions used for all amplifications were: denaturation during 2 min at 92ºC; 3 cycles of denaturation at 92ºC during 30 sec, annealing at 57ºC during 30 sec and an elongation step during 45 sec at 72ºC; followed by 25 similar cycles, where the annealing step was performed at 62ºC; concluding with a final elongation step of 10 min at 72ºC.

After PCR, each sample was loaded into an 1% (w/v) agarose gel and ran at 90V to verify if the PCR occurred as expected. The DNA was purified from the PCR amplifications using the Wizard SV Gel and PCR Clean-Up System (Promega, Madison, WI, USA) and quantified using NanoDrop 2000/2000c Spectrophotometer (Thermo Fisher Scientific Inc., Waltham, MA, USA).

A BP reaction was performed to insert the amplified sequences into an intermediate plasmid, the pDONR plasmid, using the Gateway BP Clonase Enzyme Mix (Invitrogen, Carlsbad, CA, USA). Each mix was incubated at room temperature (RT) for 2 hours, after which were transformed in *E. coli* cells and plated in LB media containing Kan, over-night. The pDONR plasmids containing the CDNF sequences were extracted (see Section 2.1.5), followed by a LR reaction, where the CDNF sequence was inserted into a series of pAdvanced Gateway (pAG) plasmids through recombination, using a Gateway LR Clonase II Enzyme Mix (Invitrogen, Carlsbad, CA, USA). The mix was incubated for 2 hours at RT, following *E. coli* transformation (Section 2.2.2; Figure 2.2.). After growth, two colonies from each transformation were collected, grown in LB liquid media and the plasmids were extracted as described in Section 2.2.3. DNA samples were sent to sequencing by gold-standard Sanger sequencing at STAB VIDA (Caparica, Almada, Portugal).

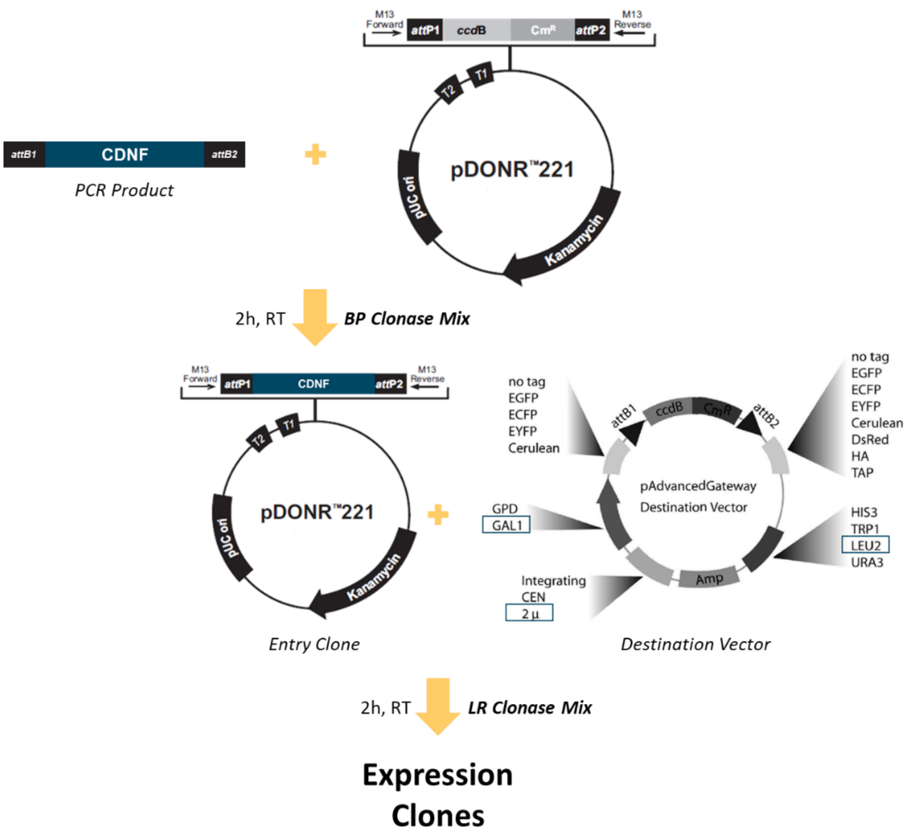

Figure 2.2 Schematic representation of the Gateway Recombination Cloning Technique procedure.

2.5 Cell Viability Assays

2.5.1 Spotting Assay

Cells were grown over-night at 30ºC in liquid media containing raffinose until they reached mid-log phase. Initial volumes corresponding to an OD of 0.1 were deposited in the first lane of a 96-well plate with sterile water to a final volume of 150µL. For the following lanes, a dilution of 1:3 was performed. Using a previously sterilized stamp, the dilutions were plated in YPD media for growth control and SC media complemented with gal to assess cell viability. The plates were incubated at optimal growth temperature of 30ºC for 48 hours and 72 hours, respectively.

2.5.2 Flow Cytometry

Cell viability was also assessed through flow cytometry. After yeast cells growth and after 6 hours of protein expression induction, a volume of cells correspondent to 1/OD was collected. Samples were centrifuge for 3 min at 3000rpm and the pellet was resuspended in phosphate buffered saline (PBS) 1X. Propidium Iodide (PI) was added at 0.1mg/mL. Cells were incubated in the dark for 25 min at 30ºC with agitation, followed by a spin down. Cells were washed twice with PBS 1X, transferred to flow cytometry tubes and vortexed. Positive and negative controls were performed according to the table 2.7. A BD FACScanto™II flow cytometer (Becton Dickinson, Franklin Lakes, Nova Jersey, USA), equipped with a 20mW solid state 488nm laser was used for GFP and PI excitation (530/30nm and 485/42nm, respectively).

Table 2.7 Positive and negative controls used for the membrane integrity assessment through flow cytometry

GFP	PI	Sample	Treatment
-	-	Empty	No PI
+	-	aSyn_WT	No PI
-	+	Empty	Yeast dead cells (95ºC 10 min); stained with PI

2.6 Detection of superoxide radical production

Flow cytometry was used to detect production of superoxide radical, using Dihydroethidium (DHE; Life Technologies, Carlsbad, CA, USA). After 6 hours of protein expression induction, a volume of cells correspondent to 1/OD was collected. Samples were centrifuge for 3 min at 3000rpm and the pellet was resuspended in PBS 1X. DHE (3mM) was added, diluted in 500µL of PBS. Cells were incubated in the dark for 15 min at 30ºC with constant agitation, followed by a spin down. Cells were washed twice with PBS 1X, transferred to flow cytometry tubes and vortexed. Positive and negative controls were performed according to the table 2.8. A BD FACScanto™II flow cytometer (Becton

Dickinson, Franklin Lakes, Nova Jersey, USA), equipped with a 20mW solid state 488nm laser was used for GFP and DHE excitation (530/30nm and 518/605nm, respectively).

Table 2.8 Positive and negative controls used for the superoxide radical production assessment through flow cytometry

GFP	DHE	Sample	Treatment
-	-	Empty	No DHE
+	-	aSyn_WT	No DHE
-	+	Empty	Yeast cells treated with H_2O_2 (0.2µM), 20 min with agitation; 30ºC; Addition of DHE

2.7 Evaluation of vacuole acidification

Vacuole acidification was assessed through flow cytometry, using LysoTracker Red DND 99 (Thermo Fisher Scientific Inc., Waltham, MA, US), a dye highly specific for acidic organelles. After 6 hours of protein expression induction, a volume of cells correspondent to 1/OD was collected. Samples were centrifuge for 3 min at 3000rpm and the pellet was resuspended in PBS 1X. LysoTracker Red DND 99 (1mM) was added, diluted in 1000µL of PBS. Cells were incubated in the dark for 30 min at 30ºC with constant agitation, followed by a spin down. Cells were washed twice with PBS 1X, transferred to flow cytometry tubes and vortexed. Unstained and GFP positive controls were performed. A BD FACSAria^{TM}II flow cytometer (Becton Dickinson, Franklin Lakes, Nova Jersey, USA) with a 375 nm solid state laser, was used for GFP and mCherry excitation (530/30nm and 575/610nm, respectively).

2.8 Protein subcellular localization through fluorescence microscopy

After 6 hours of protein expression, each sample was spun down and cells were retrieved from the pellet to observe at the fluorescence microscope. Images were acquired using an Axio Imager 2 widefield fluorescent microscope (Carl Zeiss MicroImaging GmbH, Germany) and the Zeiss Zen software (Carl Zeiss MicroImaging GmbH, Germany), with an amplification of 63X and with different filters according to the tags observed. To see aSyn tagged with GFP, the Alexa Fluor 488 filter was used, while to observe Cerulean and DsRed tag, the 4',6-diamidino-2-phenylindole (DAPI) and DsRed filters were used, respectively. To see aSyn subcellular localization after protein clearance, protein expression was ceased using liquid media complemented with glucose. Cultures were re-incubated for 6 hours or 13 hours, after which, cells were collected as before. The number of cells with inclusions and the total cell number were counted using the ImageJ – Fiji image analysis software (Rasband, 1997).

2.9 Quantification of protein expression levels

2.9.1 Protein Extraction and Quantification

A culture volume correspondent to 2/OD was collected for yeast total protein extraction. The culture was centrifuged and resuspended in MilliQ water, followed by a transference to a bead beater vial. Cell were spun down and resuspended in tris-buffered saline (TBS) 1X with proteases inhibitors (cOmplete™ ULTRA Tablets, Mini, EDTA-free, EASYpack Protease Inhibitor Cocktail by Roche, Basel, Switzerland). For cell lysis, acid-washed glass beads were added to the sample and three cycles of a 30 sec bead beater vortex followed by a 1 min ice incubation were done. Cells were smoothly centrifuged (3 min, 700g, 4˚C) and the supernatant was collected. To quantify protein, the Pierce BCA Protein Assay Kit (Thermo Fisher Scientific Inc., Waltham, MA, USA) was used according to the manufacturer protocol.

2.9.2 Protein detection through Western Blot

Protein sample buffer (200mM Tris-HCl pH 6.8, 6% 2-mercaptoethanol, 8% sodium dodecyl sulfate (SDS), 40% glycerol, 0.4% bromophenol blue) was added to each sample with the same total protein quantity (8µg), following a 10 min denaturation at 100˚C before loading into a 12% acrylamide gel. Protein samples were run in Sodium dodecyl sulfate polyacrylamide gel electrophoresis (SDS-PAGE) during 20 min at 90V. After protein deposition between stacking and resolving gel, voltage was changed to 120V. Protein was transferred to a nitrocellulose membrane using a Trans-Blot Turbo transfer system (Bio-Rad, Hercules, CA, USA), according to the manufacturer’s protocol.

Membranes were blocked with 5% Bovine Serum Albumin (NZYTech, Lisboa, Portugal)/Tris-buffered Saline – Tween 20 (5% BSA/TBS-T) (w/v), followed by an over-night incubation with a primary antibody at 4ºC (Table 2.9). The antibodies were washed three times with TBS-T, followed by a 1 hour and 30 min incubation with secondary antibodies, as depicted in table 2.9. Four washes with TBS-T were performed after incubation with secondary antibodies, after which membranes were revealed at ChemiDoc (Bio-Rad, Hercules, CA, USA) using Pierce™ ECL Western Blotting Substrate (Thermo Fisher Scientific, Waltham, MA, USA). Images recovered from ChemiDoc were treated using the Image Lab Software (Bio-Rad, Hercules, CA, USA).

To incubate a second antibody, membranes were stripped using a stripping solution (glycine, 10% SDS, ddH_2O; pH 2.0) during 45 min, followed by three washes with TBS 1X and three washes with TBS-T. Membranes were again blocked and incubated with new antibodies, restarting the membrane hybridization with new primary antibodies.

Table 2.9 Description of the antibodies used in this project

Antibody	Manufacturer	Description	Secondary Antibody
Anti-aSyn	BD Transduction Laboratories, San Jose, CA, USA	1:4000, mouse	1:10000, mouse
Anti-pS129 aSyn	Wako Chemicals USA, Inc., Richmond, VA, USA	1:4000, mouse	1:10000, mouse
Anti-PGK	Life Technologies, Grand Island, NY, USA	1:2000, mouse	1:5000, mouse
Anti-DsRed	Clontech Laboratories, Inc., Montain View, CA, USA	1:2000, rabbit	1:5000, rabbit
Anti-GFP	Neuromab, Davis, CA, USA	1:1000, mouse	1:5000, mouse

2.10 Statistical Analysis

To perform the statistical analysis, the Prism 6 (GraphPad Software Inc., La Jolla, CA, USA) was used. Statistical analysis was performed using one-way ANOVA or two-way ANOVA, with Bonferroni's multiple comparison test, comparing the mean between distinct groups. A P value $\leq$ 0.01 was considered statistically significant. Results are shown as mean ± standard deviation, for at least, three independent experiments.

3 Results and Discussion

3.1 Plasmid constructions

Several plasmids used in this study were already available in the laboratory, nevertheless, some plasmids had to be constructed, namely: aSyn_H50Q, aSyn_S129A, aSyn_S87E_S129A and aSyn_S87A_S129D. To construct these plasmids, the site-directed mutagenesis technique was performed using template plasmids and pairs of primers specific for each wanted mutation (see *Materials and Methods 2.4.1*, Table 2.3). Plasmids were sequenced and aligned with the WT aSyn sequence using the Clustal Omega bioinformatic tool, confirming the presence of the wanted mutations (*Supplementary Data,* Figure 6.1).

3.2 Evaluation of the phosphomutants effects in inclusion formation and cell viability

To unveil the role of aSyn phosphorylation, plasmids containing aSyn mutants where phosphorylation-prone residues were mutated to mimic or block phosphorylation were transformed in W303.1A yeast cells (Table 3.1). Since alanine (A) and phenylalanine (F) are phosphorylation-resistant amino acids chemically similar to serine and tyrosine, respectively, they are used to block phosphorylation in each residue; while glutamic acid (E) and aspartic acid (D) are non-phosphorylated amino-acids chemically similar to phosphorylated serine amino acid, thus mimicking phosphorylation.

Table 3.1 Phosphomutants used in this study.
Every aSyn phosphomutant was expressed in a multicopy plasmid under the regulation of a *GAL1* promoter.

Phosphomimics	Phosphoblockers	Double Mutants
S87E S129D	Y39F S87A Y125F S129A	Y39F_Y125F S87E_S129E S87E_S129A S87A_S129E S87A_S129A

Phosphomutants effects were evaluated regarding inclusion formation, clearance, and cell toxicity, through spotting assay and flow cytometry. Inclusion formation was assessed after 3 and 6 hours of protein induction.

After 3 hours of protein induction (Figure 3.1B), WT aSyn presented a higher percentage of cells with aSyn inclusions, suggesting a quicker aggregation process. Regarding Y phosphorylation, phosphorylation blockade in each Y residue individually, it revealed a decrease in inclusion formation when compared to WT aSyn. Additionally, when both Y residues (Y39 and Y125) are not phosphorylated, inclusion formation decreases even further, pointing to a toxic effect of Y residues phosphorylation and to an additive protective effect of Y phosphoblocking.

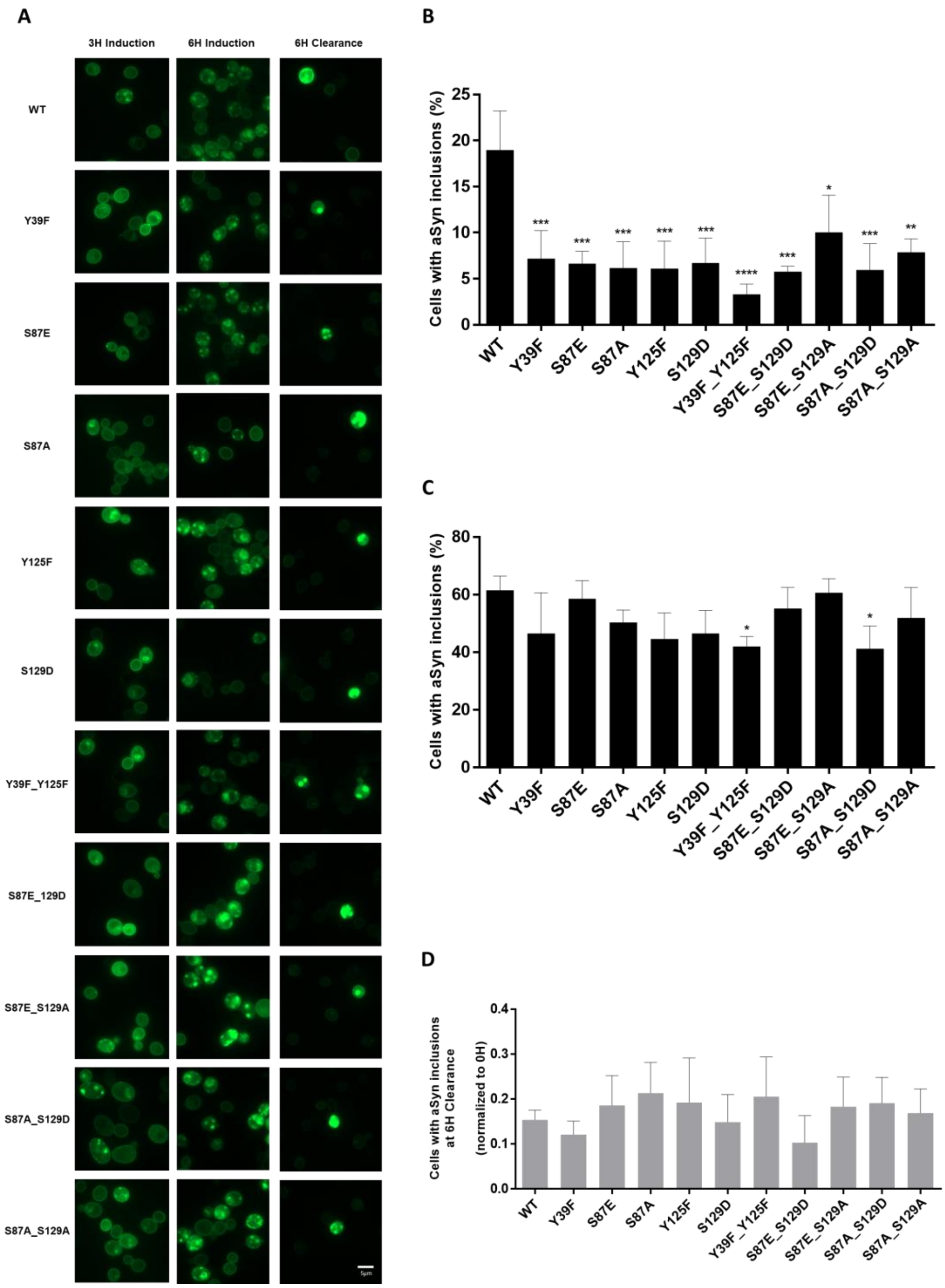

Figure 3.1 Assessment of aSyn inclusion formation and respective clearance for each aSyn phosphomutant through fluorescence microscopy.

A) Intracellular localization of WT aSyn and each aSyn mutation after 3 and 6 hours of protein expression, and after 6 hours of protein clearance in W303.1A yeast cells. **B)** Percentage of cells containing aSyn-GFP inclusions after 3 hours of protein expression. C**)** Percentage of cells containing aSyn-GFP inclusions after 6 hours of protein expression. **D)** Percentage of cells containing aSyn-GFP inclusions after 6 hours of clearance (6H Clearance), normalized to 0H Clearance. Percentage values of each mutant were normalized to 0H Clearance. (***p<0.001, ****p<0.0001; one-way ANOVA with Bonferroni's multiple comparison test; values represent mean ± SD from four biological replicas).

Previous studies revealed that phosphorylation blocking of S129 (S129A) promoted aSyn aggregation and cytotoxicity in different models (Gorbatyuk et al., 2008; Sancenon et al., 2012; Tenreiro et al., 2014a; Azeredo da Silveira et al., 2017), and other studies exposed opposite results, with S129A suppressing neuronal loss in *Drosophila melanogaster* (Chen and Feany, 2005). In yeast cells, blockade of S129 phosphorylation was revealed to highly increase toxicity in yeast cells, moreover, it also induced a significant increase in inclusion formation (Tenreiro et al., 2014a). Indeed, probably due to its high toxicity, it was not possible to grow yeast cells containing the S129A aSyn mutant expressed in a multicopy plasmid.

Nevertheless, S129A toxic effect can be supposed, since when expressing the double mutant S87E_S129A aSyn, it is possible to see an increase in aSyn aggregation, when compared to S129D aSyn, or even when compared to S87E and S87E_S129D mutants, indicating that the blocking of S129 phosphorylation effects in aSyn inclusion formation overcomes the protective effect induced by S87 phosphorylation. In contrast, blocking of S87 phosphorylation seems to induce a protective effect over blockade of S129 phosphorylation (S87A_S129A), decreasing the percentage of cells with aSyn inclusions. The protective effect of S87 phosphorylation blocking is supported by the results published by Kim *et. al*, which stated that increased levels of S87 phosphorylation increased toxicity in H19-7 cells (Kim et al., 2006). Though, other study revealed that S87 phosphorylation inhibits aSyn fibrillation and oligomerization (Paleologou et al., 2010).

With 6 hours of protein induction (Figure 3.1C), the percentage of cells containing aSyn inclusions was similar between all aSyn variants, with exception for the double tyrosine mutants (Y39F_Y125F) and the double mutant S87A_S129D, which presented a decrease in inclusion formation. These results were in agreement with the results obtained only after 3 hours of protein expression. Once again, blockage of S87 phosphorylation and blockage of both Y residues phosphorylation seem to induce a protective effect. About the double tyrosine mutant, its reductive effect in aSyn inclusion formation was also stated by Kleinknecht *et. al* in yeast cells (Kleinknecht et al., 2016).

Concerning inclusion clearance (Figure 3.1D), with only 6 hours of protein clearance, all phosphomutants presented a similar inclusion clearance, with no significant differences amongst each other. Clearance time could be increased to see more prominent differences between each phosphomutant clearance, especially since aSyn S129 and Y39 phosphorylation were already found to promote aSyn clearance in yeast cells (Mahul-Mellier et al., 2014; Tenreiro et al., 2014a).

Since a correlation between aSyn subcellular localization and cytotoxicity has been established by several groups (Outeiro and Lindquist, 2003; Zabrocki et al., 2005; Gitler, 2008), spotting assay (Figure 3.2) was performed to see the effects of each aSyn phosphomutant in cell viability. Cell viability was also assessed through flow cytometry (Figure 3.3), using PI, which marks cells with a compromised plasma membrane by binding to their nucleic acids. Flow cytometry allowed to see that every aSyn mutant is being expressed at the same levels, since the percentage of GFP+ cells is similar between samples (Figure 3.3B).

Regarding tyrosines phosphorylation, phosphorylation blockade at Y39 appears to have a cytoprotective effect when compared with WT aSyn, however, phosphorylation blockade of Y125 decreases these protective effect, inducing a similar cell growth to cells transformed with WT aSyn.

When both Y phosphorylation is being blocked, toxicity is higher, suggesting that Y125F effect overcomer the protective effect of Y39F. These results contradict the correlation between inclusion formation and toxicity.

Regarding S phosphorylation, the toxic effect of S129 phosphoblocking can be deduced, since the double mutant S87E_S129A present a decreased cell growth when compared to S87E_S129D and S87E mutants, as well as when compared to WT aSyn. Corroborating the inclusion formation assay, when phosphorylation of both S residues is being blocked, S87 phosphoblockade seem to induce a protective effect over S129 phosphoblocking, since there is an increase in cell growth when compared to S87E_S129A aSyn mutant. Moreover, similar to the obtained results, previous studies revealed that S87E_S129D aSyn restored cell viability when compared to S87E aSyn, pointing to a protective effect of S129 phosphorylation over S87 phosphorylation. Additionally, protein analysis revealed that yeast cells expressing S87E aSyn present lower phosphorylated S129 levels, suggesting that S87 phosphorylation might be reducing S129 phosphorylation and, consequently, increasing toxicity (Madaleno, 2017). However, when S87E is expressed with S129A, toxicity is increased, indicating that S129A toxic effect adds to S87E toxicity, supporting the hypothesis that S87E toxicity is induced by S129 phosphorylation levels decrease.

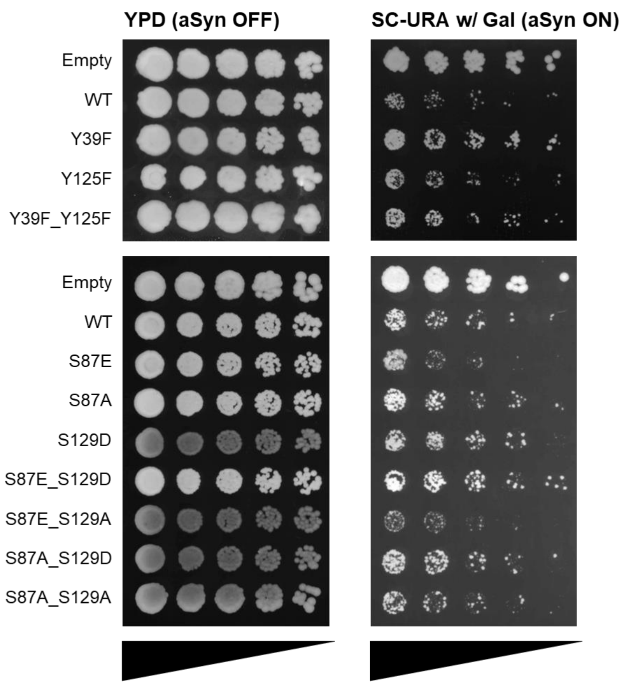

Figure 3.2 Evaluation of toxicity induced by each aSyn phosphomutant by spotting assay.
Spotting assay of the W303.1A yeast cells transformed with the indicated aSyn phosphomutants. Cell cultures were adjusted to the same OD, serially diluted, and spotted into YPD and selective media complemented with Gal as carbon source. (Image representative of four biological replicas)

In summary, blockage of S87 phosphorylation has a protective effect over S129 phosphoblocking toxicity. Nevertheless, protein should be analyzed, to see phosphorylated S129 and S87 levels, as well as total aSyn levels for each mutant, to understand how each residue phosphorylation is being affected and its effect in cell viability.

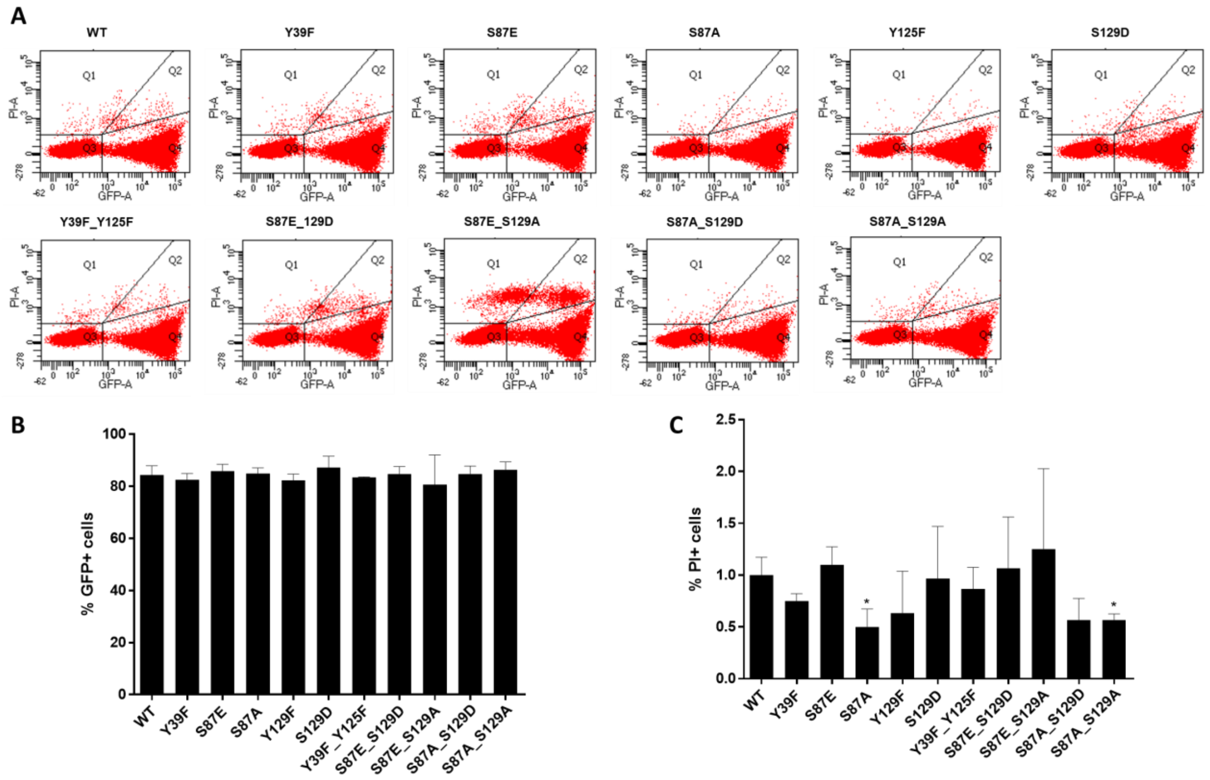

Figure 3.3 Evaluation of toxicity induced by aSyn phosphomutants through flow cytometry using PI. **A)** Representative graphs of aSyn-GFP versus PI fluorescence assessed through flow cytometry in W303.1A yeast cells transformed with each aSyn phosphomutant after 6 hours of protein expression. **B)** Frequency of GFP positive cells in the indicated yeast cells. **C)** Frequency of PI positive cells in the indicated yeast cells. (*p<0.1, one-way ANOVA with Bonferroni's multiple comparison test using WT as control; values represent mean ± SD from three biological replicas).

3.3 Evaluation of aSyn familial mutations in aSyn inclusion formation and cell toxicity

The subcellular localization of distinct aSyn variants was evaluated through fluorescence microscopy. W303.1A yeast strain cells were transformed with plasmids containing distinct aSyn variants (mutations) fused with GFP, under regulation of an inducible *GAL1* promoter. Protein expression was induced with selective media supplemented with Gal for 6 hours, after which cells were collected for microscopy (Figure 3.4).

Concerning WT aSyn, about 60% of the cells present aSyn inclusions, whereas the remaining cells do not present inclusions, presenting aSyn bound to the membrane, after 6 hours of expression induction. Regarding the A30P mutant, microscopy revealed that it does not form aggregates when overexpressed, keeping its cytoplasmic localization in a diffused manner, as described before (Outeiro and Lindquist, 2003). A decrease in the percentage of cells containing aSyn inclusions was also observed with the G51D mutation (7.74±1.06%), presenting a cytoplasmic localization in the majority of cells, as described by Fares *et. al* and Rutherford *et. al* (Fares et al., 2014; Rutherford et al., 2014).

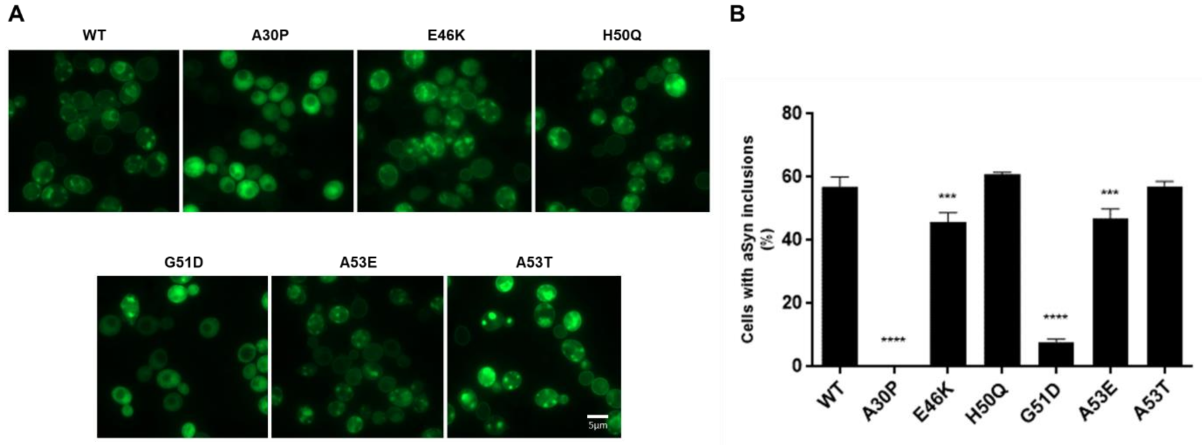

Figure 3.4 Assessment of aSyn inclusion formation for each aSyn variant through fluorescence microscopy.

A) Intracellular localization of WT aSyn and each aSyn mutation after 6 hours of protein expression in W303.1A yeast cells. **B)** Percentage of cells containing aSyn-GFP inclusions after 6 hours of protein expression (***p<0.001, ****p<0.0001; one-way ANOVA with Bonferroni's multiple comparison test; values represent mean ± SD from three biological replicas)

The E46K and A53E aSyn mutants showed a slightly decrease in inclusion formation with 45.84±2.94% and 46.9±3.06% of cells with inclusions, respectively; A53E aSyn results were in agreement with the previous studies (Ghosh et al., 2014; Rutherford and Giasson, 2016), whereas the E46K aSyn aggregation decrease showed contrary results to previous studies in SH-SY5Y cells (Pandey et al., 2006), corroborating the fact that aSyn ability to aggregate varies from different cellular models. Regarding the H50Q mutant, the percentage of cells with aSyn inclusions was similar to WT aSyn (60.91±0.64%). However, several studies support that the H50Q mutation increases aSyn aggregation (Ghosh et al., 2013; Khalaf et al., 2014; Rutherford et al., 2014; Xiang et al., 2015). While distinct studies revealed an increase in A53T aSyn aggregation when compared to WT aSyn (Narhi et al., 1999; Li et al., 2001; Lázaro et al., 2014), this assay showed a similar percentage of cells with aSyn inclusions (57.19±1.42%) when compared to WT aSyn. All of these differences in inclusion formation might be due to different cellular models used in each study, indicating that the differences in the cellular environment are sufficient to modulate aSyn ability to aggregate.

Toxicity induced by each aSyn familial mutant was evaluated through spotting assay (Figure 3.5). The A30P and the G51D mutations seem to be non-toxic, since their growth is similar to the growth of yeast cells transformed with an empty plasmid. The previous microscopy results showed that, in fact, these mutations induce less inclusion formation. On the other hand, E46K, H50Q and A53T aSyn, appear to be more toxic, presenting a similar decrease in cell growth as WT aSyn. The A53E mutation is more toxic than A30P or G51D mutation, but appears to be less cytotoxic when compared with WT aSyn and the remaining aSyn mutations.

The spotting assay and the inclusion formation assay were in agreement, since the aSyn variants with higher percentage of cells with inclusions (WT, E46K, H50Q, A53E and A53T aSyn) were the ones who presented higher toxicity.

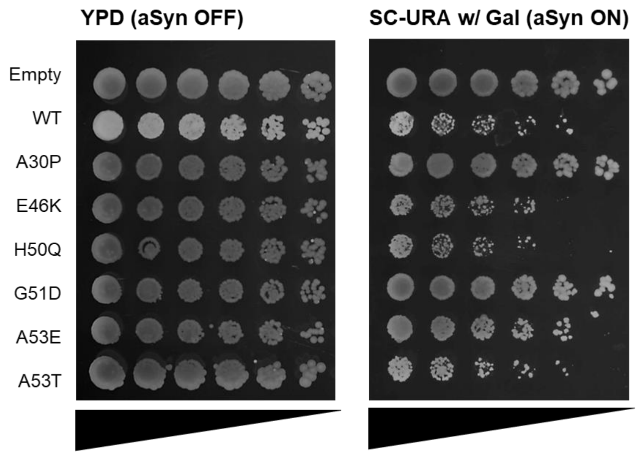

Figure 3.5 Evaluation of toxicity induced by each aSyn variant by spotting assay.
Spotting assay of the W303.1A yeast cells transformed with the indicated aSyn variants. Cell cultures were adjusted to the same OD, serially diluted, and spotted into YPD and selective media complemented with Gal as carbon source. (Image representative of three biological replicas)

To quantitatively evaluate cytotoxicity induced by each aSyn variant, flow cytometry was performed after 6 hours of protein expression (Figure 3.6). Flow cytometry results revealed that all aSyn mutants are being expressed at the same levels, since the percentage of cells expressing GFP is similar between each culture (Figure 3.6B). PI staining revealed that the E46K aSyn mutant is the most cytotoxic, when comparing to WT aSyn. The A30P mutant revealed to be the less toxic (Figure 3.3C).

However, with only 6 hours of protein induction, cell viability was still high, with low percentages of dead cells. Despite not having significant cell death, cells can still be being affected in several pathways, leading to a later cell death. To obtain a more prominent cell death, protein was expressed for a longer period, i.e., 13 hours of protein expression, after which flow cytometry was performed (Figure 3.7). After 13 hours of protein expression, aSyn was still being expressed at the same level between different variants (Figure 3.7B). Moreover, cell viability after 13 hours of protein expression decreased dramatically, with higher percentages of PI-positive cells. Nevertheless, A30P aSyn presented a low percentage of PI-positive cells, consistent with the spotting assay results and the absence of inclusions (Lázaro et al., 2014).

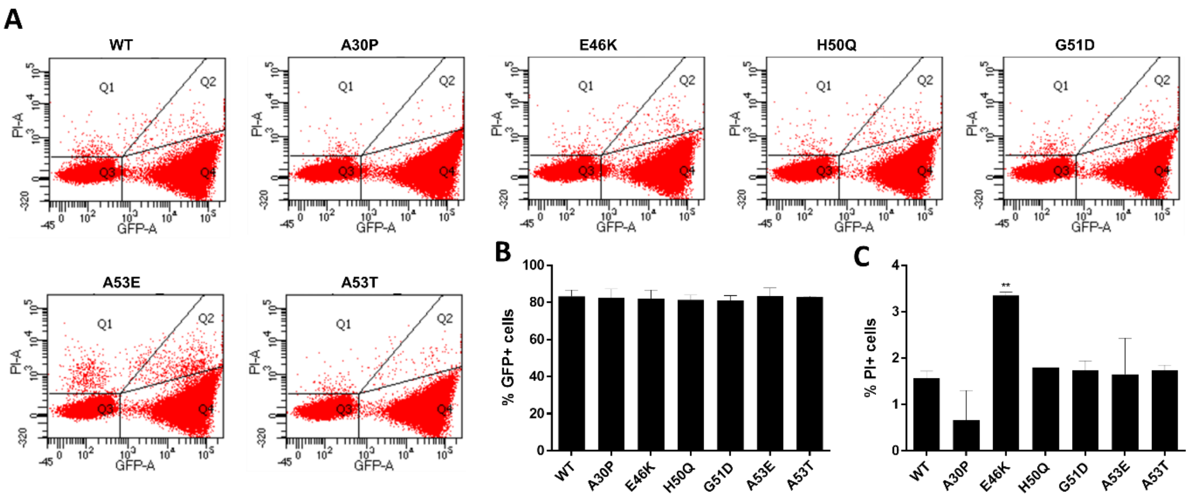

Figure 3.6 Evaluation of cytotoxicity induced by aSyn familial mutants through flow cytometry using PI after 6 hours of protein induction.

A) Representative graphs of aSyn-GFP versus PI fluorescence assessed through flow cytometry in W303.1A yeast cells transformed with each aSyn variant. **B)** Frequency of GFP positive cells in the indicated yeast cells. **C)** Frequency of PI positive cells in the indicated yeast cells. (**p<0.01, one-way ANOVA with Bonferroni's multiple comparison test using WT as control; values represent mean ± SD from three biological replicas).

The E46K was the most cytotoxic mutant, when comparing to WT aSyn, similar to the results obtained after 6 hours of protein expression and also with the results obtained by Lázaro et. al (Lázaro et al., 2014). However, the flow cytometry results did not show any consistent relation between cell viability and inclusion formation for the E46K mutation, since it forms less cytoplasmic inclusions than WT aSyn, but appears to be more cytotoxic. In a recent study, E46K was shown to be highly toxic in primary neurons model, however, it did not promote an obvious increase in aSyn aggregation. Iñigo-Marco *et. al* speculated that E46K toxicity was mediated by soluble species, not by aSyn in its aggregated form (Íñigo-Marco et al., 2017).

The remaining mutations revealed a similar percentage of PI-positive cells, as observed with the spotting assay. However, the G51D mutant presented controversial results, with a similar percentage of dead cells when comparing to WT, while in the spotting assay it revealed low cytotoxicity. Literature revision also revealed discordant conclusions (Fares et al., 2014; Rutherford et al., 2014). Further investigation is required to reach a conclusion.

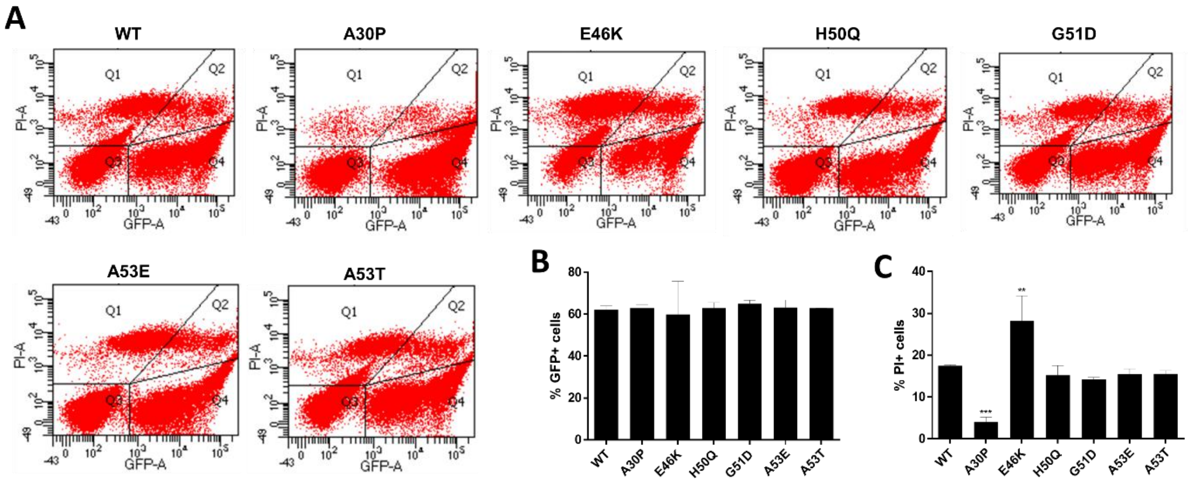

Figure 3.7 Evaluation of cytotoxicity induced by aSyn familial mutants through flow cytometry using PI after 6 hours of protein induction.

A) Representative graphs of aSyn-GFP versus PI fluorescence assessed through flow cytometry in W303.1A yeast cells transformed with each aSyn variant. **B)** Frequency of GFP positive cells in the indicated yeast cells. **C)** Frequency of PI positive cells in the indicated yeast cells. (**p<0.01, ***p<0.001, one-way ANOVA with Bonferroni's multiple comparison test using WT as control; values represent mean ± SD from three biological replicas)

3.4 Phosphorylation levels of different aSyn variants

Total aSyn and phosphorylated aSyn levels at S129 were evaluated by Western Blot, in order to search for a correlation between phosphorylation, inclusion formation and cytotoxicity (Figure 3.8). Protein was collected after 6 hours of protein expression. Western Blot revealed similar levels of total aSyn between each mutant, indicating that the toxicity differences observed for each mutant are not caused by differences in aSyn expression (Figure 3.8B). Meanwhile, phosphorylated aSyn levels at S129 differed amongst mutants were also evaluated (Figure 3.8C). When comparing to WT aSyn, A30P and A53E mutants presented higher levels of phosphorylation, while the remaining mutants were less phosphorylated, in the tested conditions.

When comparing the results obtained with familiar and phosphomutants, it is possible to hypothesize phosphorylation in residues other than S129. For instance, the A30P aSyn mutant, exhibits high levels of S129 phosphorylation and low cytotoxicity in yeast cells, accordingly to the known fact that S129 phosphorylated levels confers protection. Likewise, E46K aSyn presents decreased phosphorylation levels at S129 and high toxicity in the cell viability assay performed by flow cytometry, reinforcing the toxic role of S129 phosphorylation blockade. A53E aSyn, on other hand, was revealed to have an increased S129 phosphorylation, however, its toxicity was shown to be similar to WT aSyn, while its aggregation propensity was still high. However, phosphorylation at S87 can also be playing an important role, since blockade of S87 phosphorylation exerts a protective effect over S129 phosphorylation (Figure 3.3C).

These results were not in agreement with the results published by Mbefo et. al, where E46K is shown to be hyperphosphorylated, and A30P and A53T mutants have no significant phosphorylation levels differences when comparing to WT aSyn in BY4741 yeast cells (Mbefo et al., 2015). To corroborate this, BY4741 yeast cells were transformed with the different plasmids, grown and protein was induced and collected after 6 hours of protein expression. Western Blot analysis were also performed (Figure 3.9). These findings suggest that different yeast strains may have distinct expression of kinases and/or phosphatases and, consequently, different phosphorylation profiles.

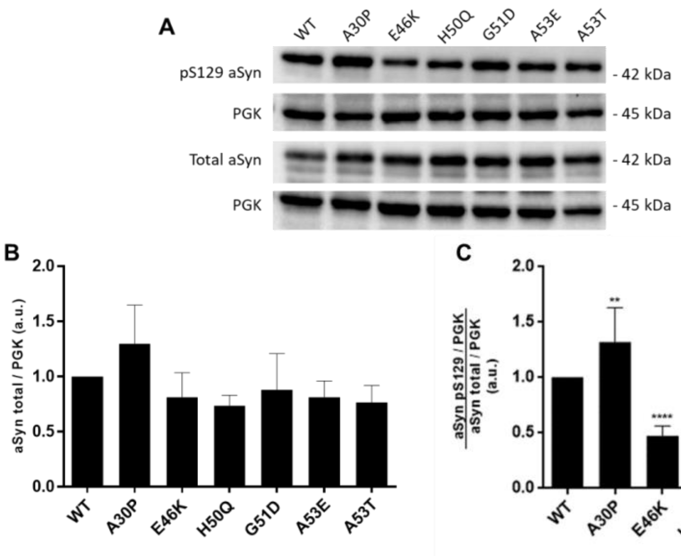

Figure 3.8 Total and phosphorylated aSyn levels after 6 hours of protein induction in W303.1A yeast cells. **A)** Total aSyn, pS129 aSyn and PGK expression levels in W303.1A yeast cells transformed with the indicated aSyn variants assessed through Western Blot analysis of total protein extracts after 6 hours of protein expression. **B)** Total aSyn expression levels normalized to total aSyn expression levels. **C)** S129 phosphorylated aSyn expression levels were normalized to the respective PGK expression levels Protein expression levels were normalized to WT aSyn. (**p<0.01, ****p<0.0001; one-way ANOVA with Bonferroni's multiple comparison test; values represent mean ± SD from six biological replicas from two independent experiments)

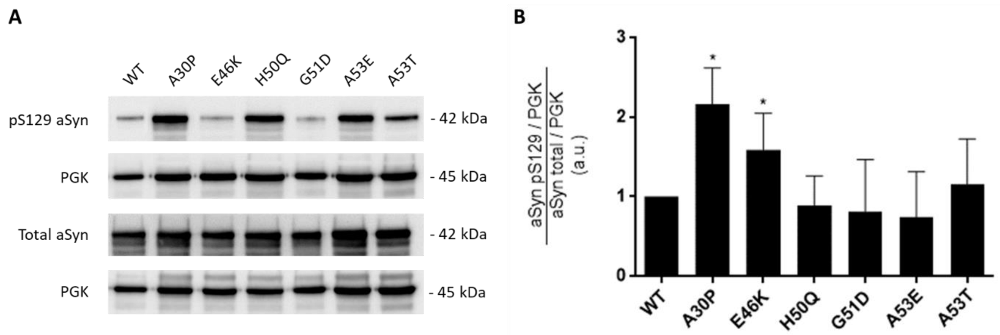

Figure 3.9 Phosphorylated aSyn levels after 6 hours of protein induction in BY4741 yeast cells. **A)** Total aSyn, pS129 aSyn and PGK expression levels in BY4741 yeast cells transformed with the indicated aSyn variants assessed through Western Blot analysis of total protein extracts after 6 hours of protein expression. **B)** S129 phosphorylated aSyn expression levels were normalized to the respective PGK expression levels Protein expression levels were normalized to WT aSyn. (*p<0.1; one-way ANOVA with Bonferroni's multiple comparison test; values represent mean ± SD from five biological replicas from two independent experiments)

3.5 Protein Clearance

To test aSyn inclusions clearance, cells were collected for microscopy after 6 hours of protein expression and after 6 hours of protein clearance (Figure 3.10). Microscopy revealed that inclusions clearance was effective for all mutations. The G51D mutant was the only mutant with total inclusions clearance, however, it induced a decreased aSyn aggregation beforehand. Regarding the percentage of cells with inclusions after clearance, all mutations showed a decrease in comparison to the WT aSyn, despite H50Q and A53E being the only mutations with a significantly lower percentage of cells with inclusions, when comparing to WT aSyn clearance.

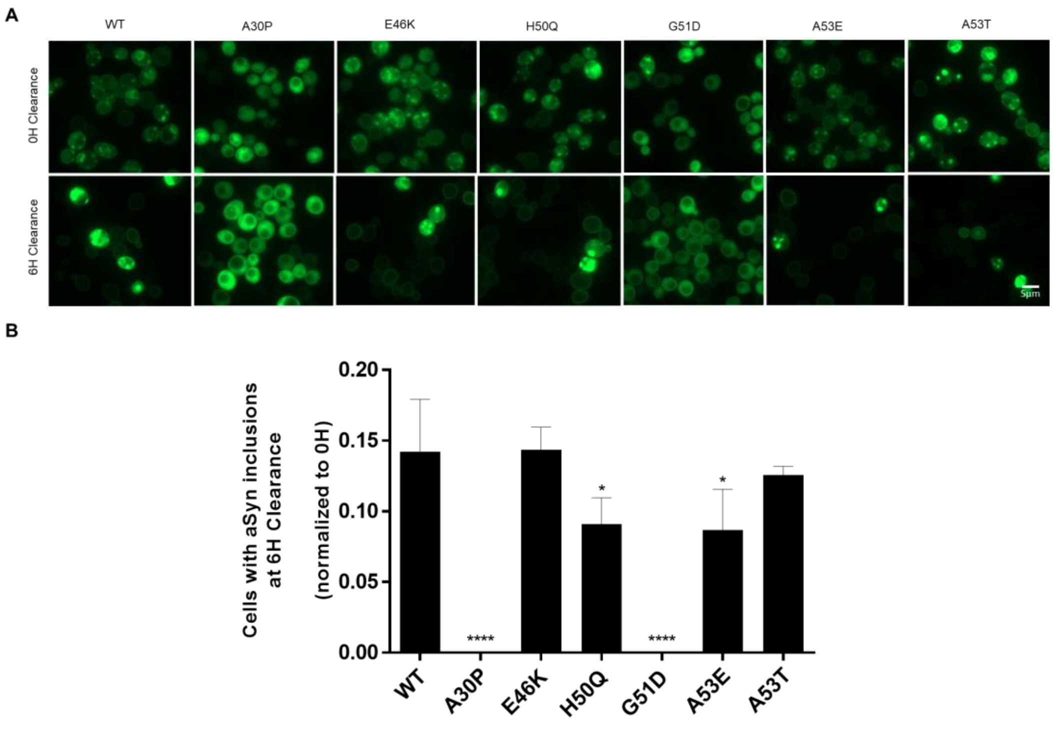

Figure 3.10 Assessment of aSyn inclusions clearance through fluorescence microscopy.
A) Intracellular localization of each aSyn mutant fused with GFP at both time points indicated in W303.1A yeast cells **B)** Percentage of cells containing aSyn-GFP inclusions before (0H Clearance) and after 6 hours of clearance (6H Clearance). Percentage values of each mutant were normalized to 0H Clearance. (*p<0.1; one-way ANOVA with Bonferroni's multiple comparison test at 6H Clearance; values represent mean ± SD from three biological replicas)

To see more a more prominent inclusion clearance, clearance time was increased for 13 hours. The percentage of cells with inclusions after 13 hours of protein clearance was lower than after 6 hours of clearance, as expected (Figure 3.11). However, with a longer clearance, the E46K, the H50Q and the A53T mutations, presented a higher percentage of cells with inclusions when comparing to the WT aSyn, despite it not being statistically different. These findings suggest that clearance of aSyn aggregates is not time-dependent, i.e., macroautophagy, responsible for degrading aggregated aSyn, acts at different time points or with distinct rates for each mutant, which would explain why, after 13 hours of protein clearance, WT aSyn presents a higher clearance when compared to the H50Q and A53E mutants. The lack of statistically differences between each sample might be due to the low percentages of all samples.

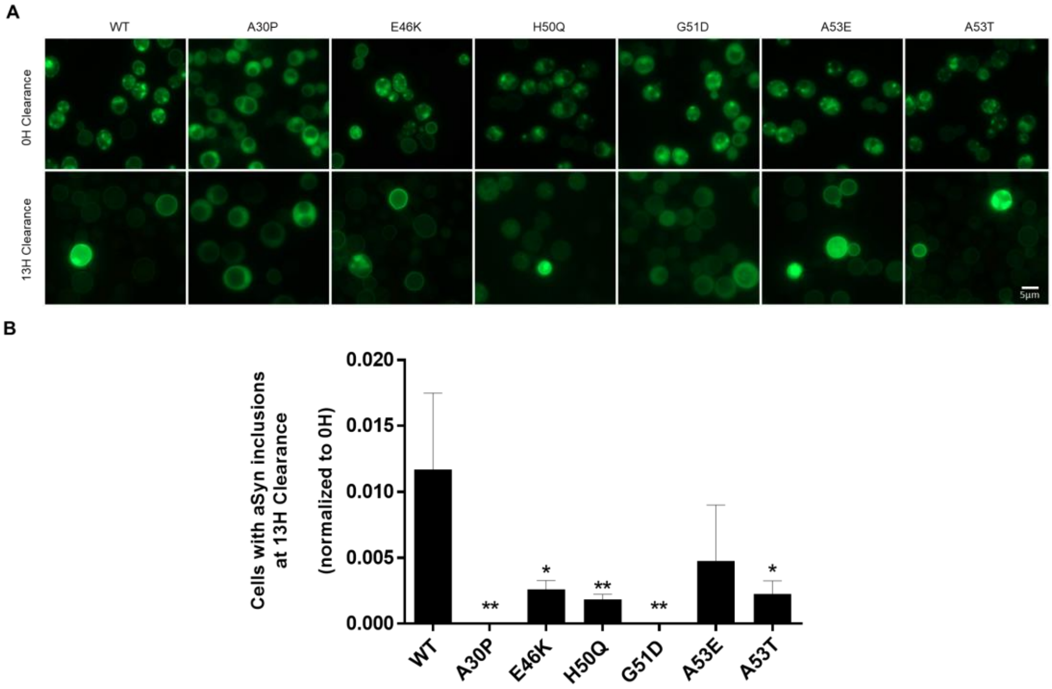

Figure 3.11 Assessment of aSyn inclusions clearance through fluorescence microscopy after 13 hours of protein clearance.

A) Intracellular localization of each aSyn mutant fused with GFP at both time points indicated in W303.1A yeast cells **B)** Percentage of cells containing aSyn-GFP inclusions before (0H Clearance) and after 13 hours of clearance (13H Clearance). Percentage values at 0H of clearance were normalized to 100% and the values at 13H of clearance were normalized to the values at 0H. (*p<0.1; two-way repeated measures ANOVA with Bonferroni's multiple comparison test; values represent mean ±SD from three independent experiments)

Protein clearance was also evaluated by Western Blot. Protein levels of total and phosphorylated aSyn at S129 were evaluated before and after 6 hours of protein clearance (Figure 3.12). Regarding total levels of aSyn, the A30P mutant presented a higher protein clearance. Nonetheless, this high clearance might be due to the high levels of total aSyn after 6 hours of protein induction (0H Clearance). Meanwhile, concerning the phosphorylated aSyn, the E46K and G51D mutants show a tendency to impair protein clearance, nevertheless there is no statistically significant differences between each aSyn variant clearance. It would be interesting to assess which clearance mechanism is being affected for each mutant, i.e., evaluate autophagy and proteasome function.

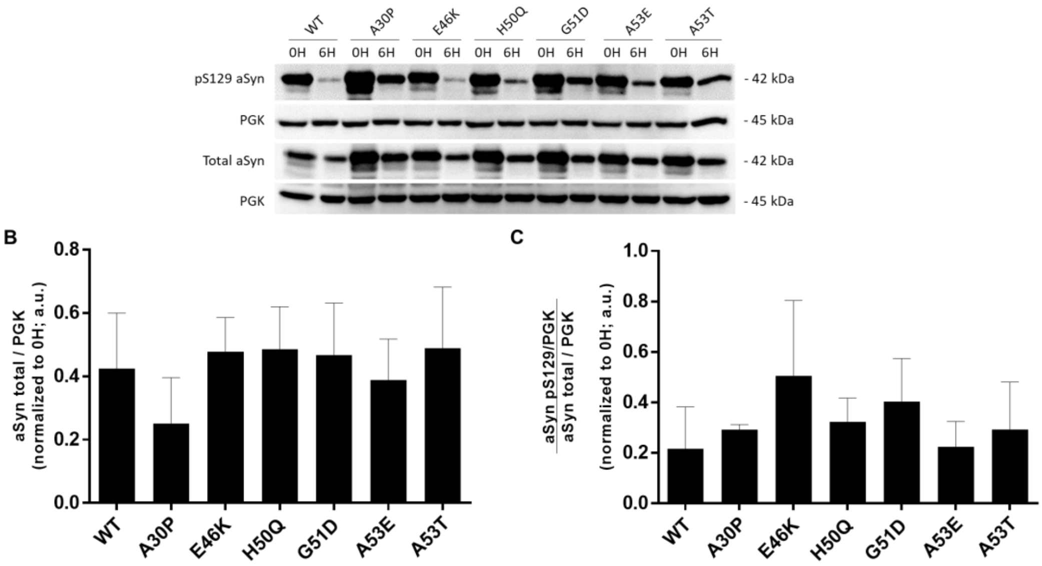

Figure 3.12 Clearance of total and phosphorylated aSyn is similar between distinct aSyn mutations.
A) Total aSyn, pS129 aSyn and PGK expression levels in W303.1A yeast cells transformed with the indicated aSyn variants assessed through Western Blot analysis of total protein extracts after 6 hours of protein expression (0H Clearance) and after 6 hours of protein clearance (6H Clearance). **B)** Total aSyn and pS129 aSyn expression levels were normalized to the respective PGK expression levels. Protein levels at 6H Clearance were normalized to levels at 0H Clearance. (two-way repeated measures ANOVA with Bonferroni's multiple comparison test; values represent mean ± SD from five biological replicas from two independent experiments)

3.5.1 Assessment of Rsp5 effect in inclusion clearance of each aSyn familial mutant

Rsp5 is a Nedd4 ortholog in *S. cerevisiae*, which was shown to promote aSyn degradation through the endosomal-vacuolar pathway and to protect from inclusion formation. In this study, we co-transformed yeast cells with a plasmid containing a Rsp5 sequence or a similar empty plasmid, with each aSyn plasmid. Inclusion formation was assessed by fluorescence microscopy at 0, 3 and 6 hours of clearance (Figure 3.13).

The results obtained were different than described by Tofaris et. al 2011. Rsp5 overexpression decreased aSyn inclusion formation only in some aSyn mutants. Regarding WT aSyn, the aSyn variant used by Tofaris et al, Rsp5 overexpression decreased inclusion formation after 3 hours of protein clearance, however, after 6 hours of protein clearance, despite the absence of significant differences, cells where Rsp5 was being overexpressed presented a higher inclusion formation than cells transformed with the control plasmid. A decrease in inclusion formation was only visible in some aSyn mutants, namely G51D, A53E and A53T. E46K aSyn mutant was the only mutant not showing any protective effect for Rsp5; this could suggest that E46K aSyn is not mainly degraded by the endosomal-vacuolar pathway or that it inhibits said pathway.

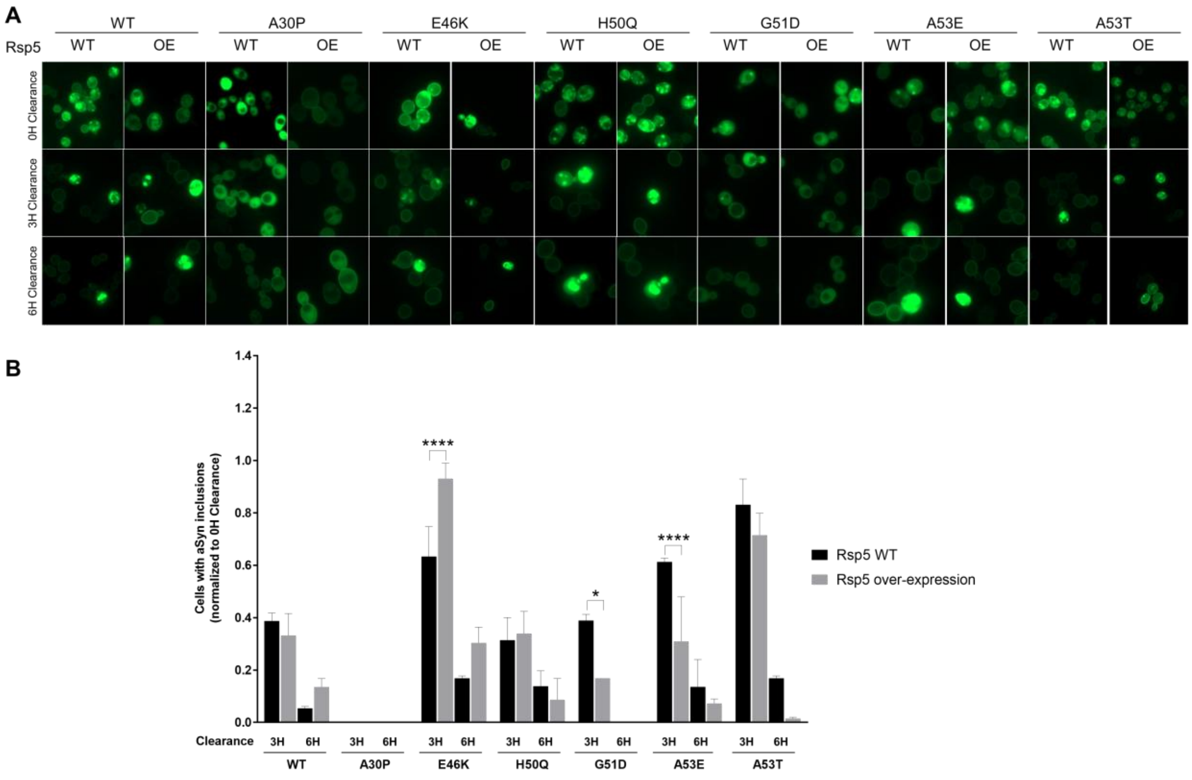

Figure 3.13 Assessment of Rsp5 effect in aSyn inclusions clearance through fluorescence microscopy after 3 and 6 hours of protein clearance.

A) Intracellular localization of each aSyn mutant fused with GFP at the time points indicated in W303.1A yeast cells co-transformed with a control plasmid or a plasmid containing a Rsp5 WT sequence. (OE – over-expression) **B)** Percentage of cells containing aSyn-GFP inclusions after 3 and 6 hours of clearance. Percentage values were normalized to the values at 0H Clearance. (*p<0.1, ****p<0.0001; two-way repeated measures ANOVA with Bonferroni's multiple comparison test; values represent mean ±SD from three independent experiments)

3.6 Vacuole acidification evaluation

Lysosomal function was found to be altered in PD, and impairment of protein degradation pathways is involved in several neurodegenerative disorders. Lysosomal acidification is required for the proper function of hydrolases involved in lysosomal degradation. In yeast cells, vacuole acidification was identified as a positive regulator for mitochondrial stability and yeast lifespan. To assess vacuolar acidification, flow cytometry was performed after 6 and 13 hours of protein induction using LysoTracker Red DND 99, a red-fluorescent probe that labels acidic organelles in live cells (Figure 3.14). LysoTracker probes contain a fluorophore connected to a weak base, since weakly basic amines accumulate in cellular compartments with low pH. They are permeant to membrane cells and typically concentrate in spherical organelles. Although, their mechanism of action is still not fully understood, but it is believed to involve protonation and retention in organelle's membranes.

LysoTracker staining revealed that A30P has a decreased vacuole acidification, when comparing to WT aSyn, which, according to Hughes and Gottschling, indicates a decrease in mitochondrial stability and yeast lifespan (Hughes and Gottschling, 2012). However, A30P was shown, both in spotting assays and flow cytometry with PI, to be less cytotoxic when comparing to the remaining aSyn variants. The observed decrease in Median Fluorescence Intensity for the A30P mutant can also be affecting hydrolases activation, reducing A30P aSyn clearance. Once again, this is not in agreement with the protein clearance assay, where A30P aSyn was shown to have a higher total aSyn clearance. Besides, A30P was shown to be highly proteolytically degraded in the vacuole, after A30P aSyn-containing vesicles merge with the vacuolar membrane with the support of Ypp1, a aSyn protective protein (Flower et al., 2007). This decrease in LysoTracker fluorescence in the A30P mutants can be a result of different vacuole morphology. Smaller vacuoles would internalize less LysoTracker and, consequently, express less fluorescence. To test this hypothesis, vacuole morphology could be assessed using probes specific for vacuoles, such as LysoTracker or FM 4-64, and visualizing at the fluorescence microscope.

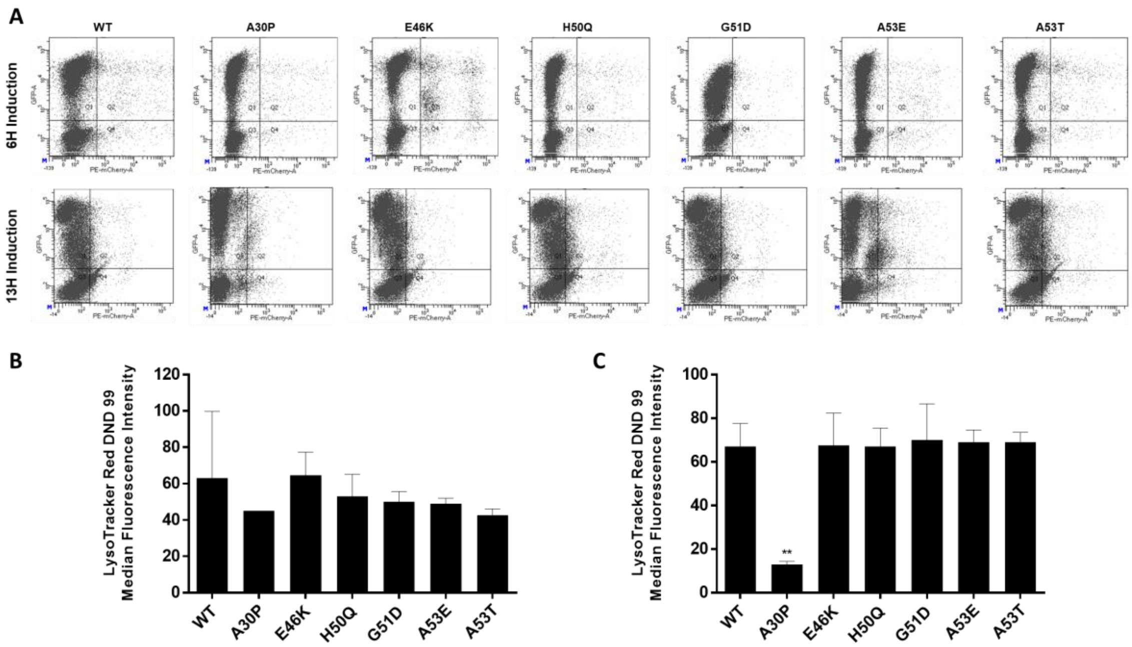

Figure 3.14 Evaluation of vacuole acidification in yeast cells transformed with each aSyn variant after 6 and 13 hours of protein induction.

A) Representative graphs of aSyn-GFP versus LysoTracker Red DND 99 fluorescence assessed through flow cytometry in W303.1A yeast cells transformed with each aSyn variant after 6 and 13 hours of protein expression. **B)** Median fluorescence intensity of each cell population after 6 hours of protein induction. **C)** Median fluorescence intensity of each cell population after 13 hours of protein induction (**p<0.01; one-way ANOVA with Bonferroni’s multiple comparison test using WT as control; values represent mean ± SD from three biological replicas)

Regarding the remaining mutants, their vacuole acidification was similar to WT aSyn, indicating a similar mitochondrial function, as well as a similar autophagy induction. This could also be assessed by evaluating autophagy flux and induction, through Western Blot, by analyzing aSyn levels before and after clearance in yeast strains where autophagy is inhibited, or using yeast cells co-transformed with aSyn variants and plasmids expressing *ATG8*, which encodes for an autophagy related protein, required for autophagosomal membranes formation, that is degraded in the vacuole. By quantifying Atg8 protein levels, it would be possible to infer autophagy induction and flux (Tenreiro et al., 2014a).

3.7 Evaluation of ROS and superoxide production

The production of ROS was evaluated through flow cytometry at 6 and 13 hours of protein induction, using DHE, a superoxide indicator (Figure 3.15). DHE usually displays blue fluorescence when in the cytosol, but when oxidized by superoxides or by other sources of ROS, it intercalates with DNA, staining the nucleus red. DHE fluorescence intensity was similar between all the aSyn mutants, having no differences when comparing to WT aSyn, i.e., the ROS production is similar amongst all aSyn variants. However, E46K and G51D seem to exhibit a more intense fluorescence, indicating a higher production of ROS. Since a higher production of ROS would induce aSyn aggregation, and vice-versa, these results are not in agreement with the inclusion formation results. However, increased ROS levels also causes oxidative stress, which leads to cell death, which is in agreement with the E46K cell viability results obtained with flow cytometry. This suggests that E46K toxicity might be mainly due to an excessive ROS production, and not due to aSyn aggregation alone.

Mitochondrial dysfunction also provokes ROS accumulation, which means that E46K and G51D could be impairing mitochondrial function, somehow, leading to ROS production and, eventually, cell death.

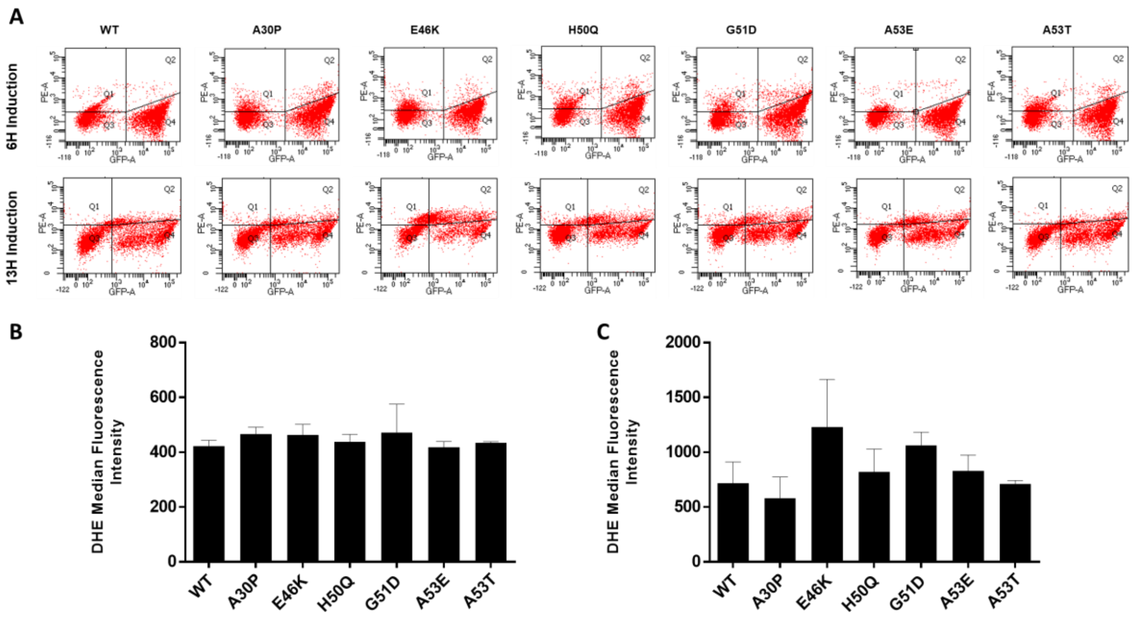

Figure 3.15 Evaluation of ROS production in yeast cells transformed with each aSyn variant after 6 and 13 hours of protein induction.

A) Representative graphs of aSyn-GFP versus DHE fluorescence assessed through flow cytometry in W303.1A yeast cells transformed with each aSyn variant after 6 and 13 hours of protein expression. **B)** Median fluorescence intensity of each cell population after 6 hours of protein induction. **C)** Median fluorescence intensity of each cell population after 13 hours of protein induction (values represent mean ± SD from three biological replicas)

3.8 CDNF effects on aSyn toxicity

3.8.1 Plasmid Construction through Gateway Recombination Technique

CDNF sequence was only available in a mammalian plasmid, so to generate constructs in yeast expression vectors with N-terminal and C-terminal fusions to fluorescent proteins and without fusion, the Gateway Recombination Cloning Technique was performed according to *Materials and Methods 2.3.2*. Three constructs were performed: (i) CDNF with no fusion; (ii) CDNF with an N-terminal fusion with Cerulean and (iii) CDNF with a C-terminal fusion with DsRed. Plasmids were sent to sequencing to confirm proper plasmid construction (*Supplementary Data*, Figure 6.2).

3.8.2 CDNF effects on cell viability, inclusion formation and aSyn expression levels

To evaluate whether the distinct CDNF constructions would affect CDNF effects, as well as to assess the putative CDNF cytoprotective effect against aSyn induced toxicity in yeast cells. W303.1A yeast cells were transformed with WT aSyn alone or co-transformed with each CDNF plasmid. Cell viability was assessed through spotting assay (Figure 3.16A), which revealed a similar aSyn cytotoxic effect in the presence of CDNF when compared to aSyn effect *per si.* Moreover, this assay allowed to conclude that, by tagging CDNF at N-terminus or C-terminus, the CDNF effect produced is similar, indicating that the tags do not affect CDNF function. The CDNF effect in the aSyn inclusions formation was also assessed through fluorescence microscopy (Figure 3.16B) after 6 hours of protein induction. CDNF tagging with both Cerulean and DsRed revealed a cytoplasmic localization. The percentage of cells with aSyn inclusions were counted to evaluate the CDNF effect in inclusion formation as well as the tags effect on CDNF function. The presence of CDNF did not affect inclusion formation, as well as the presence of each tag (Figure 3.16C).

CDNF effects on total aSyn expression levels were also evaluated through Western Blot (Figure 3.17A). There were no significant effects for each CDNF construction in the total aSyn levels (Figure 3.17B). Overall, CDNF expression did not caused any significant changes in toxicity, inclusion formation and total aSyn protein levels in yeast cells, despite the CDNF protective effect observed against aSyn oligomers in mice mesencephalon neurons cultures (Latge et al., 2015).

CDNF mechanism is still unknown, nevertheless it is believed that CDNF is involved in ER stress and UPR regulation (Voutilainen et al., 2015). Recently, it was proposed that CDNF activated the survival promoting PI3K-Akt signaling pathway (Voutilainen et al., 2017). This pathway involves the generation of PIP3 in the plasma membrane, which is responsible for activating Akt, culminating with the regulation of mammalian cell proliferation and survival. However, in *S. cerevisiae* cells, PIP3 appears to have no role in its physiology (Wera et al., 2001), ceasing the survival pathway. Accordingly, the results here obtained with no effect of CDNF expression on aSyn toxicity can be due to the non-conservation of the CDNF function in the yeast model.

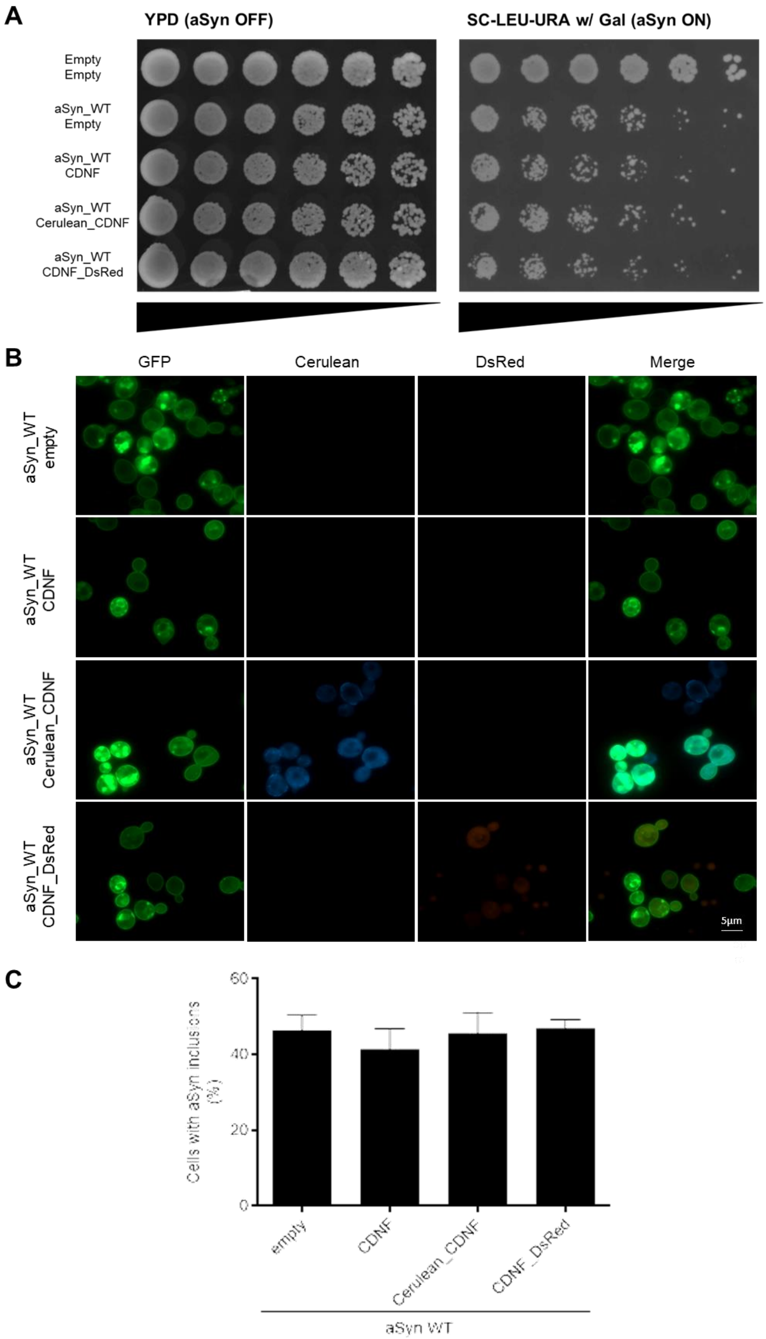

Figure 3.16 Cell viability and inclusion formation assessment through spotting assay and fluorescence microscopy, respectively.

A) Spotting assay of the indicated W303.1A yeast cells. Cell cultures were adjusted to the same OD, serially diluted, and spotted into YPD and selective media complemented with Gal as carbon source. **B)** Intracellular localization of WT aSyn and CDNF without fusion or fused with Cerulean or DsRed at N- or C-terminus, respectively, after 6 hours of protein expression. **C)** Percentage of cells containing aSyn-GFP inclusions after 6 hours of protein expression. (one-way ANOVA with Bonferroni's multiple comparison test; values represent mean ± SD from three biological replicas).

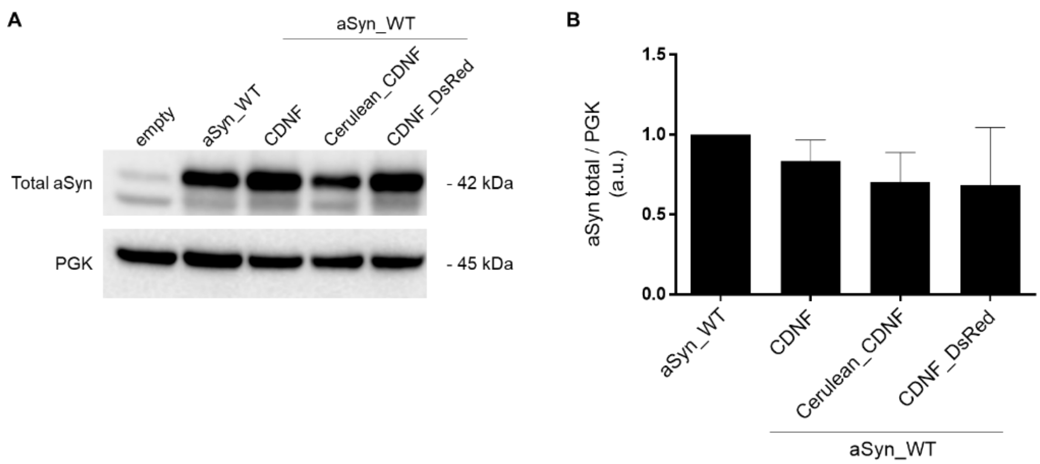

Figure 3.17 Evaluation of total aSyn levels in the presence and absence of each CDNF plasmid.

A) Total aSyn and PGK expression levels in W303.1A yeast cells transformed with the indicated CDNF variants and WT aSyn assessed by Western Blot analysis of total protein extracts after 6 hours of protein expression. **B)** Total aSyn expression levels were normalized to the PGK expression levels. Protein levels were normalized to WT aSyn. (one-way ANOVA with Bonferroni's multiple comparison test; values represent mean ± SD from three biological replicas)

4 Concluding remarks and future perspectives

PD, being the second most common neurodegenerative disease, needs, undoubtedly, a more comprehensive study. It is known that the dopaminergic neurons in the SNpC present aSyn aggregates, however, despite all the efforts, it is still unknown whether aggregation prevents or induces aSyn toxicity. Likewise, it is known that aSyn is prone to suffer several PTMs, including phosphorylation. However, it is still unclear whether phosphorylation prevents or promotes toxicity. These uncertainties are due to distinct results obtained in different cellular models.

Coding missense mutations and multiplication of the *SNCA* locus leads to familiar PD. Until now, six aSyn mutations were already identified, however, their exact effects in several cellular pathways is still not completely understood.

In this work, *S. cerevisiae* cells, being a well-established model to study PD, were used to study the effects of aSyn phosphorylation in different phosphorylation-prone residues. Similarly, toxicity of each aSyn familial mutant was also characterized using the budding yeast. Multicopy plasmids were used to express aSyn fused with GFP, under the regulation of a *GAL1* promoter.

Overexpression of each phosphomutant in yeast cells, revealed that S129 phosphorylation plays a major role, with its phosphoblockers and phosphomimics mutants presenting an effect capable of overlapping S87 phosphorylation or its blockage. Blockage of S129 phosphorylation induces a toxic effect, however, S87 phosphorylation blockade exerts a protective effect, even capable of protecting against S129 phosphoblocking. A great limitation of this work was the lack of a proper antibody specific for phosphorylated S87, making it impossible to evaluate S87 phosphorylation levels.

Regarding the Y residues, blockage of both residues revealed a protective effect in inclusion formation; however, this effect was not observed in the cell viability assay by flow cytometry, contradicting the theory that aSyn inclusion formation is related to its toxicity. The inclusion clearance assay suggested that Y125 phosphorylation impairs protein clearance, even though the differences are not significant. This could explain the observed toxicity, despite the decreased inclusion formation.

The effects of aSyn familial mutants were evaluated regarding inclusion formation, cell toxicity, protein clearance, ROS production and vacuolar acidification. Results obtained for each familial mutant, comparing to WT aSyn, are resumed in Table 4.1. In summary, A30P aSyn was revealed to be a less toxic mutation; despite E46K showing a decrease in inclusion formation, it presented the highest ROS production, suggesting that this is the mechanism by which E46K exerts its elevated toxicity; H50Q and A53T mutations presented similar results regarding inclusion formation, cell toxicity and ROS production in comparison to WT; G51D and A53E presented less inclusions, less toxicity and higher clearance, suggesting to be less toxic than WT aSyn.

Familial mutations in the *SNCA* locus induce a more severe parkinsonism with an early onset, however, the results obtained for several mutations, specially A30P, G51D and A53E aSyn, point to a lower toxicity than WT aSyn in yeast cells, while the remaining mutations presented results very similar to WT. This divergence can be due to the cellular model used. Indeed, a major limitation for the study of PD has been the inexistence of a perfect model, since every model has its advantages and limitations. For example, even *in vivo* studies in mice, were revealed to have a major limitation, since mice are not able to reproduce the DA alterations observed in PD (Burbulla et al., 2017). Yeast cells are able to reproduce several PD events; however, the yeast cellular environment is distinct than the dopaminergic neurons cellular environment. This is corroborated by the existence of several studies revealing dissimilar results in different cellular models. Indeed, it was already suggested that the result's discrepancy is due to distinct efficiencies or expression levels of distinct kinases or phosphatases in the different cellular models (Oueslati et al., 2013; Schreurs et al., 2014). Besides, the mechanisms by which each aSyn mutations is inducing toxicity might not be conserved in yeast cells.

Table 4.1 Resume table of the results obtained in distinct assays for each aSyn familial mutant.
For this table, each aSyn familial mutant was compared to WT aSyn (↑ increased results; ↓ decreased results, ≈ similar results)

	Inclusion Formation	Cell Toxicity	pS129 Levels	Protein Clearance	Lysosomal Acidification	ROS production
A30P	↓↓	↓↓	↑	↑	↓↓	≈
E46K	↓	↑	↓↓	↓	≈	↑↑
H50Q	≈	≈	↓	↑	≈	≈
G51D	↓	↓↓	↓	↑	≈	≈
A53E	↓	↑	↑	↑	≈	≈
A53T	≈	≈	↓	↓	≈	≈

Despite the rarity of familial PD cases, their exhaustive study can bring light to aSyn function and increase the understanding about this aging disorder. With this in mind, the study of each *SNCA* familial mutation should be carried on in a mammalian cellular model, since these are more similar to the affected neurons in the SNpC and different cellular models present contrasting results. Regarding the studies in *S. cerevisiae* cells, aSyn degradation should be better elucidated, to understand which degradation pathway is more prominent during aSyn clearance.

5 Bibliography

Airavaara, M.; Harvey, B. K.; Voutilainen, M. H.; Shen, H.; Chou, J.; Lindholm, P.; Lindahl, M.; Tuominen, R. K.; Saarma, M.; Wang, Y.; et al. CDNF Protects the Nigrostriatal Dopamine System and Promotes Recovery after MPTP Treatment in Mice. *Cell Transpl.* **2012a**, *21* (6), 1213–1223.

Airavaara, M.; Voutilainen, M. H.; Wang, Y.; Hoffer, B. Neurorestoration. *Park. Relat. Disord.* **2012b**, *1*, 143–146.

Anderson, J. P.; Walker, D. E.; Goldstein, J. M.; Laat, R. De; Banducci, K.; Caccavello, R. J.; Barbour, R.; Huang, J.; Kling, K.; Lee, M.; et al. Phosphorylation of Ser-129 Is the Dominant Pathological Modification of a-Synuclein in Familial and Sporadic Lewy. *J. Biol. Chem.* **2006**, *281* (40), 29739–29752.

Appel-cresswell, S.; Vilarino-guell, C.; Yu, I.; Shah, B.; Weir, D.; Thompson, C.; Szu-tu, C.; Trinh, J.; Aasly, J. O.; Rajput, A.; et al. Alpha-Synuclein P . H50Q , a Novel Pathogenic Mutation for Parkinson ' S Disease. *Mov. Disord.* **2013**, *28* (6), 811–813.

Azeredo da Silveira, S.; Schneider, B. L.; Cifuentes-diaz, C.; Sage, D.; Aebischer, P. Phosphorylation Does Not Prompt , nor Prevent , the Formation of a -Synuclein Toxic Species in a Rat Model of Parkinson ' S Disease. *Hum. Mol. Genet.* **2017**, *18* (5), 872–887.

Banerjee, K.; Sinha, M.; Le, C.; Pham, L.; Jana, S.; Chanda, D.; Cappai, R.; Chakrabarti, S. A - Synuclein Induced Membrane Depolarization and Loss of Phosphorylation Capacity of Isolated Rat Brain Mitochondria : Implications in Parkinson ' S Disease. *FEBS Lett.* **2010**, *584* (8), 1571–1576.

Baptista, M. J.; Farrell, C. O.; Daya, S.; Ahmad, R.; Miller, D. W.; Hardy, J.; Farrer, M. J.; Cookson, M. R. Co-Ordinate Transcriptional Regulation of Dopamine Synthesis Genes by a - Synuclein in Human Neuroblastoma Cell Lines. *J. Neurochem.* **2003**, *85*, 957–968.

Betarbet, R.; Sherer, T. B.; Greenamyre, J. T. Ubiquitin – Proteasome System and Parkinson ' S Diseases. *Exp. Neurol.* **2005**, *191*, S17–S27.

Bourdenx, M.; Dehay, B. What Lysosomes Actually Tell Us about Parkinson's Disease? *Ageing Res. Rev.* **2016**.

Bourdenx, M.; Stavros, N.; Sanoudou, D.; Bezard, E.; Dehay, B.; Tsarbopoulos, A. Progress in Neurobiology Protein Aggregation and Neurodegeneration in Prototypical Neurodegenerative Diseases : Examples of Amyloidopathies , Tauopathies and Synucleinopathies. *Prog. Neurobiol.* **2016**.

Brachmann, C.; Davies, A.; GJ, C.; Caputo, E.; Li, J.; Hieter, P.; JD, B. Designer Deletion Strains Derived from Saccharomyces Cerevisiae S288C: A Useful Set of Strains and Plasmids for PCR-Mediated Gene Disruption and Other Applications. *Yeast* **1998**, *14* (2), 115–132.

Breydo, L.; Wu, J. W.; Uversky, V. N. α-Synuclein Misfolding and Parkinson ' S Disease. *BBA - Mol. Basis Dis.* **2012**, *1822* (2), 261–285.

Burbulla, L. F.; Song, P.; Mazzulli, J. R.; Zampese, E.; Wong, Y. C.; Jeon, S.; Santos, D. P.; Blanz, J.; Obermaier, C. D.; Strojny, C.; et al. Dopamine Oxidation Mediates Mitochondrial and Lysosomal Dysfunction in Parkinson's Disease. *Science (80-.).* **2017**, *9080* (September), 1–12.

Burré, J.; Sharma, M.; Tsetsenis, T.; Buchman, V.; Südhof, T. C. α -Synuclein Promotes SNARE-Complex Assembly in Vivo and in Vitro. *Science (80-.).* **2010**, *329* (5999), 1663–1667.

Cabin, D. E.; Shimazu, K.; Murphy, D.; Cole, N. B.; Gottschalk, W.; Mcilwain, K. L.; Orrison, B.; Chen, A.; Ellis, C. E.; Paylor, R.; et al. Synaptic Vesicle Depletion Correlates with Attenuated Synaptic a-Synuclein. *J. Neurosci.* **2002**, *22* (20), 8797–8807.

Chaudhuri, K. R.; Schapira, A. H. V. Non-Motor Symptoms of Parkinson ' S Disease : Dopaminergic Pathophysiology and Treatment. *Lancet Neurol.* **2009**, *8* (5), 464–474.

Chen, B.; Retzlaff, M.; Roos, T.; Frydman, J. Cellular Strategies of Protein Quality Control. *Cold Spring Harb. Perspect. Biol.* **2011**, *3*, 1–14.

Chen, L.; Feany, M. B. A -Synuclein Phosphorylation Controls Neurotoxicity and Inclusion Formation in a Drosophila Model of Parkinson Disease. *Nat. Neurosci.* **2005**, *8* (5), 657–663.

Chinta, S. J.; Mallajosyula, J. K.; Rane, A.; Andersen, J. K. Mitochondrial Alpha-Synuclein Accumulation Impairs Complex I Function in Dopaminergic Neurons and Results in Increased Mitophagy in Vivo. *Neurosci Lett* **2011**, *486* (3), 235–239.

Choubey, V.; Safiulina, D.; Vaarmann, A.; Cagalinec, M.; Wareski, P.; Kuum, M.; Zharkovsky, A.; Kaasik, A. Mutant A53T a -Synuclein Induces Neuronal Death by Increasing Mitochondrial Autophagy. *J. Biol. Chem.* **2011**, *286* (12), 10814–10824.

Colacurcio, D. J.; Nixon, R. A. Disorders of Lysosomal acidification—The Emerging Role of v-ATPase in Aging and Neurodegenerative Disease. *Ageing Res. Rev.* **2016**.

Colla, E.; Jensen, P. H.; Pletnikova, O.; Troncoso, J. C.; Glabe, C.; Lee, M. K. Accumulation of Toxic a-Synuclein Oligomer within Endoplasmic Reticulum Occurs in a-Synucleinopathy In Vivo. *J. Neurosci.* **2012a**, *32* (10), 3301–3305.

Colla, E.; Coune, P.; Liu, Y.; Pletnikova, O.; Troncoso, J. C.; Schneider, B. L.; Lee, M. K. Endoplasmic Reticulum Stress Is Important for the Manfestations of a-Synucleinopathy in Vivo. *J* **2012b**, *32* (10), 3306–3320.

Cook, C.; Petrucelli, L. A Critical Evaluation of the Ubiquitin-Proteasome System. *Biochim. Biophys. Acta* **2010**, *1792* (7), 664–675.

Cooper, A. A.; Gitler, A. D.; Cashikar, A.; Haynes, C. M.; Hill, K. J.; Bhullar, B.; Liu, K.; Xu, K.; Strathearn, K. E.; Liu, F.; et al. α-Synuclein Blocks ER-Golgi Traffic and Rab1 Rescues Neuron Loss in Parkinson's Models. *Science (80-.).* **2006**, *313* (5785), 324–328.

Cuervo, A. M. Autophagy : In Sickness and in Health. *Trends Cell Biol.* **2004**, *14* (2), 70–77.

Darios, F.; Ruipérez, V.; López, I.; Villanueva, J.; Gutierrez, L. M.; Davletov, B. A-Synuclein Sequesters Arachidonic Acid to Modulate SNARE-Mediated Exocytosis. *EMBO Rep.* **2010**, *11* (7), 528–533.

Dehay, B.; Fernagut, P. Alpha-Synuclein-Based Models of Parkinson ' S Disease. *Rev. Neurol. (Paris).* **2016**, 4–11.

Dehay, B.; Bove, J.; Rodríguez-muela, N.; Perier, C.; Recasens, A.; Boya, P.; Vila, M. Pathogenic Lysosomal Depletion in Parkinson' S Disease. *J. Neurosci.* **2010**, *30* (37), 12535–12544.

Desplats, P.; Spencer, B.; Coffee, E.; Patel, P.; Michael, S.; Patrick, C.; Adame, A.; Rockenstein, E.; Masliah, E. A-Synuclein Sequesters Dnmt1 from the Nucleus - A NOVEL MECHANISM FOR EPIGENETIC ALTERATIONS IN LEWY BODY DISEASES. *J. Biol. Chem.* **2011**, *286* (11), 9031–9037.

Devi, L.; Raghavendran, V.; Prabhu, B. M.; Avadhani, N. G.; Anandatheerthavarada, H. K. Mitochondrial Import and Accumulation of ⎵ -Synuclein Impair Complex I in Human Dopaminergic Neuronal Cultures and Parkinson Disease Brain * □. *J. Biol. Chem.* **2008**, *283* (14), 9089–9100.

Dexter, D. T.; Jenner, P. Parkinson Disease : From Pathology to Molecular Disease Mechanisms. *Free Radic. Biol. Med.* **2013**, *62*, 132–144.

Dias, V.; Junn, E.; Mouradian, M. M. The Role of Oxidative Stress in Parkinson's Disease. *2Journal Park. Dis.* **2013**, *3* (4), 461–491.

Diciccio, J. E.; Steinberg, B. E. Lysosomal pH and Analysis of the Counter Ion Pathways That Support Acidification. *J. Gen. Physiol.* **2011**, *137* (4), 385–390.

Doyle, K. M.; Kennedy, D.; Gorman, A. M.; Gupta, S.; Healy, S. J. M.; Samali, A. Unfolded Proteins and Endoplasmic Reticulum Stress in Neurodegenerative Disorders. *J. Cell. Mol. Med.* **2011**, *15* (10), 2025–2039.

Duina, A. A.; Miller, M. E.; Keeney, J. B. Budding Yeast for Budding Geneticists : A Primer on the Saccharomyces Cerevisiae Model System. *Genetics* **2014**, *197* (May), 33–48.

Dunning, C. J. R.; Reyes, J. F.; Steiner, J. A.; Brundin, P. Progress in Neurobiology Can Parkinson ' S Disease Pathology Be Propagated from One Neuron to Another ? *Prog. Neurobiol.* **2012**, *97* (2), 205–219.

Ebrahimi-fakhari, D.; Cantuti-castelvetri, I.; Fan, Z.; Masliah, E.; Hyman, B. T.; Mclean, P. J.; Vivek, K. Distinct Roles in Vivo for the Ubiquitin-Proteasome System and the Autophagy-Lysosomal Pathway in the Degradation of a-Synuclein. *J. Neurosci.* **2011**, *31* (41), 14508–14520.

Eftekharzadeh, B.; Hyman, B. T.; Wegmann, S. Structural Studies on the Mechanism of Protein Aggregation in Age Related Neurodegenerative Diseases. *Mech. Ageing Dev.* **2016**, *156*, 1–13.

Eisenberg, D.; Jucker, M. The Amyloid State of Proteins in Human Diseases. *Cell* **2012**, *148* (6), 1188–1203.

Fares, M.; Ait-bouziad, N.; Dikiy, I.; Mbefo, M. K.; Jovic, A.; Kiely, A.; Holton, J. L.; Lee, S.; Gitler, A. D.; Eliezer, D.; et al. The Novel Parkinson's Disease Linked Mutation G51D Attenuates in Vitro Aggregation and Membrane Binding of a-Synuclein , and Enhances Its Secretion and Nuclear Localization in Cells. *Hum. Mol. Genet.* **2014**, *23* (17), 4491–4509.

Flower, T. R.; Clark-dixon, C.; Metoyer, C.; Yang, H.; Shi, R.; Zhang, Z.; Witt, S. N. YGR198w (YPP1) Targets A30P a-Synuclein to the Vacuole for Degradation. *J. Cell Biol.* **2007**, *177* (6), 1091–1104.

Forgac, M. Vacuolar ATPases : Rotary Proton Pumps in Physiology and Pathophysiology. *Nat. Rev.* **2007**, *8* (November), 917–929.

Franssens, V.; Bynens, T.; Brande, J. Van Den; Vandermeeren, K.; Verduyckt, M.; Winderickx, J. The Benefits of Humanized Yeast Models to Study Parkinson ' S Disease. *Oxid. Med. Cell. Longev.* **2013**.

Fujiwara, H.; Hasegawa, M.; Dohmae, N.; Kawashima, A.; Masliah, E.; Goldberg, S.; Shen, J.; Takio, K.; Iwatsubo, T. α -Synuclein Is Phosphorylated in Synucleinopathy Lesions. *Nat. Cell Biol.* **2002**, *4* (February 2002), 160–164.

Fusco, G.; Pape, T.; Stephens, A. D.; Mahou, P.; Costa, A. R.; Kaminski, C. F.; Schierle, G. S. K.; Vendruscolo, M.; Veglia, G.; Dobson, C. M.; et al. Structural Basis of Synaptic Vesicle Assembly Promoted by a-Synuclein. *Nat. Commun.* **2016**, *7* (12563), 1–11.

George, J. M. The Synucleins. *Genome Biol.* **2001**, *3* (1), 1–6.

Ghosh, D.; Mondal, M.; Mohite, G. M.; Singh, P. K.; Ranjan, P.; Anoop, A.; Ghosh, S.; Jha, N. N.; Kumar, A.; Maji, S. K. The Parkinson ' S Disease-Associated H50Q Mutation Accelerates α-Synuclein Aggregation in Vitro. *Biochemistry* **2013**, *52*, 6925–6927.

Ghosh, D.; Sahay, S.; Ranjan, P.; Salot, S.; Mohite, G. M.; Singh, P. K.; Dwivedi, S.; Carvalho, E.; Banerjee, R.; Kumar, A.; et al. The Newly Discovered Parkinson ' S Disease Associated Finnish Mutation (A53E) Attenuates α-Synuclein Aggregation and Membrane Binding. *Biochemistr* **2014**, *53* (41), 6419–6421.

Giasson, B. I.; Murray, I. V. J.; Trojanowski, J. Q.; Lee, V. M.-Y. A Hydrophobic Stretch of 12 Amino Acid Residues in the Middle of a-Synuclein Is Essential for Filament Assembly. *J. Biol. Chem.* **2001**, *276* (4), 2380–2386.

Gitler, A. D. Beer and Bread to Brains and Beyond : Can Yeast Cells Teach Us about Neurodegenerative Disease ? *Neurosignals.* **2008**, *16*, 52–62.

Goffeau, A.; Barrell, B. G.; Bussey, H.; Davis, R. W.; Dujon, B.; Feldmann, H.; Galibert, F.; Hoheisel, J. D.; Jacq, C.; Johnston, M.; et al. Life with 6000 Genes. *Science (80-.).* **1996**, *274* (5287), 546 LP – 567.

Gorbatyuk, O. S.; Li, S.; Sullivan, L. F.; Chen, W.; Kondrikova, G.; Manfredsson, F. P.; Mandel, R. J.; Muzyczka, N. The Phosphorylation State of Ser-129 in Human a-Synuclein Determines Neurodegeneration in a Rat Model of Parkinson Disease. *PNAS* **2008**, *105* (2), 763–768.

Guardia-Laguarta, C.; Area-gomez, E.; Schon, E. A.; Przedborski, S. A New Role for a -Synuclein in Parkinson ' S Disease : Alteration of ER – Mitochondrial Communication. *Mov. Disord.* **2015**, *30* (8), 1026–1033.

Gureviciene, I.; Gurevicius, K.; Tanila, H. Role of α -Synuclein in Synaptic Glutamate Release. *Neurobiol. Dis.* **2007**, *28*, 83–89.

Haitani, Y.; Nakata, M.; Sasaki, T.; Uchida, A.; Takagi, H. Engineering of the Yeast Ubiquitin Ligase Rsp5 : Isolation of a New Variant That Induces Constitutive Inactivation of the General Amino Acid Permease Gap1. *FEMS Yeast Res* **2008**, *9*, 73–86.

Hegde, M. L.; Rao, K. S. J. Challenges and Complexities of a -Synuclein Toxicity: New Postulates in Unfolding the Mystery Associated with Parkinson's Disease. *Arch. Biochem. Biophys.* **2003**, *418*, 169–178.

Heras-Sandoval, D.; Pérez-Rrojas, J. M.; Hernández-Damián, J.; Pedraza-Chaverri, J. The Role of PI3K/AKT/mTOR Pathway in the Modulation of Autophagy and the Clearance of Protein Aggregates in Neurodegeneration. *Cell. Signal.* **2014**, *26* (12), 2694–2701.

Hernandez, D. G.; Reed, X.; Singleton, A. B. Genetics in Parkinson Disease: Mendelian versus Non-Mendelian Inheritance. *J. Neurochem.* **2016**, *41* (Special Issue on Parkinson's Disease), 1–16.

Hirsch, L.; Steeves, T. The Incidence of Parkinson's Disease : A Systematic Review and Meta-Analysis. *Neuroepidemiology* **2016**, *46*, 292–300.

Hughes, A. L.; Gottschling, D. E. An Early-Age Increase in Vacuolar pH Limits Mitochondrial Function and Lifespan in Yeast. *Nature* **2012**, *492* (7428), 261–265.

Imaizumi, N.; Kwang, K.; Zhang, C.; Boelsterli, U. A. Mechanisms of Cell Death Pathway Activation Following Drug-Induced Inhibition of Mitochondrial Complex I. *Redox Biol.* **2015**, *4*, 279–288.

Íñigo-Marco, I.; Valencia, M.; Larrea, L.; Bugallo, R.; Martínez-goikoetxea, M. E46K α -Synuclein Pathological Mutation Causes Cell-Autonomous Toxicity without Altering Protein Turnover or Aggregation. *PNAS* **2017**, 1–10.

Janezic, S.; Threlfell, S.; Dodson, P. D.; Dowie, M. J.; Taylor, T. N. De Ficits in Dopaminergic Transmission Precede Neuron Loss and Dysfunction in a New Parkinson Model. *PNAS* **2013**, *110* (42), E4016–E4025.

Junn, E.; Mouradian, M. M. Human a-Synuclein over-Expression Increases Intracellular Reactive Oxygen Species Levels and Susceptibility to Dopamine. *Neurosci. Lett.* **2002**, *320*, 146–150.

Kalia, L. V; Lang, A. E.; Shulman, G. Parkinson ' S Disease. *Lancet* **2015**, *386* (9996), 896–912.

Kasten, M.; Klein, C. The Many Faces of Alpha-Synuclein Mutations. *Mov. Disord.* **2013**, *28* (6), 697–701.

Khalaf, O.; Fauvet, B.; Oueslati, A.; Dikiy, I.; Ruggeri, F. S.; Mbefo, M. K.; Vercruysse, F.; Dietler, G.; Lee, S.; Eliezer, D.; et al. The H50Q Mutation Enhances a-Synuclein Aggregation , Secretion , and Toxicity. *J. Biol. Chem.* **2014**, *289* (32), 21856–21876.

Kim, E. J.; Sung, J. Y.; Lee, H. J.; Rhim, H.; Hasegawa, M.; Iwatsubo, T.; Min, D. S.; Kim, J.; Paik, S. R.; Chung, K. C. Dyrk1A Phosphorylates a-Synuclein and Enhances Intracellular Inclusion Formation *. *J. Biol. Chem.* **2006**, *281* (44), 33250–33257.

Kleinknecht, A.; Popova, B.; Lázaro, D. F.; Pinho, R. C-Terminal Tyrosine Residue Modifications Modulate the Protective Phosphorylation of Serine 129 of α -Synuclein in a Yeast Model of Parkinson ' S Disease. *PLoS Genet.* **2016**, *12* (6), 1–39.

Kontopoulos, E.; Parvin, J. D.; Feany, M. B. A-Synuclein Acts in the Nucleus to Inhibit Histone Acetylation and Promote Neurotoxicity. *Hum. Mol. Genet.* **2006**, *15* (20), 3012–3023.

Krüger, R.; Kuhn, W.; Müller, T.; Woitalla, D.; Graeber, M.; Kösel, S.; Przuntek, H.; Epplen, J. T.; Scöls, L.; Riess, O. Ala30Pro Mutation in the Gene Encoding a-Synuclein in Parkinson's Disease. *Nat. Genet.* **1998**, *18* (2), 106–108.

Kumer, S. C.; Vrana, K. E. Intricate Regulation of Tyrosine Hydroxylase Activity and Gene Expression. *J. Neurochem.* **1996**, *67*, 443–462.

Kuwahara, T.; Tonegawa, R.; Ito, G.; Mitani, S.; Iwatsubo, T. Phosphorylation of a-Synuclein Protein at Ser-129 Reduces Neuronal Dysfunction by Lowering Its Membrane Binding Property in Caenorhabditis Elegans. *J. Biol. Chem.* **2012**, *287* (10), 7098–7109.

Larsen, K. E.; Schmitz, Y.; Troyer, M. D.; Mosharov, E.; Dietrich, P.; Quazi, A. Z.; Savalle, M.; Nemani, V.; Chaudhry, F. A.; Edwards, R. H.; et al. A-Synuclein Overexpression in PC12 and Chromaffin Cells Impairs Catecholamine Release by Interfering with a Late Step in Exocytosis. *J. Neurosci.* **2006**, *26* (46), 11915–11922.

Latge, C.; Cabral, K. M. S.; de Oliveira, G. A. P.; Raymundo, D. P.; Freitas, J. A.; Johanson, L.; Romão, L. F.; Palhano, F. L.; Herrmann, T.; Almeida, M. S.; et al. The Solution Structure and Dynamics of Full-Length Human Cerebral Dopamine Neurotrophic Factor and Its Neuroprotective Role against a -Synuclein Oligomers. *J. Biol. Chem.* **2015**, *290* (33), 20527–20540.

Lau, L. M. L. De; Breteler, M. M. B. Epidemiology of Parkinson ' S Disease. **2006**, *5* (June), 525–535.

Lautenschläger, J.; Kaminski, C. F.; Kaminski Schierle, G. S. α-Synuclein – Regulator of Exocytosis, Endocytosis, or Both? *Trends Cell Biol.* **2017**, *27* (7), 468–479.

Lavedan, C. The Synuclein Family. *Genome Res.* **1998**, *8*, 871–880.

Lázaro, D. F.; Rodrigues, E. F.; Langohr, R.; Shahpasandzadeh, H.; Ribeiro, T.; Guerreiro, P.; Gerhardt, E.; Kröhnert, K.; Klucken, J.; Pereira, M. D.; et al. Systematic Comparison of the Effects of Alpha-Synuclein Mutations on Its Oligomerization and Aggregation. *PLoS Genet.* **2014**, *10* (11).

Lee, J.; Yu, W. H.; Kumar, A.; Lee, S.; Mohan, P. S.; Peterhoff, C. M.; Wolfe, D. M.; Martinez-vicente, M.; Massey, A. C.; Uchiyama, Y.; et al. Lysosomal Proteolysis and Autophagy Require Presenilin 1 and Are Disrupted by Alzheimer-Related PS1 Mutations. *Cell* **2013**, *141* (7), 1146–1158.

Lesage, S.; Anheim, M.; Letournel, F.; Bousset, L.; Pieri, L.; Madiona, K.; Alexandra, D.; Melki, R.; Verny, C.; Brice, A. G51D a -Synuclein Mutation Causes a Novel Parkinsonian – Pyramidal Syndrome. *Ann. Neurol.* **2013**, *73*, 459–471.

Li, J.; Uversky, V. N.; Fink, A. L. Effect of Familial Parkinson ' S Disease Point Mutations A30P and A53T on the Structural Properties , Aggregation , and Fibrillation of Human a-Synuclein †. *Biochemistryhemistr* **2001**, *40*, 11604–11613.

Lindahl, M.; Saarma, M.; Lindholm, P. Unconventional Neurotrophic Factors CDNF and MANF : Structure , Physiological Functions and Therapeutic Potential. *Neurobiol. Dis.* **2017**, *97*, 90–102.

Lindholm, P.; Voutilainen, M. H.; Laurén, J.; Peränen, J.; Leppänen, V.; Andressoo, J.-O.; Lindahl, M.; Janhunen, S.; Kalkkinen, N.; Timmusk, T.; et al. Novel Neurotrophic Factor CDNF Protects and Rescues Midbrain Dopamine Neurons in Vivo. *Nature* **2007**, *448* (July), 73–78.

Liu, G.; Zhang, C.; Yin, J.; Li, X.; Cheng, F.; Li, Y.; Yang, H. A-Synuclein Is Differentially Expressed in Mitochondria from Different Rat Brain Regions and Dose-Dependently down-Regulates Complex I Activity. *Neurosci. Lett.* **2009**, *454*, 187–192.

Liu, S.; Ninan, I.; Antonova, I.; Battaglia, F.; Trinchese, F.; Narasanna, A.; Kolodilov, N.; Dauer, W.; Hawkins, D.; Arancio, O. A -Synuclein Produces a Long-Lasting Increase in Neurotransmitter Release. *EMBO J.* **2004**, *23* (22), 4506–4516.

Madaleno, C. da S. Alpha-Synuclein Phosphorylation Role on Parkinson's Disease, Universidade de Lisboa, 2017.

Mahul-Mellier, A.-L.; Fauvet, B.; Gysbers, A.; Dikiy, I.; Oueslati, A.; Georgeon, S.; Lamontanara, A. J.; Bisquertt, A.; Eliezer, D.; Masliah, E.; et al. C-Abl Phosphorylates a -Synuclein and Regulates Its Degradation : Implication for a -Synuclein Clearance and Contribution to the Pathogenesis of Parkinson ' S Disease. *Hum. Mol. Genet.* **2014**, *23* (11), 2858–2879.

Maroteaux, L.; Campanelli, J. T.; Scheller, R. H. Synuclein : A Neuron-Specific Presynaptic Nerve Terminal Protein Localized to the Nucleus and Presynaptic Nerve Terminal. *J. Neurosci.* **1988**, *8* (August), 2804–2815.

Massano, J.; Ferreira, M. An Updated Review of Parkinson ' S Disease Genetics and Clinicopathological Correlations. *Acta Neurol. Scand.* **2016**, No. May, 1–12.

Mbefo, M. K.; Fares, M.; Paleologou, K.; Oueslati, A.; Yin, G.; Tenreiro, S.; Pinto, M.; Outeiro, T.; Zweckstetter, M.; Masliah, E.; et al. Parkinson Disease Mutant E46K Enhances ␣ -Synuclein Phosphorylation in Mammalian Cell Lines , in Yeast , and in Vivo *. **2015**, *290* (15), 9412–9427.

Mclean, P. J.; Kawamata, H.; Hyman, B. T. A-Synuclein- Enhanced Green Fluorescent Protein Fusion Proteins Form Proteasome Sensitive Inclusions in Primary Neurons. *Neuroscience* **2001**, *104* (3), 901–912.

Menezes, R.; Tenreiro, S.; Macedo, D.; Santos, C. N.; Outeiro, T. F. From the Baker to the Bedside : Yeast Models of Parkinson ' S Disease. **2015**, *2* (8), 262–279.

Middleton, E. R.; Rhoades, E. Effects of Curvature and Composition on a-Synuclein Binding to Lipid Vesicles. *Biophys. J.* **2010**, *99* (7), 2279–2288.

Mukaetova-Ladinska, E. B.; McKeith, I. G. Pathophysiology of Synuclein Aggregation in Lewy Body Disease. *Mech. Ageing Dev.* **2006**, *127*, 188–202.

Mumberg, D.; Müller, R.; Funk, M. Yeast Vectors for the Controlled Expression of Heterologous Proteins in Different Genetic Backgrounds. *Gene* **1995**, *156*, 119–122.

Muntané, G.; Ferrer, I.; Martinez-Vicente, M. Synuclein Phosphorilation and Truncation Are Normal Events in the Adult Human Brain. *Neuroscience* **2012**, *200*, 106–119.

Narhi, L.; Wood, S. J.; Steavenson, S.; Jiang, Y.; Wu, G. M.; Anafi, D.; Kaufman, S. A.; Martin, F.; Sitney, K.; Denis, P.; et al. Both Familial Parkinson's Disease Mutations Accelerate a-Synuclein Aggregation. *J. Biol. Chem.* **1999**, *274* (14), 9843–9846.

Nemani, V. M.; Lu, W.; Berge, V.; Nakamura, K.; Onoa, B.; Lee, M. K.; Chaudhry, F. A.; Nicoll, R. A.; Edwards, R. H. Increased Expression of a -Synuclein Reduces Neurotransmitter Release by Inhibiting Synaptic Vesicle Reclustering after Endocytosis. *Neuron* **2010**, *65* (1), 66–79.

Noyce, A. J.; Lees, A. J.; Schrag, A.; Weston, R. L. The Prediagnostic Phase of Parkinson ' S Disease. *J Neurol Neurosurg Psychiatry* **2016**, *87*, 871–878.

Oldfield, C. J.; Dunker, A. . Intrinsically Disordered Proteins and Intrisically Disorder Protein Regions. *Annu. Rev. Biochem* **2014**, *83*, 553–584.

Oueslati, A. Implication of Alpha-Synuclein Phosphorylation at S129 in Synucleinopathies : What Have We Learned in the Last Decade ? *J. Parkinsons. Dis.* **2016**, *6*, 39–51.

Oueslati, A.; Fournier, M.; Lashuel, H. A. *Role of Post-Translational Modifications in Modulating the Structure , Function and Toxicity of a-Synuclein : Implications for Parkinson ' S Disease Pathogenesis and Therapies*; Elsevier B.V., 2010; Vol. 183.

Oueslati, A.; Schneider, B. L.; Aebischer, P.; Lashuel, H. A. Polo-like Kinase 2 Regulates Selective Autophagic α -Synuclein Clearance and Suppresses Its Toxicity in Vivo. *PNAS* **2013**, *110* (41), E3945–E3954.

Outeiro, T. F.; Lindquist, S. Yeast Cells Provide Insight into Alpha-Synuclein Biology and Pathobiology. *Science (80-.).* **2003**, *302* (5651), 1772–1775.

Ozansoy, M.; Ba, A. N. The Central Theme of Parkinson ' S Disease : α -Synuclein. **2013**, No. October 2012, 460–465.

Padmaraju, V.; Bhaskar, J. J.; Rao, U. J. S. P.; Salimath, P. V. Role of Advanced Glycation on Aggregation and DNA Binding Properties of a-Synuclein. *J. Alzheimer's Dis.* **2011**, *24*, 211–221.

Paillusson, S.; Gomez, P.; Radu, S.; Daniel, S.; Paul, L.; Devine, M. J.; Noble, W.; Hanger, D. P.; Miller, C. C. J. α-Synuclein Binds to the ER – Mitochondria Tethering Protein VAPB to Disrupt Ca2+ Homeostasis and Mitochondrial ATP Production. *Acta Neuropathol.* **2017**, *134* (1), 129–149.

Paleologou, K. E.; Schmid, A. W.; Rospigliosi, C. C.; Kim, H.; Lamberto, G. R.; Fredenburg, R. A.; Lansbury, P. T.; Fernandez, C. O.; Eliezer, D.; Zweckstetter, M.; et al. Phosphorylation at Ser-129 but Not the Phosphomimics S129E / D Inhibits the Fibrillation of a-Synuclein. *J. Biol. Chem.* **2008**, *283* (24), 16895–16905.

Paleologou, K. E.; Oueslati, A.; Shakked, G.; Rospigliosi, C. C.; Kim, H.-Y.; Lamberto, G. R.; Fernandez, C. O.; Schmid, A.; Chegini, F.; Gai, W. P.; et al. Phosphorylation at S87 Is Enhanced in Synucleinopathies, Inhibits a-Synuclein Oligomerization and Influences Synuclein-Membrane Interactions. *J Neurosci* **2010**, *30* (9), 3184–3198.

Pandey, N.; Schmidt, R. E.; Galvin, J. E. The Alpha-Synuclein Mutation E46K Promotes Aggregation in Cultured Cells. *Exp. Neurol.* **2006**, *197*, 515–520.

Parihar, M. S.; Parihar, A.; Fujita, M.; Hashimoto, M.; Ghafourifar, P. Mitochondrial Association of Alpha-Synuclein Causes Oxidative Stress. *Cell. Mol. Fife Sci.* **2008**, *65*, 1272–1284.

Parihar, M. S.; Parihar, A.; Fujita, M.; Hashimoto, M.; Ghafourifar, P. Alpha-Synuclein Overexpression and Aggregation Exacerbates Impairment of Mitochondrial Functions by Augmenting Oxidative Stress in Human Neuroblastoma Cells. *Int. J. Biochem. Cell Biol.* **2009**, *41*, 2015–2024.

Pasanen, P.; Myllykangas, L.; Siitonen, M.; Raunio, A.; Kaakkola, S.; Lyytinen, J.; Tienari, P. J.; Pöyhönen, M.; Paetau, A. A Novel a -Synuclein Mutation A53E Associated with Atypical Multiple System Atrophy and Parkinson ' S Disease-Type Pathology. *Neurobiol. Aging* **2014**, *35* (9), 2180.e1–e2180.e5.

Paxinou, E.; Chen, Q.; Weisse, M.; Giasson, B. I.; Norris, E. H.; Rueter, S. M.; Trojanowski, J. Q.; Lee, V. M.; Ischiropoulos, H. Induction of a-Synuclein Aggregation by Intracellular Nitrative Insult. *J. Neurosci.* **2001**, *21* (20), 8053–8061.

Peelaerts, W.; Baekelandt, V. α-Synuclein Strains and the Variable Pathologies of Synucleinopathies. *J. Neurochem.* **2016**, *41* (Special Issue on Parkinson's Disease), 1–19.

Perez, R. G.; Waymire, J. C.; Lin, E.; Liu, J. J.; Guo, F.; Zigmond, M. J. A Role for a-Synuclein in the Regulation of Dopamine Biosynthesis. *J. Neurosci.* **2002**, *22* (8), 3090–3099.

Perier, C.; Tieu, K.; Guégan, C.; Caspersen, C.; Jackson-lewis, V.; Carelli, V.; Martinuzzi, A.; Hirano, M.; Przedborski, S.; Vila, M. Complex I Deficiency Primes Bax-Dependent Neuronal Apoptosis through Mitochondrial Oxidative Damage. *PNAS* **2005**, *102* (52), 19126–19131.

Petroi, D.; Popova, B.; Taheri-talesh, N.; Irniger, S.; Shahpasandzadeh, H. Aggregate Clearance of a-Synuclein in Saccharomyces Cerevisiae Depends More on Autophagosome and Vacuole Function Than on the Proteasome. *J. Biol. Chem.* **2012**, *287* (33), 27567–27579.

Petrova, P. S.; Raibekas, A.; Pevsner, J.; Vigo, N.; Moore, M. K.; Peaire, A. E.; Shridhar, V.; Smith, D. I.; Kelly, J.; Durocher, Y.; et al. MANF - A New Mesencephalic, Astrocyte-Derived Neurotrophic Factor with Selectivety for Dopaminergic Neurons. *J. Mol. Neurosci.* **2003**, *20*, 173–187.

Petrucci, S.; Ginevrino, M.; Maria, E. Phenotypic Spectrum of Alpha-Synuclein Mutations : New Insights from Patients and Cellular Models. *Park. Relat. Disord.* **2016**, *22*, S16–S20.

Polymeropoulos, M. H.; Lavedan, C.; Leroy, E.; Ide, S. E.; Dehejia, A.; Dutra, A.; Pike, B.; Root, H.; Rubenstein, J.; Boyer, R.; et al. Mutation in the α -Synuclein Gene Identified in Families with Parkinson ' S Disease Mutation in the a-Synuclein Gene Identified in Families with Parkinson ' S Disease. *Science (80-.).* **1997**, *276*, 2045–2047.

Popova, B.; Kleinknecht, A.; Braus, G. H. Posttranslational Modifications and Clearing of α-Synuclein Aggregates in Yeast. *Biomolecules* **2015**, *5*, 617–634.

Proukakis, C.; Dudzik, C. G.; Brier, T.; Mackay, D. S.; Cooper, J. M.; Millhauser, G. L.; Houlden, H.; Schapira, A. H. V. A Noval a-Synuclein Missense Mutation in Parkison's Disease. *Neurology* **2013**, *80*, 1062–1064.

Rasband, W. S. ImageJ https://imagej.nih.gov/ij/.

Rodríguez-Escudeiro, I.; Roelants, F. M.; Thorner, J.; Nombela, C.; Molina, M.; Cid, V. J. Reconstitution of the Mammalian PI3K / PTEN / Akt Pathway in Yeast. *Biochem J* **2005**, *390*, 613–623.

Rotin, D.; Kumar, S. Physiological Functions of the HECT Family of Ubiquitin Ligases. *Nat. Rev.* **2009**, *10* (June), 398–409.

Rubinsztein, D. C.; Marin, G.; Kroemer, G. Autophagy and Aging. *Cell* **2011**, *146*, 682–695.

Rutherford, N. J.; Giasson, B. I. The A53E a-Synuclein Pathological Mutation Demonstrates Reduced Aggregation Propensity in Vitro and in Cell Culture. *Neurosci. Lett.* **2016**, *597*, 43–48.

Rutherford, N. J.; Moore, B. D.; Golde, T. E.; Giasson, B. I. Divergent Effects of the H50Q and G51D SNCA Mutations on the Aggregation of a-Synuclein. *J. Neurochem.* **2014**, *131*, 859–867.

Samuel, F.; Flavin, W. P.; Iqbal, S.; Pacelli, C.; Sri Renganathan, S. D.; Trudeau, L.-E.; Campbell, E. M.; Fraser, P. E.; Tandon, A. Effects of Serine 129 Phosphorylation in a-Synuclein Aggregation, Membrane Association, and Internalization. *J. Biol. Chem.* **2016**, *291*, 4374–4385.

Sancenon, V.; Lee, S.; Patrick, C.; Griffith, J.; Paulino, A.; Outeiro, T. F.; Reggiori, F.; Masliah, E.; Muchowski, P. J. Suppression of a -Synuclein Toxicity and Vesicle Trafficking Defects by Phosphorylation at S129 in Yeast Depends on Genetic Context. **2012**, *21* (11), 2432–2449.

Schreurs, S.; Gerard, M.; Derua, R.; Waelkens, E.; Taymans, J. In Vitro Phosphorylation Does Not Influence the Aggregation Kinetics of WT α -Synuclein in Contrast to Its Phosphorylation Mutants. *Int. J. Mol. Sci.* **2014**, *15*, 1040–1067.

Scott, D. A.; Tabarean, I.; Tang, Y.; Cartier, A.; Masliah, E.; Roy, S. A Pathologic Cascade Leading to Synaptic Dysfunction in a-Synuclein-Induced Neurodegeneration. *Neurobiol. Dis.* **2010**, *30* (24), 8083–8095.

Sidhu, A.; Wersinger, C.; Vernier, P. Does Alpha-Synuclein Modulate Dopaminergic Synaptic Content and Tone at the Synapse? *FASEB J.* **2004**, *18* (6), 637–647.

Smith, W. W.; Jiang, H.; Pei, Z.; Tanaka, Y.; Morita, H.; Sawa, A.; Dawson, V. L.; Dawson, T. M.; Ross, C. A. Endoplasmic Reticulum Stress and Mitochondrial Cell Death Pathways Mediate A53T Mutant Alpha-Synuclein-Induced Toxicity. *Hum. Mol. Genet.* **2005**, *14* (24), 3801–3811.

Stefanis, L.; Larsen, K. E.; Rideout, H. J.; Sulzer, D.; Greene, L. A. Expression of A53T Mutant But Not Wild-Type a-Synuclein in PC12 Cells Induces Alterations of the Ubiquitin-Dependent Degradation System , Loss of Dopamine Release , and Autophagic Cell Death. *J. Neurosci.* **2001**, *21* (24), 9549–9560.

Sugiyama, M.; Yamagishi, K.; Kim, Y.-H.; Kaneko, Y.; Nishizawa, M.; Harashima, S. Advances in Molecular Methods to Alter Chromosomes and Genome in the Yeast Saccharomyces Cerevisiae. *Appl Microbiol Biotecnol* **2009**, *84*, 1045–1052.

Sullivan, A. M.; Toulouse, A. Neurotrophic Factors for the Treatment of Parkinson ' S Disease. *Cytokine Growth Factor Rev.* **2011**, *22*, 157–165.

Sung, Y.; Eliezer, D. Residual Structure, Backbone Dynamics, and Interactions within the Synuclein Family. *J Mol Biol* **2007**, *372* (3), 689–707.

Swart, C.; Haylett, W.; Kinnear, C.; Johnson, G.; Bardien, S.; Loos, B. Neurodegenerative Disorders : Dysregulation of a Carefully Maintained Balance ? *Exp. Gerontol.* **2014**, *58*, 279–291.

Tagliafierro, L. Up-Regulation of SNCA Gene Expression : Implications to Synucleinopathies. *Neurogenetics* **2016**, *17*, 145–157.

Tenreiro, S.; Outeiro, T. F. Simple Is Good : Yeast Models of Neurodegeneration. **2010**, *10*, 970–979.

Tenreiro, S.; Reimão-Pinto, M. M.; Antas, P.; Rino, J.; Wawrzycka, D.; Macedo, D.; Rosado-Ramos, R.; Amen, T.; Waiss, M.; Magalhães, F.; et al. Phosphorylation Modulates Clearance of Alpha- Synuclein Inclusions in a Yeast Model of Parkinson ' S Disease. *PLoS Genet.* **2014a**, *10* (5).

Tenreiro, S.; Eckermann, K.; Outeiro, T. F. Protein Phosphorylation in Neurodegeneration : Friend or Foe ? *Front. Mol. Neurosci.* **2014b**, *7* (May), 1–30.

Thayanidhi, N.; Helm, J. R.; Nycz, D. C.; Bentley, M.; Liang, Y.; Hay, J. C. A-Synuclein Delays Endoplasmic Reticulum (ER) -to-Golgi Transport in Mammalian Cells by Antagonizing ER / Golgi SNAREs. *Mol. Biol. Cell* **2010**, *21*, 1850–1863.

Thomas, B. J.; Rothstein, R. Elevated Recombination Rates in Transcriptionally Active DNA. *Cell Press* **1989**, *56*, 619–630.

Tofaris, G. K.; Tae, H.; Hourez, R.; Jung, J.; Pyo, K.; Goldberg, A. L. Ubiquitin Ligase Nedd4 Promotes α -Synuclein Degradation by the Endosomal – Lysosomal Pathway. *PNAS* **2011**, *108* (41), 17004–17009.

Turrens, J. F. Mitochondrial Formation of Reactive Oxygen Species. *J. Physiol.* **2003**, *522* (2), 335–344.

Tyson, T.; Steiner, J. A.; Brundin, P. Sorting out Release, Uptake and Processing of Alpha-Synuclein during Prion-like Spread of Pathology. *J. Neurochem.* **2016**, *41* (Special Issue on Parkinson's Disease), 1–15.

Uversky, V. N. Intrinsic Disorder in Proteins Associated with Neurodegenerative Diseases. *Front. Biosci.* **2009**, *14*, 5188–5238.

Varkey, J.; Isas, J. M.; Mizuno, N.; Jensen, M. B.; Bhatia, V. K.; Jao, C. C.; Petrlova, J.; Voss, J. C.; Stamou, D. G.; Steven, A. C.; et al. Membrane Curvature Induction and Tubulation Are Common Features of Synucleins and Apolipoproteins. *J. Biol. Chem.* **2010**, *285* (42), 32486–32493.

Villacé, P.; Mella, R. M.; Kortazar, D. Mitochondria in the Context of Parkinson's Disease. *Neural Regen. Res.* **2017**, *12* (2), 214–215.

Vogiatzi, T.; Xilouri, M.; Vekrellis, K.; Stefanis, L. Wild Type a-Synuclein Is Degraded by Chaperone-Mediated Autophagy and Macroautophagy in Neuronal Cells. *J. Biol. Chem.* **2008**, *283* (35), 23542–23556.

Volles, M. J.; Lansbury Jr, P. T. Zeroing in on the Pathogenic Form of a -Synuclein and Its Mechanism of Neurotoxicity in Parkinson's Disease. *Biochemistry* **2003**, *42* (26).

Volles, M. J.; Lansbury Jr, P. T. Relationships between the Sequence of a-Synuclein and Its Membrane Affinity, Fibrillization Propensity, and Yeast Toxicity. *J Mol Biol* **2007**, *366* (5), 1510–1522.

Voutilainen, M. H.; Arumäe, U.; Airavaara, M.; Saarma, M. Therapeutic Potential of the Endoplasmic Reticulum Located and Secreted CDNF / MANF Family of Neurotrophic Factors in Parkinson ' S Disease. *FEBS Lett.* **2015**, *589* (24), 3739–3748.

Voutilainen, M. H.; Lorenzo, F. De; Stepanova, P.; Bäck, S.; Yu, L.; Lindholm, P.; Pörsti, E.; Saarma, M.; Männistö, P. T.; Tuominen, R. K. Evidence for an Additive Neurorestorative Effect of

Simultaneously Administered CDNF and GDNF in Hemiparkinsonian Rats : Implications for Different Mechanism of Action. *eNeuro* **2017**, *4* (February), 1–14.

Wales, P.; Pinho, R.; Lázaro, D. F.; Outeiro, T. F. Limelight on Alpha-Synuclein : Pathological and Mechanistic Implications in Neurodegeneration. *J. Parkinsons. Dis.* **2013**, *3*, 415–459.

Watson, J. B.; Hatami, A.; David, H.; Masliah, E.; Roberts, K.; Evans, C. E.; Levine, M. S. Aterations in Corticostriatal Synaptic Plasticity in Mice Overexpressing Human a-Synuclein. *Neuroscience* **2009**, *159* (2), 501–513.

Waxman, E. A.; Giasson, B. I. Characterization of Kinases Involved in the Phosphorylation of Aggregated a-Synuclein. *J Neurosci Res* **2011**, *89* (2), 231–247.

Weissman, A. M. Themes and Variations on Ubiquitylation. *Nat. Rev.* **2001**, *2* (March), 169–178.

Wera, S.; Bergsma, J. C. T.; Thevelein, J. M. Phosphoinositides in Yeast: Genetically Tractable Signalling. *FEMS Yeast Res* **2001**, *1*, 9–13.

Wijayanti, I.; Watanabe, D.; Oshiro, S.; Takagi, H. Isolation and Functional Analysis of Yeast Ubiquitin Ligase Rsp5 Variants That Alleviate the Toxicity of Human a -Synuclein. *J. Biochem.* **2015**, *157* (4), 251–260.

Winklhofer, K. F.; Haass, C. Mitochondrial Dysfunction in Parkinson ' S Disease. *Biochim. Biophys. Acta* **2010**, *1802* (1), 29–44.

Wolfe, D. M.; Lee, J.; Kumar, A.; Lee, S.; Orenstein, S. J.; Nixon, R. A. Autophagy Failure in Alzheimer ' S Disease and the Role of Defective Lysosomal Acidification. *Eur. J. Neurol.* **2013**, *37* (January), 1949–1961.

Wong, Y. C.; Krainc, D. α -Synuclein Toxicity in Neurodegeneration : Mechanism and Therapeutic Strategies. *Nat. Publ. Gr.* **2017**, *23* (2), 1–13.

Wooten, G. F.; Currie, L. J.; Bovbjerg, V. E.; Lee, J. K.; Patrie, J. Are Men at Greater Risk for Parkinson's Disease than Women? *J. Neurol. Neurosurg. Psychiatry* **2004**, *75*, 637–640.

Wu, N.; Joshi, P. R.; Cepeda, C.; Masliah, E.; Levine, M. S. Alpha-Synuclein Overexpression in Mice Alters Synaptic Communication in the Corticostriatal Pathway. *J. Neurosci. Res.* **2010**, *88* (8), 1764–1776.

Xiang, W.; Menges, S.; Schlachetzki, J. C. M.; Meixner, H.; Hoffmann, A.; Schlötzer-schrehardt, U.; Becker, C.; Winkler, J.; Klucken, J. Posttranslational Modification and Mutation of Histidine 50 Trigger Alpha Synuclein Aggregation and Toxicity. *Mol. Neurodegener.* **2015**, *10* (8), 1–16.

Xu, L.; Pu, J. Alpha-Synuclein in Parkinson ' S Disease : From Pathogenetic. *Parkinsons. Dis.* **2016**, *2016*.

Xu, S.; Zhou, M.; Yu, S.; Cai, Y.; Zhang, A.; Chan, P.; Ue, K. Oxidative Stress Induces Nuclear Translocation of C-Terminus of. *Biochem. Biophys. Res. Commun.* **2006**, *342*, 330–335.

Zabrocki, P.; Pellens, K.; Vanhelmont, T.; Vandebroek, T.; Griffioen, G.; Wera, S.; Leuven, F. Van; Winderickx, J. Characterization of a -Synuclein Aggregation and Synergistic Toxicity with Protein Tau in Yeast. *FEBS J.* **2005**, *272*, 1386–1400.

Zarranz, J. J.; Alegre, J.; Go, J. C.; Lezcano, E.; Ros, R.; Ampuero, I.; Hoenicka, J.; Rodriguez, O.; Ser, T.; Mun, D. G. The New Mutation , E46K , of a -Synuclein Causes Parkinson and Lewy Body Dementia. *Ann. Neurol.* **2003**, *55* (2), 164–173.

Zhou, W.; Chang, L.; Fang, Y.; Du, Z.; Li, Y.; Song, Y.; Hao, F.; Lv, L.; Wu, Y. Cerebral Dopamine Neurotrophic Factor Alleviates A-Beta-25-35-Induced Endoplasmic Reticulum Stress and Early Synaptotoxicity in Rat Hippocampal Cells. *Neurosci. Lett.* **2016**, *633*, 40–46.

6 Supplementary Data

Figure 6.1 Sequence alignments between aSyn WT sequence and the described aSyn mutants. Plasmids were obtained through site-directed mutagenesis, according to *Material and Methods 2.4.1.*

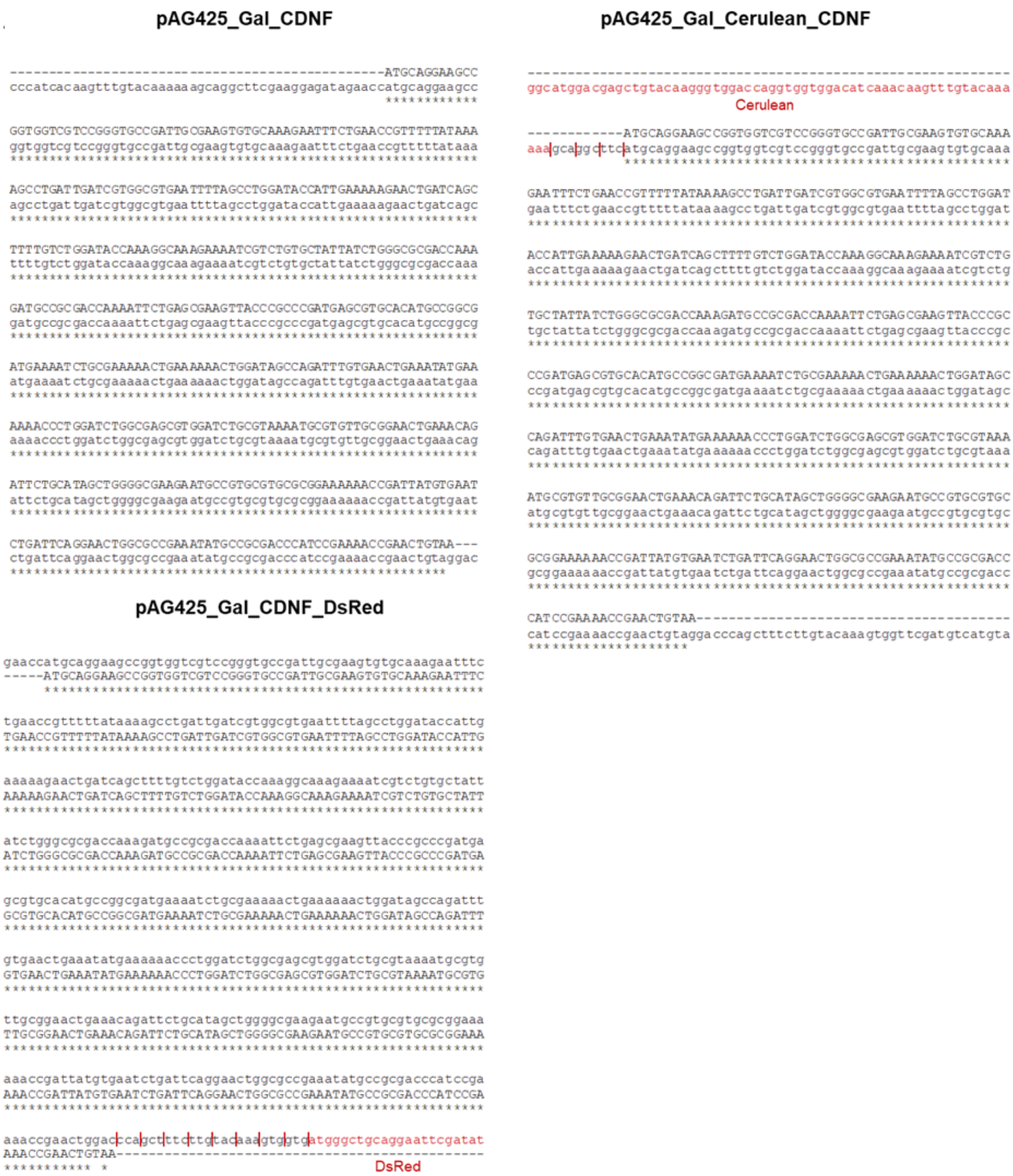

Figure 6.2 Sequence alignments between CDNF sequence and the described plasmids.

Plasmids were obtained through Gateway Recombination Cloning Technique, according to *Material and Methods 2.3.2.*